UNIVERSITÀ
DEGLI STUDI
DI PADOVA

UNIVERSITA' DEGLI STUDI DI PADOVA

Department of Chemical Sciences

Ph.D. Course in Molecular Sciences

Curriculum: Pharmaceutical Sciences

XXX Series

THESIS TITLE

Metabolomics in natural products research: application to *in vivo* bioactivity studies involving nutraceuticals

Coordinator: Prof. Leonard Prins

Supervisor: Dr. Stefano Dall'Acqua

Ph.D. student: Gregorio Peron

TABLE OF CONTENTS

ABSTRACT

The analysis of urinary metabolite changes can provide information on the effects of food supplements or health-promoting products on healthy subjects or animal models. Specimen collection is non-invasive, long-term experiments can be easily conducted and urinary biomarkers of oxidative stress can also be measured, offering the opportunity to study the effects of a nutritional intervention and evaluate the redox status of the considered organism. Compared to other biological fluids or matrices (plasma and feces for example), sample preparation is more straightforward in the case of urine because of lower sample complexity and lower protein/peptide content. Finally, urine samples the metabolic end-products from the organism destined for excretion, therefore, it is prone to high biological variations.

Three natural extracts were selected for the work here reported, namely *Polygonum cuspidatum* Sieb. et Zucc. (rich in resveratrol), *Vaccinium macrocarpon* Aiton (cranberry, rich in type A procyanidins) and green *Coffea canephora* Pierre ex Froehn. beans (GCBE, rich in chlorogenic acids), on the basis of their distribution on the nutraceuticals market and on the basis of the information regarding their *in vivo* activity actually available in literature. In fact, these largely sold products are aimed to prevent disorders or aging (as in the case of *P. cuspidatum* and resveratrol), or in general to maintain a healthy status. On the other hand, in many cases scientific data regarding the efficacy and safety of nutraceuticals and their phytochemical composition are scarce, so there is the need to study in deep these products and how they exert their activity. For this reason, considering the heterogeneity of the products studied and the complexity of the interactions between nutraceuticals and living organisms, metabolomics analyses represent an attractive approach.

In the first part of the work, the effects of *P. cuspidatum* dry extract were studied in healthy adult rats during a 49-days supplementation, using a combined ^{1}H NMR and UPLC-HRMS metabolomics approach. The variations of urinary composition were studied using ^{1}H NMR, UPLC-HRMS and multivariate statistical analysis. Because of the reported antioxidant activity of resveratrol, the urinary levels of two oxidative stress biomarkers were measured by targeted HPLC–MS/MS analyses and, due to the supposed “anti-aging” effects of resveratrol, multivariate models were designed in order

to compare the aging effects between control and treated animals. Specific biomarkers were then selected and identified, and their amounts in urine were monitored throughout the experimental period.

UPLC-MS metabolomics approaches were used to evaluate the mode of action of cranberry against uropathogenic *Escherichia coli* in two independent experiments, using an animal model and enrolling healthy adult volunteers, respectively. The experimental design was similar for the two trials, and the aim was to observe if the results obtained from the first animal experiment were reproducible in humans, being cranberry supplements claimed for treatment of UTIs in human consumers. In the first experiment, healthy Sprague−Dawley rats were orally supplemented with a standardized cranberry extract for 35 days, to mimic a prolonged consumption of cranberry by healthy subjects. 24-h urinary outputs were collected weekly during the experiment, and samples were subjected to UPLC−MS analysis using an untargeted approach. In a second experiment on the same animal model, a single dose of cranberry was administered to animals and the changes of urinary composition at 2, 4, 8, and 24 h after extract administration were monitored. Anti-adhesive properties of all the urine samples were studied. Furthermore, the markers related to cranberry intake were discovered using a multivariate data analysis approach. Finally, a specific chromatographic method was developed for the measurement of unmodified PAC-A in urine. In the experiment involving human volunteers, these consumed an oral sachet containing 360 mg of dry cranberry extract and 100 mg of quercetin. Urine samples were collected at 2, 4, 6, 8 ad 24 hours after product administration and the anti-adhesive properties of urine samples were tested using an in vitro assay on *E. coli*. In order to correlate possible observed bioactivity with modification of urinary composition, LC-MS-based targeted and untargeted metabolomics approaches were used.

Finally, a clinical trial on a small number of healthy adult volunteers was performed to study the effects of a prolonged (30 days) supplementation with 400 mg of green coffee bean extract. The 24-h urinary samples were collected weekly, and analyzed by LC-MS. Multivariate data analysis approaches were applied and also targeted analysis were performed to measure urinary oxidative stress biomarkers, namely allantoin and 8-hydroxydeoxyguanosine (8-OHdG), in order to assess the potential antioxidant activity of GCBE *in vivo*.

On the best of our knowledge, and on the basis of the data available in literature,

the works presented in this thesis project are the first reporting the application of metabolomics approaches in the bioactivity studies of *P. cuspidatum* in animal model and of GCBE in human volunteers. Regarding cranberry, the data here reported are the first to correlate the metabolomics analysis of urine after the intake of a cranberry-containing supplement and the results obtained from anti-adhesive assays of the same urine samples against uropathogenic bacteria.

LIST OF ABBREVIATIONS

8-OHdG: 8-Hydroxydeoxyguanosine

AUC: Area Under the Curve

CGA: Chlorogenic Acid

DAD: Diode Array Detector

ESI: Electrospray Ionization

GC: Gas Chromatography

GCBE: Green Coffee Bean Extract

HILIC: Hydrophilic Interaction Liquid Chromatography

HMDB: Human Metabolome Database

HPLC: High Pressure Liquid Chromatography

HR: High Resolution

LC: Liquid Chromatography

MS: Mass Spectrometry

MS/MS: Tandem Mass Spectrometry

MS^e: Tandem Mass Spectrometry using alternating low-energy/high-energy

MS^n: Multi-step Tandem Mass Spectrometry

NMR: Nuclear Magnetic Resonance

OPLS-DA: Orthogonal Partial Least Squares Discriminant Analysis

PAC: Proanthocyanidin

PCA: Principal Component Analysis

PLS-DA: Partial Least Squares Discriminant Analysis

PPAR-α: Peroxisome Proliferator-activated Receptor alpha

ptPLS2: post transformation of Partial Least Squares regression

QC: Quality Control

QTOF: Quadrupole-Time of Flight

tdds®: Turbo Dependent Data Scanning

TQD: Triple Quadrupole Detector

UPLC: Ultra Performance Liquid Chromatography

UTI: Urinary Tract Infection

VIP: Variable Importance on Projection

INTRODUCTION

1. From nature to nutraceuticals: natural products used as food supplements

1.1. Nutraceuticals: a definition

The term "nutraceutical" was coined in 1989 by DeFelice, who described it as "a food, or part of a food, that provides medical or health benefits, including the prevention and/or treatment of a disease" (Brower, 1998). Nowadays, term "nutraceutical" is widely used in marketing and has no actual regulatory definition (Espín et al., 2007, Kalra, 2003). Nutraceuticals are non-medicinal health-promoting products that are used by a large part of the population in the developed countries. These products are available without medical prescription in pharmacies and regular markets. Because of the non-regulatory meaning of "nutraceuticals", these products can either be considered as food supplements (Espín et al., 2007) or herbal products (non-registered medicinal herbal products). Because of their "non-medicinal" nature, no proof of efficacy and no premarketing approval is required for these products in Europe or in the USA by the U.S. Food and Drug Administration (FDA) (unless drug-like efficacy is claimed) (Van Breemen, 2015). Nevertheless, nutraceuticals are commonly used for their reported health-promoting and/or disease-preventing properties, as, for example, in the prevention of aging-associated diseases or in the management of oxidative, inflammation, arthritis, osteoporosis, gastrointestinal diseases, cardiovascular diseases, depression, diabetes and cancer (Bernal et al., 2011, Sut et al., 2016, Wang et al., 2016).

Many nutraceuticals contain natural products in their composition, usually in the form of dried extracts or as pure or isolated compounds. Especially considering dried extracts, natural sources for nutraceutical products are complex matrixes, whose quali-quantitative chemical composition is often not completely defined (Espín et al., 2007). For this reason, although these products are present in the market with health-promoting claims, in many cases the consumer does not know exactly what is the composition of the product that is taking. Furthermore, in many cases little is known about the specific

biological activities that are exerted by phytochemicals (Espín et al., 2007), and about their mechanism(s) of action and their pharmacokinetics and metabolic fates, especially if they are administered as part of complex matrixes or extracts. In fact, unlike in the case of single drugs, the components of natural extracts could interact among others, so possible synergic or antagonistic effects between them could be possible (Gertsch, 2011, Wagner and Ulrich-Merzenich, 2009, Yang et al., 2014). Due to the fact that these products are "food or part of a food" (Brower, 1998), they are generally considered safe and tolerable, but the literature regarding their efficacy and tolerability is often controversy, showing inconsistent results in some cases and/or reporting investigations that are not well-designed. As suggested by Van Breemen (Van Breemen, 2015), to ensure the safety and efficacy of botanical dietary supplements, their development should be performed in a similar way to that of pharmaceuticals. Thus, first of all a complete chemical characterization of extracts and the assessment of mechanisms of action of active constituents should be required. Furthermore, the chemical standardization of the active compounds and the biological standardization based on pharmacological activity should be performed, along with the preclinical evaluation of the toxicity, the study of the metabolism of active compounds and potential drug-botanical interactions, and finally, clinical studies on safety and efficacy (Van Breemen, 2015). On the other hand, all these procedures are more complex and time-consuming compared to single drugs, considering that many "nutraceutical" ingredients are complex mixtures that are obtained by extracting natural materials (plant, marine or terrestrial organism, microorganism, or fermentation product, etc.). Products standardization, for example, could not be performed by using a single "marker" compound or a "class" of marker compounds, because this is not sufficient to assess their quality and efficacy. In addition, the pharmacokinetic profile (ADME: absorption, distribution, metabolism, and excretion) of all the constituents of the extracts should be analyzed, in order to understand the relative influence of the matrix on the absorption of active constituents (Sut et al., 2016). In fact, the bioavailability of several phytochemicals could be limited by their poor solubility, by their susceptibility to degradation in the gastro-intestinal environment, by extensive metabolism or by the presence of other constituents in the matrix that could hamper their absorption (such as fibers or hemicellulose). An additional issue is the possible interaction of natural products with gut microbiota. In fact, dietary phytochemicals can cause selective stress or stimulus to the resident intestinal flora, creating food-microbiome networks that

could interfere with both the expected bioactivity of the product and the normal activity of intestinal flora (Ni et al., 2015). For all these reasons, the study of nutraceuticals is a challenge that can be solved using a medicinal chemistry approach, but considering the presence of multiple active agents.

1.2. Classical *in vitro* approaches to study the bioactivity of botanicals and nutraceuticals

As for the development of new drugs, appropriate *in vitro* bioassays are needed to identify bioactive components of nutraceuticals, to assess their mechanism of action and to test their efficacy and toxicity. For bioactivity assessment, bioassays on crude extracts, purified fractions or pure isolated compounds are performed. All these approaches have advantages and disadvantages that should be taken in account. The study of crude extracts may be considered attractive for assessing the effect of the whole mixture, however the complex chemical composition and the presence of interfering compounds (such as tannins, chlorophyll or fatty acids, for example) could hamper the assays and can lead to unexpected false positive or negative results (Sut et al., 2016). Another problem is the low water solubility of some phytocompounds, therefore an adequate non-toxic solvent for cells should be used. Usually, DMSO is used for this purpose, because of its valuable solvent properties and its relatively low effect on cell viability. However, DMSO might also have an effect on cells viability (Butterweck and Nahrstedt, 2012), furthermore dissolving the extract in DMSO might solubilize compounds that would never have been dissolved under more moderate conditions, so the effects of such compounds might be measured in the assay. Another problem is related to the color and auto-fluorescence of crude botanical extracts that could interfere with several assays.

Another classical strategy to study the bioactivity of natural extracts and do identify the active constituents is the bioassay-guided fractionation (Koehn and Carter, 2005) (Figure 1). It consists in preliminary bioassays that are used to test the specific bioactivity of the whole botanical extract. This latter is subsequently fractionated by chromatographic techniques to separate the constituents with different physicochemical properties, and each fraction is tested using the same bioassay. Active fractions are fractionated and tested again, and the entire process is repeated until the compounds responsible for the activity are isolated and identified by means of spectroscopic

techniques (Koehn and Carter, 2005).

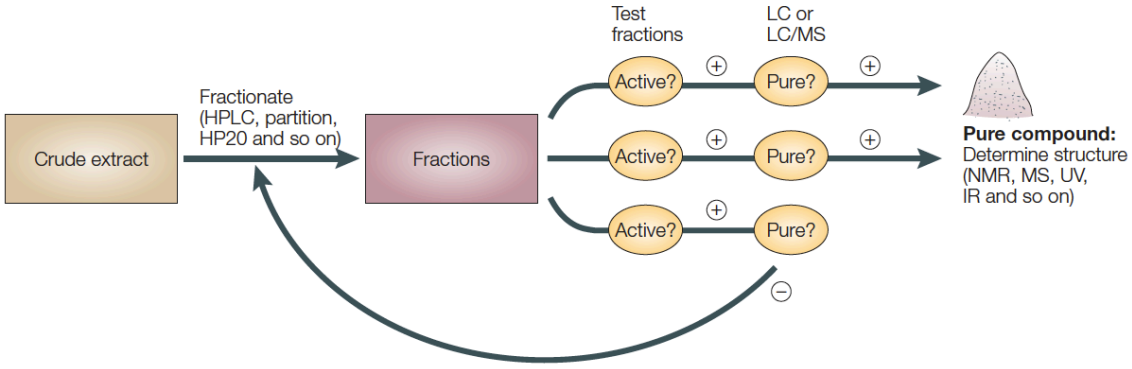

Figure 1. Generic scheme for bioassay-guided fractionation. Taken and re-adapted from (Koehn and Carter, 2005).

The most important limitation of the bioassays as described above is that they consist in reductionist approaches, aimed to investigate the activity of single compounds on specific targets. However, as stated before, the effects of complex natural extracts could not be linked to the activity of single compounds on specific targets, but to the complex action of multiple constituents or to the multi-targeting activity of several compounds (Gertsch, 2011), so reductionist approaches could not be suitable for a complete investigation. Moreover, all *in vitro* bioassays don't take in account the aspects related to pharmacokinetics and possible activation of pro-drugs that could be observable *in vivo*, along with the possible interactions between the phytoconstituents and gut microbiome. Thus, after a preliminary *in vitro* study, *in vivo* bioassays are required to depict a more complete profile on the activity and toxicity of natural extracts.

1.3. *In vivo* bioactivity studies

A more complete study on the bioactivity of natural extracts is performing *in vivo* experiments using animal models, although it is a model that present differences and, in many cases, approximations compared to humans. In fact, variations in the body weight, organ size, hepatic and renal blood flow, metabolism, distribution, and elimination rate result in significantly different pharmacokinetic profiles between animals and humans (Ting et al., 2014, Van Breemen, 2015). Hence, also murine experiments should be

considered as approximate representations of what could be observed in humans.

A first important aspect to consider in the performance of animal experiments is the route of administration of the studied product. Generally, the expected clinical route of administration should be chosen, that for nutraceutical products would be oral. However, in some experiments the intraperitoneal administration was reported, because it is very easy to perform in comparison with other administration routes (Pferschy-Wenzig and Bauer, 2015). This application route has some drawbacks, such as unpredictable absorption characteristics, which depend on the exclusion through the GI tract, microbiota metabolism and portal system (Sut et al., 2016).

The metabolic activities of the different systemic organs (most importantly, liver, heart and lungs) must be considered, given that they may impact the amount of ingested compounds (McClements, 2015, Ting et al., 2014). In fact, several phytochemicals are subjected to extensive metabolism by hepatic enzymes, which can lead to either the activation (pro-drugs) or the inactivation of these compounds. Therefore, the bioactivity of a native herbal product might be markedly changed by these *in vivo* metabolic reactions. To mimic *in vivo* metabolism, *in vitro* preparations such as S9-liver homogenate, microsomes, cryopreserved hepatocytes, cryopreserved liver slices and fresh liver, lung, kidney and intestinal slices have also been compared for their ability to metabolize xenobiotics (Sut et al., 2016). However, the intestinal environment is even more complex. Gut microbiota exerts an enormous impact on the nutritional and health status of the host by modulating its immune and metabolic functions. The microbiome provides additional enzymatic activities that are involved in the transformation of dietary compounds and on several phytoconstituents (Laparra and Sanz, 2010). For these reasons, the biological roles of nutraceuticals, phytochemicals and functional food components may be strongly related to gut microbiota interactions, and for an exhaustive study of their activity an *in vivo* model is required.

Other information on the possible health benefits of nutraceuticals can be obtained from standard randomized clinical trials. In these trials, the ‘patient’ population should be composed by healthy individuals, the dosages are typically low and interference with components from the diet may be highly significant (Possemiers et al., 2011). In fact, botanical dietary supplements are not intended to treat a disease, but rather to modify an imbalance within normal physiological boundaries (Possemiers et al., 2011), so they are intended to promote a healthy status. Thus, nutraceutical trials have to be managed in a different way than conventional clinical pharmaceutical trials. Usually, from

pharmaceutical trials higher specific dosages, disease-specific clinical endpoints, and a specific patient population mean that will have more significant results than nutraceutical studies, in which the supplements may be administered to a wide range of healthy individuals. First of all, given the inherent phytochemical variability of the herbal materials used in the preparation of nutraceuticals, a detailed description of herbal products used in clinical trials is an essential prerequisite for the performance of the experiment (Pferschy-Wenzig and Bauer, 2015). The plant part, the extraction solvent, and the manufacturing process should always be reported for the correct interpretation of trial results. Also inter-individual variation following exposure to active ingredients could have a profound impact on the final clinical outcomes. In fact, nutraceuticals are subjected to bacterial metabolism that can generate active or inactive metabolites. Considering the high variability of gut microbiome, bioactivity in different individuals will be influenced by the final circulating metabolite patterns that can be highly modified both in concentration and composition. Thus, innovative analytical approaches such as metabolomics could be useful tools for the study of activity, metabolism and excretion of nutraceuticals.

2. Metabolomics: an innovative tool for *in vivo* studies

2.1. The "Omics" cascade

Since the end of '90s, the availability of increasingly sensitive and accurate chromatographic and spectroscopic instruments have contributed to the development of systems biology, a branch of science that aims to study the complex interactions within biological systems, using a holistic approach (Lavrik and Zhivotovsky, 2014). The sequencing of DNA maps from various animal species during the late '90s, including humans, gave birth to genomics, the first of the so called "omics" techniques that focuses on the characterization of genetic material. Starting from the available genomic data, transcriptomics aims to characterize set of mRNA molecules in one cell or a population of cells; during the last years, its usefulness as a tool to identify new potential biochemical targets of drug therapies was reported (Dopazo, 2014). Proteomics approaches were subsequently developed to investigate signaling networks in living systems at the protein and protein-protein interaction levels. Finally, analytical

approaches aimed at studying and characterizing global metabolite profiles in living systems under different conditions and stimuli were developed, and these were named metabolomics (Figure 2).

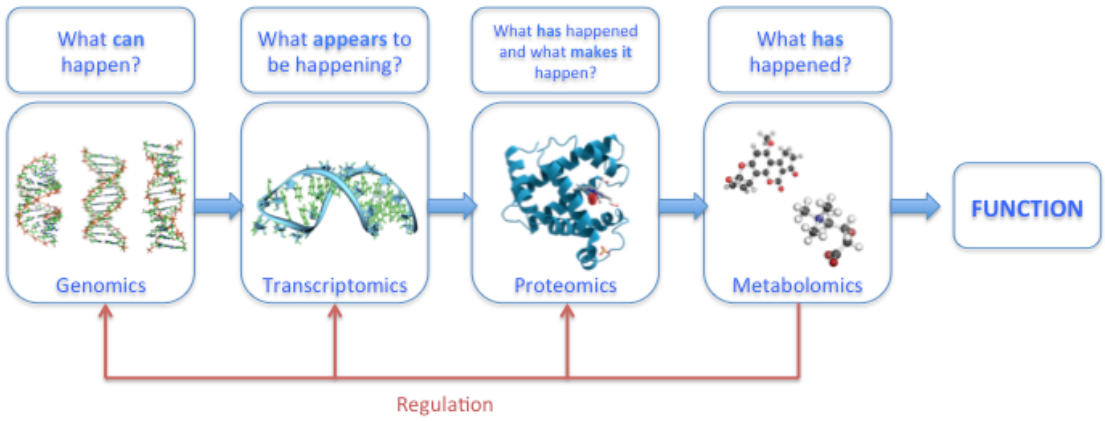

Figure 2. The OMICS cascade.

Metabolomics focuses on metabolic pathways and processes as well as on specific compounds, and it relates processes and compounds to growth, development, stress, disease or environmental changes. Nowadays metabolomics has become an important tool in life sciences and it has acquired an important role in studies on plant interactions with other plants, insects and other living organisms (i.e., animals or humans), in the quality control of food or medicine and in the diagnosis of pathologies and drug research.

2.2. Metabolomics: an evaluable tool for natural products research

Metabolomics is focused on the high-throughput identification, characterization and quantification of small molecules (MW < 1000 Da) composing the metabolome, the end product of cell metabolism (Han et al., 2008). This branch of systems biology was born between the ‘70s and ‘80s, when researchers began to study urinary metabolic composition by gas chromatography–mass spectrometry (GC-MS). However, the term metabolomics appeared in the scientific literature only in 1998 (Mishra and Tiwari, 2011).

Nowadays metabolomics approaches are extensively applied in studies involving natural products. The mapping of metabolite profiles of natural extracts to an extensive degree is one of its applications in this research field, and researchers frequently apply

metabolomics to quality control of herbal products. In fact, variations in metabolic profiles may occur because of environmental changes during the growth or harvesting of plants, or because of adulteration, for example, and these changes could alter the bioactivity profiles of natural products (Chang et al., 2011). Moreover, the metabolome is the final downstream product of gene transcription, and its changes are amplified in comparison with the transcriptome and proteome changes (Urbanczyk-Wochniak et al., 2003). An analytical methodology that allows for the monitoring of an entire class of metabolites in an unbiased manner, such as that of metabolomics, can be a useful tool (Van Der Kooy et al., 2009).

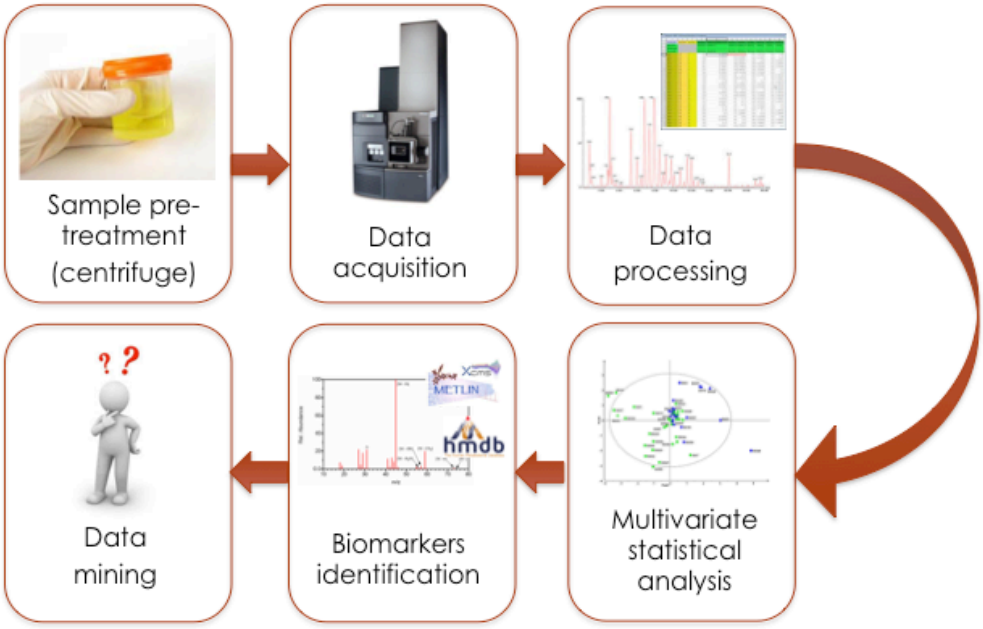

Figure 3. Scheme representing a typical metabolomics workflow.

Another application of metabolomics is the metabolic fingerprinting of biological fluids, such as urine, blood, cerebro-spinal fluid, saliva, lymph and synovial fluid (Wang et al., 2005). The composition of biofluids could change following stimuli, such as environmental, dietary or pharmacological, among others, and monitoring these variations could be useful to assess the efficacy, mechanism(s) of action and toxicity of drugs or natural products, for example. Urine and saliva could be easily sampled in a scarcely invasive way and pre-analytical sample treatment is straightforward, due to low protein and fats content, so they are frequently used for these types of investigations. Several high-throughput spectroscopic (NMR, MS, MS-MS) and chromatographic

(HPLC, GC, GC-MS, LC-MS, and TLC) techniques are widely employed in metabolomics, and each approach presents its own strength and weakness (Sut et al., 2016) (Table 1).

A typical untargeted metabolomics methodological pipeline comprises several steps, concerning samples collection and analysis, data pre-processing, multivariate statistical analysis and model building, and finally data mining (Figure 3). Along metabolite-identification methods, spectral pre-processing methods are highly dependent on the analytical technique used (e.g., NMR, LC-MS, or GC-MS). The different steps are described in the next paragraphs.

2.2.1. Sampling

Sampling times and protocols greatly affect the reproducibility of the data, so it should be performed with extreme care, as the risk to introduce variations in samples is high. Metabolomics approaches could be used to study biological samples of different physicochemical nature, such as blood, plasma, cell metabolites or excretion liquids. Each kind of sample needs a suitable sampling method that could be highly or scarcely invasive, as for blood sampling and urine harvesting, respectively. All samples must be collected, stored and treated in the same way, so a protocol must be drawn up to ensure standardization of the procedures. Blood collection can be carried out at regular and selected intervals, and small amounts (few drops) can be collected. Furthermore, compared to urine, it is less subject to microbial contamination. On the other hand, enzymatic activity is higher in blood and the risk of sample degradation is high; for this reason, blood samples must be handled at low temperatures. Blood is composed of plasma and a cell fraction; this latter should be discarded by centrifugation and anticoagulant agents (EDTA or heparin) should be added (Savorani et al., 2013). On the other hand, urine sampling is less invasive than blood collection, and this creates a lower stress in the animals or volunteers involved in the studies. Also sample pre-treatment is simpler and less time-consuming than blood, usually consisting only in a centrifugation step to discard proteins and in a further dilution with water.

In general, it is important to keep the samples at low temperatures to prevent analytes from undergoing degradation and structural modifications and to block enzymatic reactions. In this way, the sample metabolome is maintained stable until analysis. A common practice is to freeze the samples between -20 °C and -80 °C

immediately after harvesting. Subsequently, thawing and reheating cycles, which represent a thermal stress for samples, should be avoided.

Depending on the type of analysis, the samples will undergo different treatments. For example, in targeted analyses, it could be necessary to purify the analytes to reduce the background noise, so, after protein precipitation and centrifugation, solid phase or liquid phase extractions are performed. As an example, if intracellular metabolites are to be analyzed, it is necessary to lysate the cells, extrapolate the metabolites with non-polar (e.g. chloroform) or polar (H_2O/MeOH mixtures) solvents, and finally remove the pellets through a centrifugation step.

2.2.2. NMR and MS platforms in metabolomics and data acquisition

Among others, nuclear magnetic resonance (NMR) is considered one of the best-suited analytical platforms, because of its advantages relative to other methods. NMR is characterized by high reproducibility and short analysis times, furthermore pre-analytical sample preparation is usually fast and simple and structures of known or unknown compounds in complex matrixes can be elucidated by analyzing the spectra (Kim et al., 2011, Yuliana et al., 2013). Moreover, multidimensional NMR methods may offer additional tools for structural elucidation, because they provide information for all the H and C atoms in molecules with highly reproducible chemical shifts, coupling constants and atom correlation (Wolfender et al., 2013). Other advantages are that NMR is non-destructive, non-biased and can easily be used in quantification; furthermore, it requires little or no separation and needs no chemical derivatization (Wishart, 2008). Analyte quantification is simple because it only requires an internal standard, whereas in other methods compounds must be quantified using calibration curves (Yuliana et al., 2013). However, NMR presents two major drawbacks that limit its use in metabolomics. The most relevant is related to its low sensitivity, especially if compared to modern mass spectrometric technologies (Verpoorte et al., 2007). The required amount of sample is often higher than the amounts needed for other analytical platforms and signals generated by compounds that are present in low quantities could not be detected, leading to a loss of information. Another limitation, especially concerning the analysis of complex samples, is the large number of signals measured in a single spectrum and their overlapping, which are factors that may hamper identification of parent compounds (Kim et al., 2011, Wolfender et al., 2013).

Table 1. Advantages and disadvantages of the main analytical platforms used in metabolomics.

Analytical platform	Advantages	Disadvantages
NMR	• Fast data acquisition • High reproducibility • High resolution • Simple sample preparation • Non-destructive • No chemical derivatization required	• Low sensitivity • High amounts of sample required • Complex spectra • Multiple peaks related to a single metabolite
LC-MS	• High sensitivity • Analysis conditions could be adapted to metabolites • Wide analytical range • Derivatization not required	• Long analysis time • Poor spectra databases
GC-MS	• High sensitivity • Analysis conditions could be adapted to metabolites • Wide analytical range • Rich spectra databases	• Long analysis time • Not suitable for thermolabile compounds • Derivatization could be necessary

On the other hand, mass spectrometry (MS) is the other most used analytical technique in metabolomics. First of all, MS can be used by directly infusing samples in the instrument, and this approach is known as direct infusion MS (DIMS) (Wolfender et al., 2015). The advantage of this approach is the fast time of analysis, but long sample pre-treatment may be needed, especially while working with complex matrices as natural extracts or biological samples. For this reason, MS is usually hyphenated with different chromatographic techniques, those provide compound separation prior to MS detection: the most used in metabolomics are gas chromatography-MS (GC-MS) and liquid chromatography-MS (LC-MS). GC is employed for the analysis of volatile and thermo-stable compounds, whether LC is suitable for the analysis of a broader range of molecules (Wolfender et al., 2013). Compared to NMR, the main advantage of MS is its higher sensitivity, which allows for the detection of compounds at trace amounts

(Dettmer et al., 2007). Furthermore, chromatographic and mass spectrometric conditions could be optimized according to the sample to analyze. For LC-MS, for example, different stationary phases (normal phase, reverse-phase C-8, C-18, and HILIC) and mobile phases (water, acetonitrile, methanol, and buffers) could be selected to improve separation. Also, the mass spectrometric parameters could be properly set, in order to optimize the detection of specific classes of constituents. Specific ionization sources could be selected (ESI and APCI are the most frequently used) as several analyzers could be used to reach a proper resolution (QTOF, Orbitrap and FT-ICR have acquired larger popularity, among others). In particular, two steps are critical for MS-based metabolomics, i.e., metabolite ionization and ion separation by the mass analyzer (Wolfender et al., 2013, Wolfender et al., 2015). Ionization is a chemical process in which the yield depends primarily on the chemical properties of the compounds. Thus, the use of positive and negative ionization modes allows for the detection of different metabolites, and therefore the comprehensive coverage of most metabolites requires that both ionization modes be used (Wolfender et al., 2015). The number of features detected is, however, also related to the capacity of the mass analyzer to separate ions at different *m/z* values, and thus to its resolution. Currently, high-resolution analyzers such as Q-TOF ($R \cong 20.000$) and orbitrap ($R \cong 500.000$) are frequently employed in metabolomics, through which molecular weights and molecular formulas can be determined with high accuracy. Furthermore, by employing tandem, ion-trap or orbitrap analyzers, multistage fragmentation MS spectra (MS^n) and simultaneous fragmentation MS spectra at low and high collision energies (MS^e) could be acquired. Important information on features identities are strictly related to fragmentation patterns, and helpful data for molecular identification could be collected through MS^n and MS^e experiments (Herrero et al., 2012, Zhang et al., 2012). The main disadvantage of MS is that, unlike NMR, metabolites detection is not universal, and MS ionization is strongly compound-dependent; thus, the intensities of the observed ions cannot be directly related to the concentration of the analytes (Wolfender et al., 2013), and their quantitation must be performed on the basis of the appropriate calibration curves (Yuliana et al., 2013).

Usually, for both NMR and MS-based metabolomics, three different approaches could be used, namely targeted and untargeted analyses (Boccard et al., 2010) and metabolic fingerprinting (Krastanov, 2010) (Figure 4).

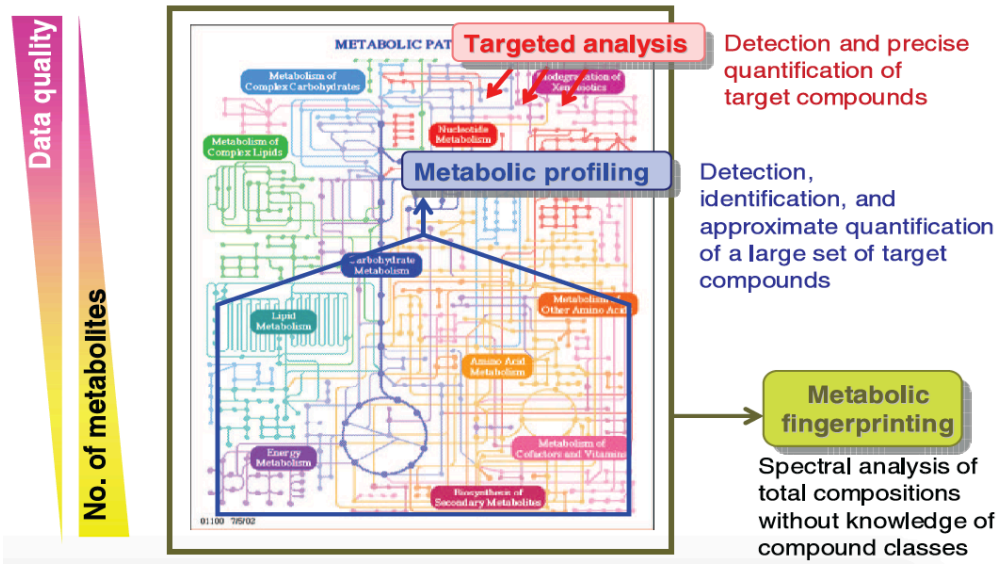

Figure 4. The different approaches in metabolomics analysis. Taken from (Krastanov, 2010).

In targeted metabolomics, quantitative methods are used to analyze specific variables one by one, and their statistical significance can be tested using univariate methods (Commisso et al., 2013). On the other hand, if the aim is to provide a comprehensive view of the system under investigation, an untargeted metabolomics approach is employed, through which all the obtained variables are considered simultaneously and many known and unknown metabolites are quantified. By using both targeted and untargeted metabolomics, the behavior of known metabolites could be described, but only the untargeted approach allows for the detection of synergic effects between variables that cannot be observed at an individual level (Commisso et al., 2013). Finally, metabolic fingerprinting is an approach that is not driven by a priori hypothesis. It is used for complete metabolome comparison, without knowledge of compound identification. Usually, a spectral analysis is used to perform fingerprint analysis. Metabolite variation is observed principally on the total chromatographic pattern changes without the previous knowledge of the compounds investigated, therefore, metabolite identification is not mandatory (Krastanov, 2010).

2.2.3. Raw data pre-processing

After data acquisition by NMR and MS, data processing using statistical tools and subsequent data mining is required to interpret the obtained results. Prior to statistical

processing, raw data should be treated in order to make them suitable. In fact, NMR and MS spectra typically show differences, as peak shape, width, and position due to noise, sample differences or factors related to the instrumentation employed (Blekherman et al., 2011, Smolinska et al., 2012). The aim of preprocessing is to make different samples comparable, by correcting these differences for better detection and quantification of metabolites (Vettukattil, 2015). Preprocessing in NMR-based metabolomics typically includes baseline correction, alignment, binning, normalization, and scaling (Smolinska et al., 2012). Baseline correction aims to correct baseline distortions caused by systematic artifacts (Vettukattil, 2015). Alignment is performed to correct peak shifts due to differences in instrumental factors or temperature and due to changes of pH (as for urine samples (Krumsiek et al., 2016)). Binning divides the spectra into segments and replaces the data values within each bin by a representative value (Smolinska et al., 2012). Normalization is used to correct for some systematic variations between samples, as sample dilution factor (Krumsiek et al., 2016), in order to make samples more comparable with each other. Usually, normalization is a multiplication of every row (sample) by a sample specific constant (Craig et al., 2006). Scaling methods are data pretreatment approaches that aim to adjust for the differences in fold differences between metabolites by converting the data into differences in concentration relative to the scaling factor. They divide each variable by a factor, the scaling factor, which is different for each variable. Most commonly used scaling methods are autoscaling (also referred as Unit of Variance scaling) and Pareto scaling. Autoscaling uses the standard deviation as the scaling factor, and after processing all metabolites have a standard deviation of one. In Pareto scaling, instead of the standard deviation, the square root of the standard deviation is used as the scaling factor. In this way, large fold changes are decreased more than small fold changes, thus the large fold changes are less dominant compared to clean data (van den Berg et al., 2006).

Also for MS data baseline correction, normalization, peak alignment and scaling must be performed to render data suitable for further statistical analysis. These procedures are the same described for NMR analysis. Furthermore, for MS raw data, noise filtering, de-isotoping, spectral deconvolution and peak detection must be performed. Noise filtering is often applied to improve peak detection (Blekherman et al., 2011), and it is usually performed using different noise filters (Yang et al., 2009). De-isotoping can be used to cluster the isotopic peaks corresponding to the same compounds together to simplify the data matrix (Vettukattil, 2015). Deconvolution is

used to separate overlapping peaks in order to improve peak detection and quantification.

Nowadays, many analytical platforms present several of these processing in simplified mode and using user-friendly software. With LC-MS systems, dedicated build-in software have been developed to help in the generation of datasets that can be then used in multivariate analysis. On the other hand, free downloadable software as MZmine (http://mzmine.github.io), for example, can also be used, and they allow the operator to pre-process and process data in different modes. However, in some cases, to obtain readable data for calculation programs, raw data from the instruments need to be converted using other specific software.

2.2.4. Multivariate statistical data analysis

After preprocessing, data are used to perform multivariate statistical analysis and to extract information. From a statistical point of view, in targeted analysis variables are analyzed using classical univariate methods, but the consideration of the large number of variables involved in untargeted metabolomics is not feasible using the same methods, thus multivariate statistical tools must be applied. For exploratory data analysis, unsupervised techniques such as Principal Component Analysis (PCA) could be used, although more complex supervised methods such as the Partial Least Squares Discriminant Analysis (PLS-DA) and Orthogonal Partial Least Squares Discriminant Analysis (OPLS-DA) may be employed to extract hidden information that helps to explain the system's behavior (Figure 5) (Commisso et al., 2013). In unsupervised methods data is unlabeled and unclassified, and they allow to discover the groups or trends in the dataset. On the other hand, supervised methods are employed in discovering biomarkers, classification and prediction, and prior to analysis data are classified (e.g., treated and control groups in *in vivo* bioactivity studies) (Krumsiek et al., 2016).

From a high-dimensional dataset comprising hundreds or thousands of metabolites, only a few combinations of them that best explain the total variation in the original dataset have to be found. PCA is a dimension reduction algorithm that replaces all correlated variables by a smaller number of uncorrelated variables, named principal components (PCs), that still retain most of the information in the original dataset (Krumsiek et al., 2016). If the first few PCs can explain a large proportion of variation

in the data, it could be visualized using a two-dimensional or three-dimensional plot, called score plot, which is mainly used to discover groups. Another graph, indicated as loading plot, present the variables that are responsible for separating the groups, whose are represented by the points that are further from the origin than most other points in the plot (Krumsiek et al., 2016).

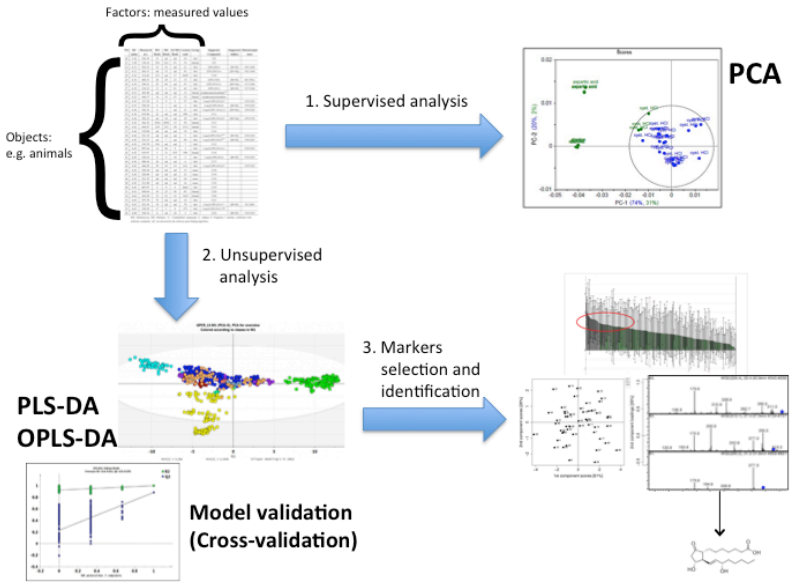

Figure 5. Example of data mining procedures. Data matrix is used to perform supervised (PCA) and unsupervised (PLS-DA, OPLS-DA) analyses, and from the models markers are selected and further identified.

Usually, in metabolomics PCA is used to find (dis)similarities between groups of observation in a dataset when variation within the groups is sufficiently less than variation between the groups, otherwise for classification, prediction and biomarkers selection supervised methods are preferred, mainly ones based on PLS (Projection to Latent Structures or Partial Least Squares) algorithms. PLS is a latent variable approach (i.e. a dimension reduction method) used to find the fundamental relations between two matrices (X and Y), and it is used to model the covariance structures in these two spaces. In other words, a PLS model will try to find the multidimensional direction in the X space that explains the maximum multidimensional variance direction in the Y space. PLS regression is particularly suited when the matrix of predictors has more variables than observations, and when there is multi-colinearity among X values. There are many variants of the PLS and corresponding algorithms, whose may have different

orthogonal conditions and different methods to estimate scores and loading matrices (Ren et al., 2015). One of the most used in metabolomics is PLS-DA (Nguyen and Rocke, 2002), where Y is a vector whose values represent class memberships. On the other hand, OPLS-DA, another popular method (Trygg and Wold, 2002), can be embedded as an integrated part of PLS modeling to remove systematic variation in X that is orthogonal to Y, thus also enhancing the interpretation of PLS.

PLS methods have a tendency to over-fit models to data, even identifying excellent class separation in completely random variables (Westerhuis et al., 2008), so validation is a critical step in ensuring model reliability. Model validation requires partitioning the data into a training set used to build a model and a validation set used to assess predictive ability of the model, where the validation set is in no way used to generate the trained model (Anderssen et al., 2006, Broadhurst and Kell, 2006). The quality assessment (Q^2, comprised between 0 and 1) statistic is typically reported as a result of cross-validation and provides a qualitative measure of consistency between the predicted and original data. Also the R^2 values (fitting values, comprised between 0 and 1) of a given model may be used to assess its degree of fit to the data (Gromski et al., 2015).

From multivariate analysis different visual plots are obtained, from whose the data could be analyzed. The scores scatter plot shows how the observations are distributed in the model and how they separate according to their dissimilarities, while the loadings scatter plot shows how the variables distribute in the model and how they contribute to describe the observations trend. For PCA, observations appear grouped in scores only when within-class variation is less than between-class variation, conversely, in PLS and OPLS the data tend to be over-fitted and the models could show class separation even with random data (Worley and Powers, 2013). For this reason, the use of PLS or OPLS models necessitates validation, as previously described. Due to the complementary nature of scores and loadings as explanations of the data matrix, the two may be used together. In the loadings plot, variables with loadings in a given position contribute to observations whose scores are found in a similar position in a scores plot, so the loadings closest to the scores are expected to have the highest contribution to class separation. One of the most useful method of variable selection is to use VIP (Variable Importance on Projection)-based models, from whose it is possible to extract a reduced subset of descriptive variables on the basis of their VIP values. In this case, only variables having VIP value over a specific threshold are considered as significant

descriptors for a specific observation group, and the threshold could be estimated by maximizing the $Q2_{validated}$ of the model (Peron et al., 2017).

2.2.5. Variables identification

On the basis of the analytical platform used, NMR or MS, variable identification can be performed in different ways. In both the cases, spectral signals can be identified by comparing them with reference data from the literature or with freely available web libraries of reference compounds (Wolfender et al., 2013). Among these latter, the most commonly used are Human Metabolome Database (HMDB, http://www.hmdb.ca; for both NMR and MS), Metlin (https://metlin.scripps.edu; for MS) and MassBank (http://www.massbank.jp; for MS). The second strategy is to identify the metabolites by studying the collected spectra. Concerning NMR, along with 1D NMR techniques, 2D NMR methods are required for identification (Wolfender et al., 2013). 2D NMR correlations between protons (^{1}H-^{1}H) or proton-carbons (^{1}H-^{13}C) can be useful to confirm whether the observed signals are derived from a single variable or not. Correlation spectroscopy (COSY) is a common experiment that shows which signals in a ^{1}H-NMR have mutual spin-spin couplings. The resulting spectrum has the conventional 1D NMR spectrum along the diagonal cross-peaks at chemical shifts that correspond to pairs of coupled nuclei. Another commonly used 2D correlation technique is total correlation spectroscopy (TOCSY), which provides information such as the unbroken chains of coupled protons in the same molecule (Wolfender et al., 2013). A direct correlation between carbons and protons can be detected by heteronuclear multiple quantum coherence (HMQC) or heteronuclear single quantum coherence (HSQC). In the resulting spectra, any carbon that is directly attached to a proton is detected, and so, the chemical shift of a ^{13}C connected to a specific proton can be obtained. Long-range correlations between carbons and protons can be observed by heteronuclear multiple bond correlation (HMBC) spectra, by which carbon-carbon correlations can be indirectly obtained with the aid of HMQC or HSQC. In addition, correlations between quaternary carbons such as carboxylic acid and nearby protons can be observed in the spectra. The long-range couplings in HMBC spectra can provide information on the connectivity between two moieties that are connected only by quaternary carbons or heteroatoms.

Concerning MS-based approaches, the first useful information that could be

obtained from the analysis is the molecular weight (MW) of the metabolites. Using High Resolution (HR) mass spectrometers, the accurate MW value could be obtained (i.e., accuracy to the forth decimal point). This data, together with the isotopic patterns, could be used to determine the molecular formula of the compounds. Currently, most HR-MS instruments (TOF, Orbitrap) routinely provide mass accuracy < 5 ppm, and this can reach 1 ppm or less on high-end FT-ICR-MS (Tsybin et al., 2011, Wolfender et al., 2013). An effective biomarker identification could be performed comparing HR experimental *m/z* values and calculated molecular formula with compound libraries and databases (HMDB, Metlin, MassBank). To obtain additional structural information, molecular ion species could be fragmented in tandem analyses using MS/MS, MS^n (using Ion-trap mass spectrometers) or MS^e experiments. For high-resolution measurements in MS/MS, either a hybrid instrument such as a Q-TOF-MS or an Ion Trap-MS such as an Orbitrap provides high quality spectra for metabolite identification. Concerning GC-MS, the electron impact MS spectra (EI-MS) that can be recorded are very reproducible, due to the high energy used in the ion source. This has the important advantage that large EI-MS databases, such as NIST database, can be used for spectra comparison and further peak annotation. In general, identification in GC-MS is also completed by the calculation of experimental measurement of retention index, such as Kovats index in different chromatographic columns.

In order to assess the identity of detected compounds, the best approach could be the use of different techniques. Furthermore, the identification could be confirmed by the comparison with authentic standards, when available, that can be added to the real sample in spiking experiments, allowing an unequivocal identification. However, this approach presents the strong drawback of the non-commercially availability of several standard compounds, furthermore it can be extremely expensive and time-consuming. Thus, for many applications, HR-MS coupled to fragmentation pattern analysis and NMR assignments can be considered sufficient to tentatively identify the metabolites.

3. Natural extracts used as nutraceuticals: focus on *Polygonum cuspidatum* Sieb. et Zucc., *Vacciunium macrocarpon* L. and green coffee (*Coffea canephora* Pierre ex Froehn.) beans

3.1. *Polygonum cuspidatum* Sieb. et Zucc.

3.1.1. Plant description

Figure 6. *Polygonum cuspidatum*.

Poligonum cuspidatum Sieb et Zucc. (Japanese knotweed, Figure 6) is an herbaceous perennial plant of the family Polygonaceae, native to Asia. *P. cuspidatum* appears as a shrub that could reach 1-3 m in height. The round stems are hollow and covered with scales, the shoots grow from spreading rhizomes that can reach 20 m in length. The leaves are broadly oblong-ovate or ovate-lanceolate, 8-15 cm long and 5-12 cm wide. The tips of the leaves are abruptly acuminate, while the bases of the leaves are truncate. The numerous, greenish-white flowers are borne in panicles from the upper axils. The flowers are functionally unisexual: each of the male and female flowers still have the complementary organs, but they are vestigial. The inflorescences of the male flowers tend to be upright, while those of the female flowers tend to be drooping. Flowers appear from August to September. The fruit are papery and winged, and are 6-10 mm long. These fruits contain black, smooth, shiny, 3-angled achenes that are 3-4 mm long (Seiger, 1996).

P. cuspidatum is frequently used as active ingredient of nutraceuticals and food supplements, due to its content in resveratrol. In fact, *P. cuspidatum* is considered one of the best sources of resveratrol, because it is a world-diffused invasive plant and it contains higher amounts of this compound than other plants or fruits (Wang et al., 2013).

3.1.2. Resveratrol: a multi-target phytocompound

Resveratrol (3,5,4'-trihydroxystilbene; structure reported in Figure 7) is a simple polyphenol that has received widespread attention because of its supposed beneficial health effects. It is found in grapes, berries and peanuts (Jasinski et al., 2013) and in various plants, and it is used as component of several nutraceutical products. Resveratrol exists in two isomers, *trans*-resveratrol and *cis*-resveratrol, and their glucosides, *trans*-piceid and *cis*-piceid, but actually, the most studied is the aglycone of *trans*-isomer, being the most stable (Caruso et al., 2004).

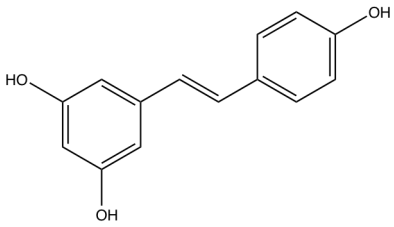

Figure 7. Resveratrol structure.

Scientific interest in resveratrol has grown since the late 1990s, when it was first demonstrated to prevent carcinogenesis in mice (Jang et al., 1997). Since then, its potential health promoting effects have been studied through numerous *in vitro* and *in vivo* experiments. A large number of pharmacological targets were discovered and numerous health benefits and disease-preventing activities, such as chemo-preventive (Chen et al., 2004) and anti-inflammatory (Tomé-Carneiro et al., 2012) ones, were related to resveratrol administration in animal models. Furthermore, many authors have considered resveratrol for its supposed usefulness in cancer, cardiovascular disease, ischemic injuries, and also as a possible enhancer of stress resistance. Finally, others considered this compound for its effects on the lifespan extension of various organisms from yeast to vertebrates (Baur et al., 2006, Pearson et al., 2008). Because of its antioxidant properties and its caloric restriction mimetic role (Pearson et al., 2008), also a preventive activity in many age-related and metabolic diseases has been attributed to resveratrol, most importantly in inflammation and obesity-related disorders such as diabetes and cardiovascular diseases (Baur et al., 2006, Howitz et al., 2003). However, the mechanism by which it exerts such a range of beneficial effects is not yet clear. A summary of the effects of resveratrol is reported in Figure 8.

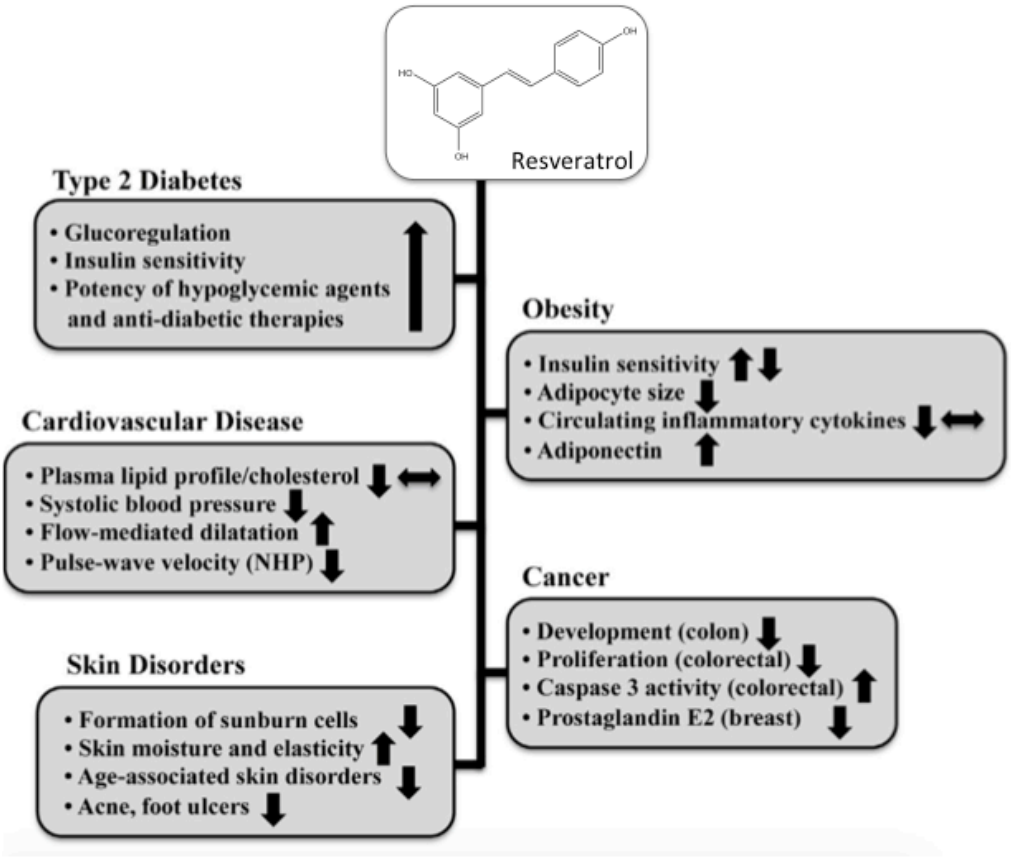

Figure 8. Summary of the *in vivo* effects of resveratrol. The symbol ↔ denotes lack of effect, and ↑ ↓ opposite action in some trials. The figure was re-adapted from (Novelle et al., 2015).

Several papers were published describing *in vitro* and *in vivo* effects of resveratrol, but doubts on its effectiveness are still present because of its low bioavailability. In fact, as several other polyphenols, it is absorbed at the intestinal level, but it is rapidly metabolized both in the intestinal lumen and in the liver to more hydrophilic derivatives, that are then excreted in the urine as glucuronides and sulfates. Moreover, gut microbiota transforms resveratrol in dihydroresveratrol and also this metabolite is absorbed and further metabolized and conjugated (Juan et al., 2010). Resveratrol could exert such different biological activities through multiple targets and multiple molecular mechanisms, thus metabolomics-based approaches offer the opportunity to get new information for the study of the bioactivity of this natural product (Sut et al., 2016).

A recent review summarized the results of *in vivo* trials reporting the effectiveness of resveratrol in clinical management of chronic diseases (Wahab et al., 2017). Concerning type 2 diabetes, resveratrol was reported to exert tissue-specific anti-hyperglycemic effect in insulin deficient states (Kang et al., 2012) and to induce an

improvement in insulin sensitivity and glucose-regulation in diabetic subjects (Hausenblas et al., 2015, Liu et al., 2014). Also chronic experiments were reported, in whose, for example, a 28-days consumption of 5 g daily of resveratrol by diabetic type-2 patients caused a significant reduction in insulin and glucose levels (Elliott et al., 2009). In another chronic study, a reduction of the level of oxidative stress markers as well as an amelioration of insulin resistance related to the activation of AKT signaling were observed in male diabetic patients (Brasnyó et al., 2011), after consumption of 5 mg of resveratrol twice a day, for one month. Concerning cardiovascular disorders (CVD), resveratrol was reported to decrease systolic blood pressure without affecting diastolic blood pressure, after daily treatment with 150 mg/day (Bhatt et al., 2012, Liu et al., 2015, Movahed et al., 2013). The mechanism of action was further supposed to be related to the improvement of endothelial function by stimulation of Ca^{2+}-activated potassium-channels and by increasing nitric oxide signaling (Magyar et al., 2012). Resveratrol was also reported to affect the levels of pro-inflammatory cytokines in plasma, as shown after supplementation of CVD patients with 350 mg/die dose of resveratrol for six months to one year. In this trial, a reduction of the production of IL-6, IL-10 and TNF (three of the main pro-inflammatory cytokines) was reported (Tomé-Carneiro et al., 2013). Similarly, other authors showed a decreased production of inflammatory biomarkers, such as high sensitivity CRP (hs-CRP), and increased circulating levels of various anti-inflammatory biomarkers, such as adiponectin (Militaru et al., 2013).

The effects of resveratrol supplementation were also studied in healthy subjects, also if in this case the number of clinical trials is scarce and sometimes controversial. Some authors reported that positive effects of resveratrol consumption are exerted only in pathological subjects, while no significant preventive activity was observable in healthy consumers. Thus, the metabolic condition of patients seems to state the effectiveness of resveratrol treatment (Wahab et al., 2017), although further investigations are required.

3.1.3. The anti-aging effects of resveratrol

The term aging refers to a gradual decline of all physiological functions (e.g. decreased kidney and heart capacities, lowered secretion of sexual hormones, bone and joint degeneration) that, in humans, starts after puberty. Still nowadays, the exact

mechanisms on the basis of aging are not known, but several factors play a concomitant role in the decrease of body functions. One theory states that aging could be related to two interconnected processes, referred as primary and secondary aging (Fontana and Klein, 2007). Primary aging consists in progressive decline of biological functions and of physical structure that occurs with advancing age, independent of other factors. On the other hand, secondary aging is related to the deterioration of organ structure and function that is mediated by diseases (e.g. diabetes or hypertension) or to harmful lifestyle (e.g. smoking or excessive alcohol intake) and environmental factors (Fontana and Klein, 2007).

Figure 9. Free radical oxidative stress and related dysfunctions.

As reported by Fontana and Klein (Fontana and Klein, 2007), several complex and interrelated factors are involved in aging mechanisms, including oxidative stress–induced protein and DNA damage in conjunction with inadequate DNA damage repair,

chronic inflammation states caused by increased adipokine and cytokine production, alterations in fatty acid metabolism, including excessive free fatty acid release into plasma with subsequent tissue insulin resistance, accumulation of cellular metabolic end-products that interfere with normal cell function and, finally, loss of post-mitotic cells, resulting in a decreased number of neurons and muscle cells as well as deterioration in structure and function of cells in all tissues and organs (Fontana and Klein, 2007).

Several studies highlight the implication of oxidative stress in the development of a variety of degenerative processes, diseases and syndromes, including, for example, atherosclerosis and cardiovascular diseases, chronic inflammatory diseases (e.g. rheumatoid arthritis or psoriatic arthritis), neurological disorders and cell mutations leading to cancer (Pham-Huy et al., 2008) (Figure 9). However, also normal metabolism leads to a mild oxidative stress. This could induce several damages to biomolecules and cells that, in some cases, cannot be totally repaired or removed by cells. A low percentage of metabolized oxygen produced by mitochondrial processes is converted to the superoxide ion, which can be converted subsequently to hydrogen peroxide, hydroxyl radical and eventually other reactive species, referred as Reactive Oxygen Species (ROS). These latter, including peroxides and singlet oxygen, can in turn generate free radicals that can cause damages to DNA and structural proteins (Beckman and Ames, 1998, Casteilla et al., 2002). Oxidative stress and related damages could be prevented in some extent with the regular intake of exogenous antioxidants from fruits and vegetables, such as vitamin C and E, carotenoids and polyphenols. In fact, their antioxidant properties (although largely investigated only *in vitro*) are often claimed to be responsible for the protective effects of these food components against several diseases (Rietjens et al., 2002). Resveratrol, that is frequently claimed to prevent aging (Baur et al., 2006), was reported to exert antioxidant activity *in vitro* and in animal models, although the molecular mechanisms on the basis of its activity are not yet established. As an example, in a study by Chen and collaborators was observed that resveratrol could alleviate juglone-induced lethal oxidative stress in *Caenorhabditis elegans*, and it extended the lifespan of the same species under conditions of acute oxidative damage and oxidative stress caused by high concentrations of glucose (Chen et al., 2013). However, no extension of the normal life span of *C. elegans* was observed either in liquid or solid growth media containing different concentrations of resveratrol only (Chen et al., 2013).

Another activity of resveratrol on the basis of its supposed anti-aging effects is related to the activation of a family of NAD^+-dependent deacetylases named sirtuins, whose main function might be to promote survival and stress resistance in times of adversity (Baur et al., 2006). Extra copies of the genes that encode for sirtuins are associated with extended lifespan in yeast, worms and flies (Kaeberlein et al., 1999, Rogina and Helfand, 2004, Tissenbaum and Guarente, 2001), and, in particular, activation of SIRT1 is related to survival and extended lifespan in mice. An *in vitro* screen for activators of SIRT1 identified resveratrol as the most potent of 18 inducers of deacetylase activity (Baur et al., 2006). *In vivo* studies showed an extension of the lifespans of *Saccaromyces cerevisiae*, *Caenorhabditis elegans* and *Drosophila melanogaster* after treatment with resveratrol, but only if the gene that encodes SIR2 was present in these organisms (Baur et al., 2006). In a more recent study by Park and collaborators, it was reported that resveratrol indirectly activates SIRT1 through a signaling cascade involving cAMP, Epac1 (a cAMP effector protein) and AMPK (Park et al., 2012). In mice on a high-fat diet, the same authors showed that administration of the PDE4 inhibitor rolipram induced similar beneficial metabolic effects to resveratrol, including prevention of diet-induced obesity (Guarente et al., 2012, Park et al., 2012).

3.2. *Vaccinium macrocarpon* Ait. (cranberry)

3.2.1. Plant description

Vaccinium macrocarpon Ait. (cranberry) is a low-growing, trailing, woody vine with a perennial habit (Figure 10). This plant is native to North America. It is characterized by vertical upright branches (uprights), whose are formed from the buds along the stems, usually 30 to 180 cm long. Leaves are tiny, 0.5 - 1.5 cm long, evergreen, thick, and oval/oblong in shape with entire margins. During the growing season, they are dark green and glossy, turning reddish-brown during the dormant season. The uprights have a vertical growth habit and form

Figure 10. *Vaccinium macrocarpon*.

the terminal buds that contain the flower buds. Most of the fruit is formed from the flowers on the uprights, with some berries arising from flowers on the runner ends. Flowers are borne singly in leaf axils on the basal portion of a newly expanded, terminal mixed bud. Flowers, white/pink colored, are inverted, have four petals and inferior ovaries. The fruit are bright red berries with waxy bloom at maturity, giving dark red to black appearance; color changes from green to white, then red during development (Brown and Mcneil, 2006) . 90% of the world's annual production comes from the states of Massachusetts, New Jersey and Wisconsin in the US, and 8% comes from the provinces of Quebec and British Columbia in Canada. The fruit is harvested in September and October (Guay, 2009).

3.2.2. Procyanidins in cranberry and their activity as anti-adhesive agents

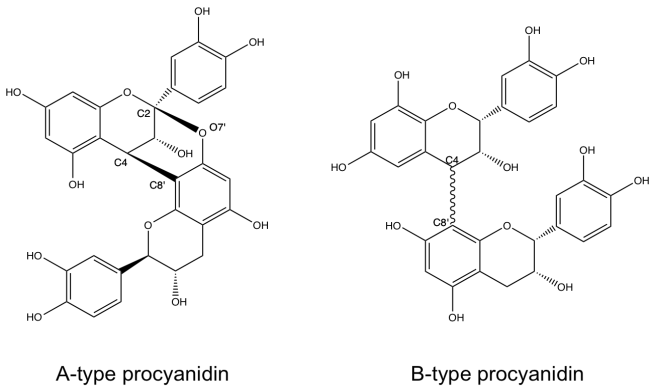

Figure 11. Structures of PAC-A and PAC-B.

Cranberry fruits are a good natural source of phenolic compounds, most importantly anthocyanins, flavones, phenolic acids and flavan-3-ols, namely procyanidins (PACs), (Feliciano et al., 2016). These latters could be monomers, dimers or higher order polymers, and in cranberry the main monomer is (−)-epicatechin. The building blocks of PACs can be condensed either via C4 β → C8' and C2 β → O7' interflavanoid bonds (A-type procyanidins) or via a single C4 → C8' interflavanoid bond (B-type procyanidins) (Figure 11). PAC with at least 1 A-type linkage (PAC-A2 or bigger) account for 51‑91% of total PACs in cranberry (Blumberg et al., 2013), hence this berry is considered one of the richest source of these compounds.

In nature, anthocyanidins and proanthocyanidins protect the plant from infections through their anti-adhesion properties. The class of PAC-A is considered to exert anti-adhesive activity against p-fimbriated uropathogenic bacteria, although their effectiveness as anti-adhesive agents is still under debate. Due to their peculiar composition, cranberry fruits are employed in the preparation of juices, sauces and dried

extracts, whose are used as active ingredients of food supplements or nutraceuticals for prevention and treatment of non-complicated urinary tract infections (UTIs) (Hisano et al., 2012).

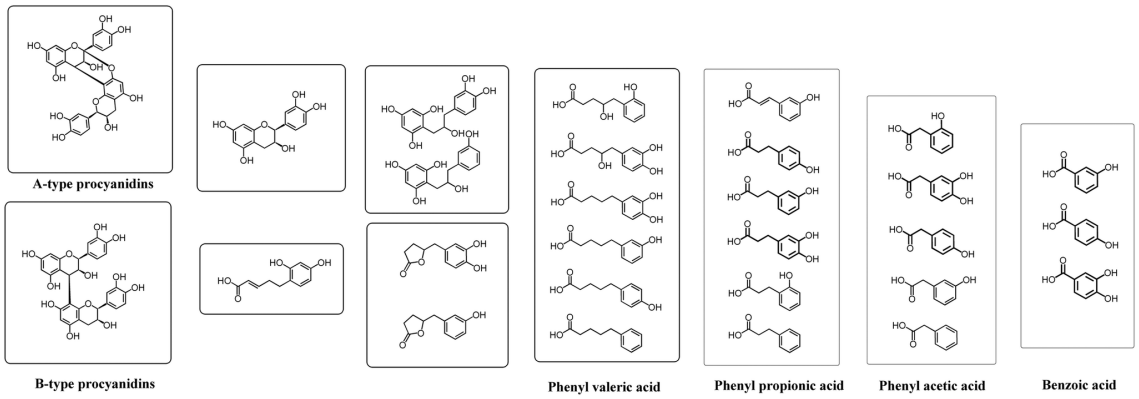

Figure 12. Examples of microbial degradation products of flavan-3-ol derivatives. Image taken from (Zhang et al., 2016).

The efficacy of cranberry in prevention and treatment of UTIs is supported by clinical evidence and was reported by several published papers; in many cases, authors have claimed its activity to oligomeric A-type procyanidins (Foo et al., 2000, Howell et al., 1998, Howell et al., 2005). Nevertheless, a comprehensive understanding of possible mechanisms of action is still lacking and, due to poor bioavailability of PACs, many doubts about their activity are emerging. In fact, intact oligomeric PACs are scarcely absorbed by the intestine, while large amounts of low molecular weight catabolites are absorbed after biotransformation by the colon microflora (Del Rio et al., 2013). The highest amounts of ingested flavan-3-ols are converted to phenolic and aromatic acids of microbial origin (phenols and benzoic, phenylacetic and phenylpropionic acids, valerolactone derivatives) (Zhang et al., 2016), that enter the bloodstream and are excreted in urine (Del Rio et al., 2013, Monagas et al., 2010). Examples of such metabolites are reported in Figure 12. Furthermore, several studies available in the literature report effective anti-adhesive activity of isolated PAC-A *in vitro* (Gupta et al., 2016, Polewski et al., 2016, Rodríguez-Pérez et al., 2016), without taking in account the whole composition of cranberry phytocomplex and all the factors that may positively or negatively contribute to its effects *in vivo*, mainly related to pharmacokinetic processes.

The mechanism exerted by PAC-A relies in hindering bacterial binding to urinary epithelium, thus promoting its elimination in urine. Uropathogenic bacteria bind to the

uroepithelium thanks to the presence of lipids and carbohydrates in lipopolysaccharides (LPS) and in the extracellular matrix that allow the binding of the bacteria to the epithelium by non-specific short-range interactions (van der Waals forces, H-bonds, hydrophobic interactions) (Johnson-White et al., 2006, Wojnicz et al., 2012). Furthermore, some bacteria could bind to specific carbohydrate ligands thanks to the presence of appendages on their surface, named fimbriae. PACs are big oligomers with a hydrophobic aromatic skeleton and hydrophilic -OH and –COOH residues, so they can interact with both hydrophobic and hydrophilic elements of bacteria. Experiments conducted *in vitro* show that cranberry constituents decrease hydrophobicity, thus decreasing the opportunity for short-range interactions, as well as reducing all other nonspecific interactions (Liu et al., 2008), hampering the binding capacity of bacteria to the epithelium.

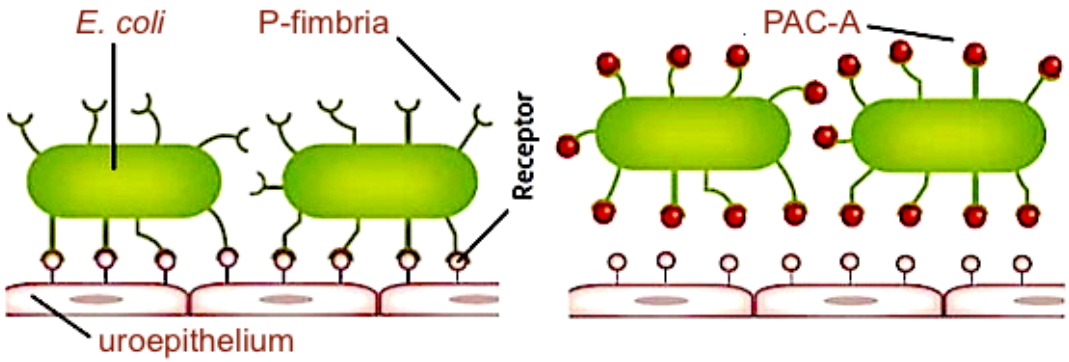

Figure 13. Interaction of P-fimbriated E. coli with uroepithelium and supposed mechanism of action of PAC-A.

The fimbriae present on the surface of uropathogenic bacteria allow the formation of specific bonds with carbohydrate moieties on the epithelium (Figure 13). In a paper by Liu and collaborators was shown that cranberry extract provoked a decrease in P-fimbriae length of a P-fimbriated *E.coli* strain (*E.coli* HB101pDC1), from 148 to 48 nm after cranberry juice treatment, which resulted in a reduced adhesion of bacteria to human kidney epithelial cells (Liu et al., 2008). The adhesion forces were measured by atomic force microscopy (AFM) and it was observed that they decreased from 9.64 to 0.5 nN after cranberry juice treatment (Liu et al., 2008). This phenomenon was due to conformational changes, meaning that the fimbriae were more compressed on the bacterial surface in the presence of cranberry and their binding activity was reduced.

Recently, many papers dealing with the use of cranberry in the treatment of UTIs

in human subjects were published, reporting positive activity results. Occhipinti and coll. studied the efficacy of supplementation with a commercially available product containing a 36% PAC-A cranberry extract (Occhipinti et al., 2016). The effects of treatment were monitored in a group composed by 30 female and 5 male volunteers, with at least 2 culture-documented symptomatic UTIs in the year prior to recruitment. The experiment took 7 days, during whom volunteers were given 1 capsule containing 112 mg cranberry extract, twice per day. Results showed that the administration of cranberry supplement significantly ameliorated UTI in the treated group compared to control. Furthermore, authors reported a significant variability in the effects of treatment related to the age of volunteers (Occhipinti et al., 2016). In another recently published study, the efficacy and tolerability of a treatment with cranberry extract were evaluated in patients with subclinical or uncomplicated recurrent UTI (r-UTI) (Singh et al., 2016). Treated group received one capsule twice a day of a commercially available supplement containing cranberry extract (60 mg PAC-A per capsule), for 12 weeks. 33% of patients in treated group developed r-UTI over 12 weeks, compared to 89% in placebo-treated group, showing that the overall efficacy and tolerability of treatment with cranberry supplement were superior to placebo in terms of reduced bacterial adhesion (Singh et al., 2016). Conversely, a meta-analysis reported in a recent review showed that, compared to control groups, cranberry products did not significantly reduce the occurrence of symptomatic UTI overall, and the efficacy of treatment was heterogeneous (Jepson et al., 2012). Hence, the contrasting opinions about the efficacy of cranberry in the treatment of UTIs underline the need for new investigations on the mode of action of this herbal remedy.

3.3. Green coffee beans (*Coffea canephora* Pierre ex Froehn.)

3.3.1. Plant description

Coffee plants (*Coffea* species) are member of the family of *Rubiaceae*. They are shrubs or small trees native to tropical and southern Africa and tropical Asia that are cultivated mainly for the production of the “beans”. In fact, the trees produce edible red or purple fruits (called cherries) that contain two seeds, the so-called "coffee beans". These latters are commonly used to prepare beverages after roasting, while the non-roasted (referred as green coffee beans) are frequently used in the preparation of food

supplements due to their beneficial effects. Coffee plants have bright green opposite leaves with smooth margins. The flowers grow in clusters on the axils of the leaves and are white colored. Fruits are born from them (Davis et al., 2006).

Figure 14. *Coffea arabica*.

Among the approximately 40 species of coffee plants, two are the most diffused: *C. arabica* and *C. canephora*. *C. arabica* (Figure 14) is a shrub which grows 9 to 12 m tall, but the height can be regulated in order to give more crops (up to 4.5 m). The plant stands out from a deep root system and has an open branching system. It has opposite, bright green leaves with elongated form (6–12 cm long and 4–8 cm broad). The blossom is small and white colored. The drupaceous fruit, dark green, glossy at first, becomes dark red when it ages. *C. arabica* is native to Ethiopia, where it grows in the wild at altitudes of about 1.000 – 2.000 m above sea level, although nowadays it is cultivated in several tropical and sub-tropical regions in the world at altitudes of about 1.300 – 2.800 m above sea level. On the other hand, *C. canephora* is a shrub that could reach approximately the same height of *C. arabica*, but it grows at lower altitudes, being cultivated at 700 m above sea level, and it needs higher temperatures (24-30 °C) (Davis et al., 2006). *C. canephora* is easier to cultivate than *C. arabica*, due to its higher resistance to diseases, especially in regard to *Hemileia vastatrix*, *Pellicularia koleroga* and nematodes (Santana-Buzzy et al., 2007). It is much more productive than the *arabica* variety, producing more oval seeds having higher caffeine content. *C. canephora* is native to West Africa, but as *C. arabica* is nowadays cultivated in many tropical areas of the world.

3.3.2. Green coffee and chlorogenic acids: their usage in weight-management

Green coffee bean extract (GCBE) is produced from coffee beans that have not been roasted, mainly obtained from *C. canephora* (Thom, 2007). Roasting can cause partial degradation of the phenylpropanoid esters of quinic acid (as chlorogenic acids, CGA) during high temperature treatments (Farah and Donangelo, 2006). CGA are esters of hydroxycinnamic acids, mainly caffeic, ferulic and p-coumaric acids, with (-)-quinic acid (Figure 15), and are considered the main constituents of GCBE (Farah and Donangelo, 2006).

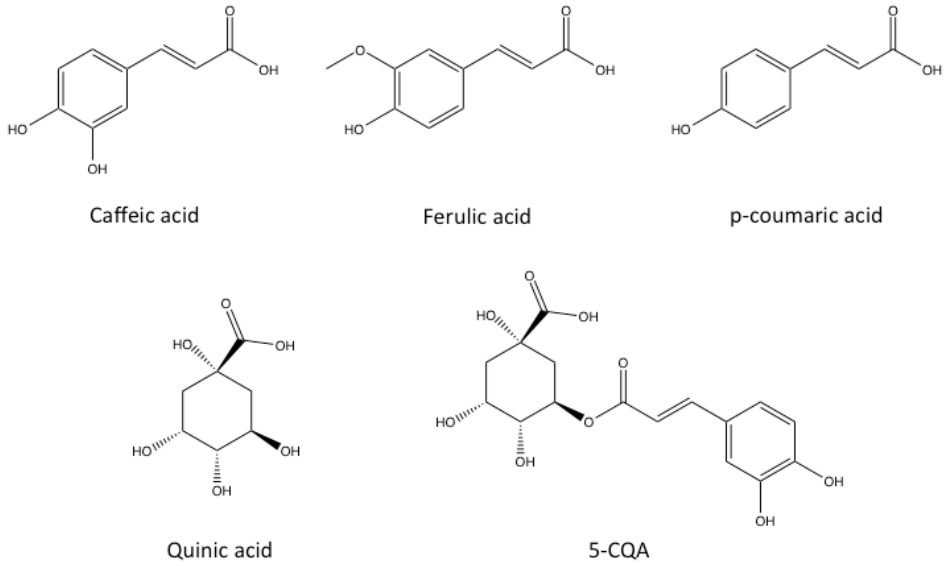

Figure 15. Structures of main CGA constituents in coffee; CQA: Caffeoylquinic acid.

Although the content of CGA may vary according to several factors as species and cultivar, degree of maturation, agricultural practices, climate and soil, the amounts of total CGA in regular green coffee beans, on dry matter basis, may vary from 4 to 8.4 % for *C. arabica*, and from 7 to 14.4 % for *C. canephora*, with some hybrids presenting intermediate levels (Farah and Donangelo, 2006). Examples of CGA present in coffee beans are reported in Figure 16. GCBE is supposed to exert weight loss and anti weight-gaining activities, whose are thought to be related to the high content of CGA. Among constituents of GCBE there is also caffeine, which is also considered to exert potential weight loss activity (Shimoda et al., 2006).

The effects of consumption of GCBE observed in animal models and in humans

are related to modulation of glucose metabolism, inhibition of fat accumulation, weight reduction and alteration of body fat distribution, exerted by CGA (Shimoda et al., 2006). Moreover, other proposed mechanisms are the reduction of the intestinal absorption of glucose (Shimoda et al., 2006) and the inhibition of the enzymatic activity of hepatic glucose-6-phosphatase (Arion et al., 1997, Shimoda et al., 2006). More recently, in an *in vivo* study CGA of green coffee were demonstrated to improve the blood lipid metabolism in rats by alleviating the levels of fatty acids and triglycerides and modulating the multiple factors in liver through AMP-activated protein kinase (AMPK) pathway, showing a possible mode of action of this ingredient in the management of obesity (Sudeep et al., 2016). The presence of caffeine can be considered useful because of its stimulant effect, hence it increases energy expenditure in humans, contributing to weight loss effects of coffee (Dulloo et al., 1989). Furthermore, other proposed mechanisms for caffeine effects on weight loss include increased thermogenesis, which consequently enhances lipolysis and lipid metabolism (Dulloo et al., 1989, Greenberg et al., 2006).

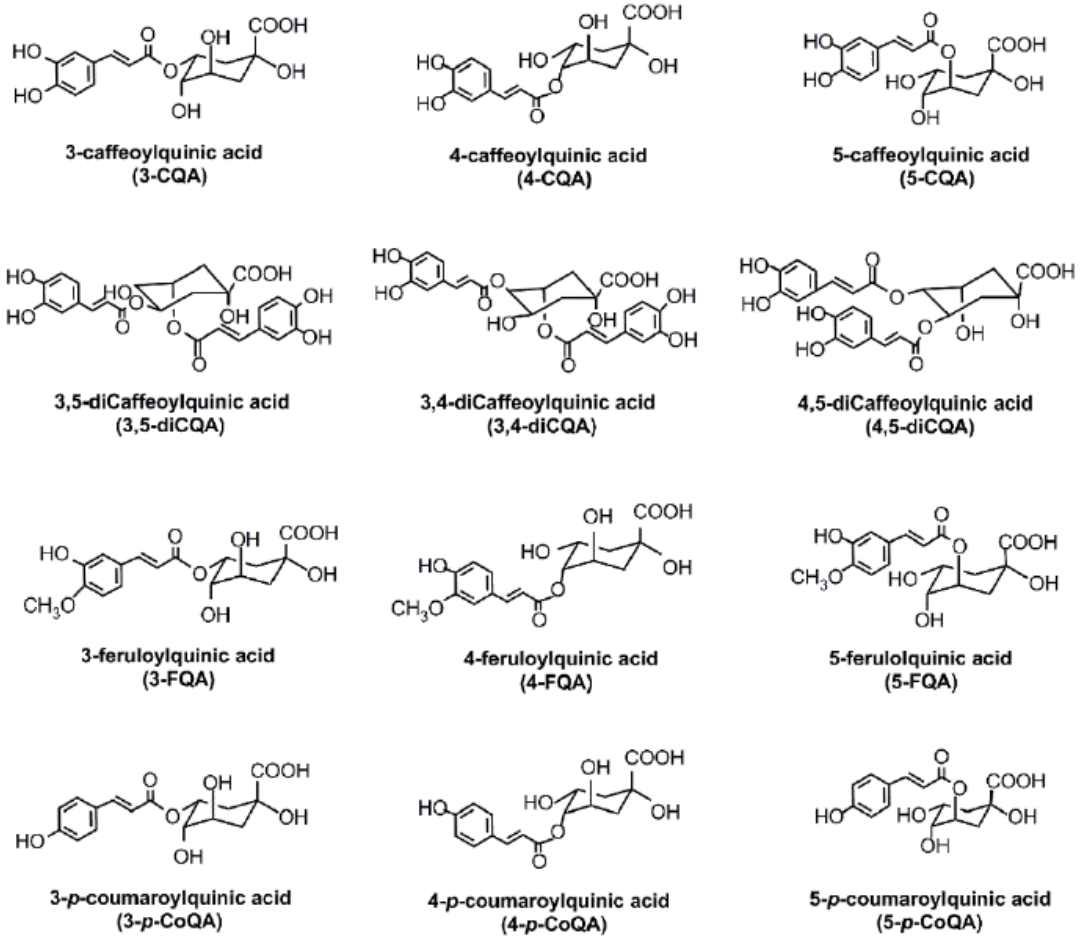

Figure 16. Structures of some typical CGA present in green coffee.

Food supplements containing GCBE are increasing in use to control weight gain, but the efficacy of these products is still under debate, due to contradictory data published in literature. In a review of 2013, Buchnan and Beckett indicated that a limited number of clinical studies were published related to the efficacy of GCBE, and that in most of them the clinical significance of the weight loss was minimal (Buchanan and Beckett, 2013). The same authors underlined the significant limitation of the reviewed studies as lack of blinding, direct comparisons, safety assessment, lack of comprehensive endpoints, very low sample size, and not inclusion of lifestyle modifications (Buchanan and Beckett, 2013). On the other hand, other papers reported moderate effects of GCBE on weight loss (Onakpoya et al., 2011, Quick and Kiefer, 2013, Shimoda et al., 2006). Revuelta-Iniesta and coll. compared the effects of a 2-weeks green coffee and black coffee consumption in 20 healthy subjects, observing that that systolic blood pressure were significantly reduced after green coffee, as well as body mass index and abdominal fat, with no changes in energy intake. Furthermore, cortisol/cortisone ratio in urine was reduced after green coffee, suggesting that green coffee can play a role in reducing cardiovascular risk factors overall (Revuelta-Iniesta and Al-Dujaili, 2014).

Other papers focused their attention only on CGA, without studying the effects of a treatment with a complete green coffee extract. For example, Cho and coll. compared the effects of treatment with CGA and caffeic acid (0.02% w/w) in obese mice (Cho et al., 2010). Both caffeic acid and CGA significantly lowered body weight, visceral fat mass and plasma leptin and insulin levels, compared to the high-fat control group. They also reported lowered triglyceride (in plasma, liver and heart) and cholesterol (in plasma, adipose tissue and heart) levels. Both treatments significantly inhibited fatty acid synthase, 3-hydroxy-3-methylglutaryl CoA reductase and acyl-CoA:cholesterol acyltransferase activities, while they increased fatty acid β-oxidation activity and peroxisome proliferator-activated receptors α (PPAR-α) expression in the liver compared to the high-fat group (Cho et al., 2010). Hence, despite the large diffusion of GCBE, studies are still needed to fully understand the possible mode of action and the role that this plant extract may have as treatment of obesity and its clinical relevance.

The green coffee extract may present some effect in the weight management but the evaluation of its effects and mode of action may be difficult due to the complex phytochemical composition and due to the multiple possible molecular targets of its constituents.

AIM OF THE WORK

The aim of the thesis project here presented was that to apply both LC-MS and NMR metabolomics approaches to study the *in vivo* bioactivity of selected natural extracts used as food supplements, namely *P. cuspidatum* (rich in resveratrol), cranberry (rich in type A procyanidins) and green coffee beans (rich in chlorogenic acids). The three extracts were selected on the basis of their commercial value as active ingredients of nutraceuticals and on the basis of the information regarding their *in vivo* activity actually available in literature.

In the first part of the work, the effects of *P. cuspidatum* dry extract were studied in healthy adult rats during a prolonged supplementation, using a combined ^{1}H NMR and UPLC-HRMS metabolomics approach. Rats were supplemented with a *P. cuspidatum* extract (100 mg/kg containing 20% of resveratrol) for 49 days and the variations of urinary composition were studied using ^{1}H NMR, UPLC-HRMS and multivariate statistical analysis. Because of the reported antioxidant activity of resveratrol, the urinary levels of 8-hydroxydeoxyguanosine (8-OHdG) and allantoin, two well-known oxidative stress biomarkers, were measured by targeted HPLC–MS/MS analyses. Monitoring the urinary amounts of allantoin and 8-OHdG is a straightforward strategy to assess the oxidative status of an organism, due to the non-invasive recovery of urine and the rapid sample preparation. Finally, due to the supposed "anti-aging" effects of resveratrol, mainly related to its caloric restriction mimetic role and to its antioxidant activity, multivariate models were designed in order to compare the aging effects between control and treated animals. Specific biomarkers were then selected and identified, and their amounts in urine were monitored along the experimental period.

Regarding cranberry, an UPLC-MS metabolomics approach was used to evaluate the mode of action of cranberry against uropathogenic *E. coli* in two independent experiments, using an animal model and enrolling healthy adult volunteers, respectively. The experimental design was similar for the two trials, and the aim was to observe if the results obtained from the first animal experiment were reproducible in humans, being cranberry supplements claimed for treatment of UTIs in human consumers. In the first one, healthy Sprague−Dawley rats were orally supplemented

with a standardized cranberry extract (100 mg/kg of extract, containing 15% of total PACs, every day) for 35 days, to mimic a prolonged consumption of cranberry by healthy subjects. The 24-h urinary outputs were collected weekly at days 0, 7, 14, 21, and 35 during the experiment, and samples were subjected to UPLC−MS analysis using an untargeted approach. In a second experiment on the same animal model, a single dose of cranberry (oral gavage of 100 mg/kg of extract containing 15% of total PACs) was administered to animals (n = 6) and the changes of urinary composition at 2, 4, 8, and 24 h after extract administration were monitored. Anti-adhesive properties of all the urine samples were studied. Furthermore, the markers related to cranberry intake were discovered using a multivariate data analysis approach. Finally, a specific chromatographic method was developed for the measurement of unmodified PAC-A in urine. In the experiment involving human volunteers, they consumed an oral sachet containing 360 mg of dry cranberry extract (fully characterized for the PAC and flavonoid contents) and 100 mg of quercetin, in order to administrate both the potential active class of constituents. Urine samples were collected at 2, 4, 6, 8 ad 24 hours after product administration and the anti-adhesive properties of urine samples were tested using an *in vitro* assay on *E. coli*. In order to correlate possible observed bioactivity with modification of urinary composition, LC-MS-based targeted and untargeted metabolomics approaches were used.

Finally, a clinical trial on a small number of healthy adult volunteers was performed to study the effects of a prolonged supplementation with GCBE. Ten healthy adult volunteers with normal body mass index (BMI), no metabolic, cardiovascular, overweight or obesity problems assumed 400 mg of dry GCBE daily for 30 days. The 24-hours urinary samples were collected weekly, and analyzed by LC-MS. Multivariate data analysis approaches were applied and also targeted analysis were performed to measure urinary oxidative stress biomarkers, namely allantoin and 8-hydroxydeoxyguanosine (8-OHdG), in order to assess the potential antioxidant activity of GCBE *in vivo*.

MATERIALS AND METHODS

1. *Polygonum cuspidatum*

1.1. Materials

P. cuspidatum dried extract was purchased from a local supplier. Resveratrol content was measured by HPLC-DAD and the amount found was 20.0 ± 0.1% w/w. Allantoin, 8-hydroxydeoxyguanosine (8-OHdG) and resveratrol standards were purchased from Sigma Aldrich. HPLC-grade acetonitrile and formic acid were purchased from Sigma Aldrich. Deionized water used in HPLC and UPLC analysis was filtered through a Milli-Q system equipped with a 0.22 μm cut-off filter (Millipore). Sodium 3-trimethylsilylpropionate-2,2,3,3,-d4 (TSP) was purchased from Sigma Aldrich.

1.2. Methods

1.2.1. Determination of resveratrol content in P. cuspidatum extract

Resveratrol content in *P. cuspidatum* extract was measured by HPLC-DAD. An Agilent 1260 HPLC system equipped with a diode array detector (DAD) was employed. Dried extract was exactly weighted (50 mg) and extracted with 25 mL of a mixture methanol/water 50/50. Extraction was performed on ultrasound bath for 10 minutes at room temperature. Sample was centrifuged and supernatant was collected in a flask. Solid matter was re-extracted with other 15 mL of solvent in the same conditions. After centrifugation liquids were pooled in a 50 mL volumetric flask and used for the HPLC analysis. Quantification was obtained on the basis of calibration curve, obtained analyzing standard resveratrol solutions in a concentration range of 1.4-140 μg/mL reading chromatograms at 325 nm. The equation of the obtained linear curve was $y = 83.706x + 5.6543$ (R^2: 0.9996).

1.2.2. Experimental design

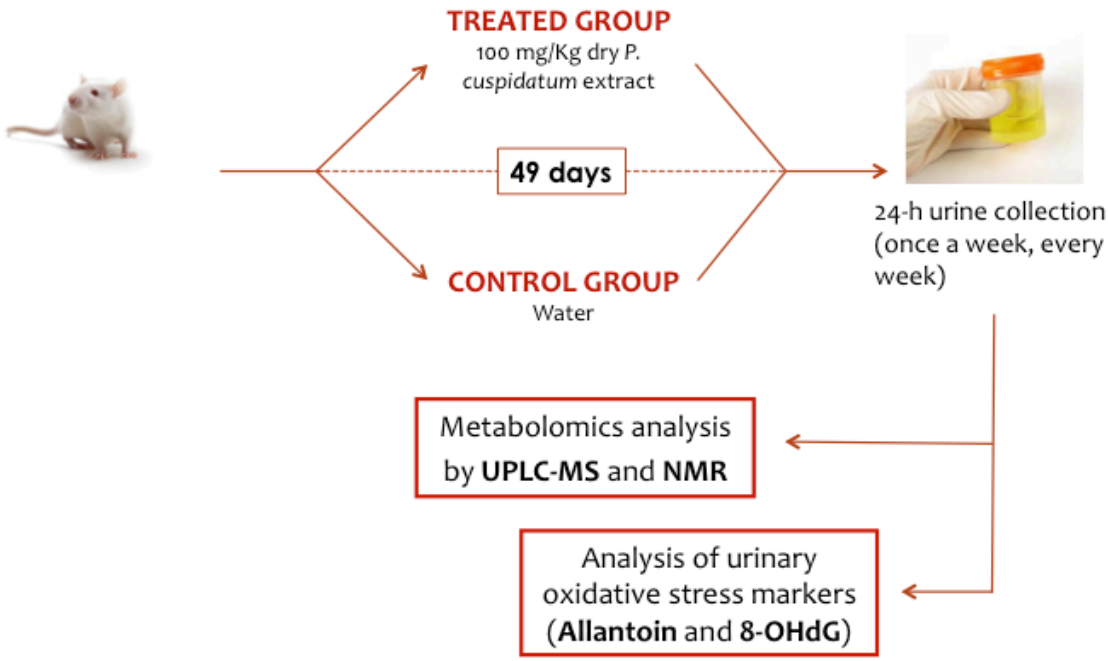

Figure 17. Scheme of *P. cuspidatum* experiment.

A longitudinal design was implemented to evaluate the effects of *P. cuspidatum* supplementation on the metabolite content of the 24-hours urine collected during the 49 days of experiment (Figure 17). The treated group received daily by gavage 100 mg/kg of *P. cuspidatum* extract suspended in water, while an equal dose of water was given to the control group. 24-hours urinary outputs were collected at day 0, 7, 14, 21, 28, 35 and 49 during the experiment and the samples were subjected to UPLC-HRMS and ^{1}H-NMR analysis. The *P. cuspidatum* dose (100 mg/kg) was selected on the basis of the resveratrol content (20.0 ± 0.1% w/w, corresponding to 20 mg/kg resveratrol), and considering previous published studies on rats showing both efficacy (Emlia Juan et al., 2002, Tiwari and Chopra, 2011) and safety of such resveratrol oral dose (Emlia Juan et al., 2002).

All animal procedures were approved and conformed to the directives of the Ethical Committee for animal experiments of the University of Padova (CEASA). Six male and six female Sprague-Dawley rats, 6 ± 2 weeks of age and weighing 108.0 ± 2.0 g, where used for the study. Animals were fed standard laboratory diet and water ad libitum and were maintained in a temperature- and photoperiod- controlled room (12-h light/dark cycle). Rats were divided randomly in a *P. cuspidatum* treated group (three

males and three females) and a control group (three males and three females). No differences were observed between control and treated groups at the beginning of the experiment on the basis of a preliminary metabolomics investigation. Rats were housed individually in metabolic cages for the collection of the 24-h urine outputs. Urine samples were then stored at -80 °C to avoid chemical degradation.

1.2.3. UPLC-HR-MS analysis of 24-h urine output

To obtain a metabolic profile of urine, a UPLC-QTOF HRMS full-scan method was used. An Agilent 1290 Infinity UPLC system equipped with a Waters Xevo G2 QTOF mass spectrometer was employed. The detector was equipped with an electrospray (ESI) ionisation source and was operating in positive resolution mode. The sampling cone voltage was adjusted to 40 V, the source offset to 80 V. The capillary voltage was adjusted to 1500 V. The nebulizer gas used was N_2 at a flow rate of 800 L/h. The desolvation temperature was 450 °C. The mass accuracy and reproducibility were maintained by infusing lock-mass (leucine–enkephalin, *m/z* 556.2771) thorough Lock-spray at a flow rate of 20 µL/min. Centroided data were collected for each sample in the mass range 50 – 1200 Da, and the *m/z* value of all acquired spectra was automatically corrected during acquisition based on lockmass. An Agilent XDB C-8 column (2.1 mm x 150 mm, 3.5 µm) was used as stationary phase. The mobile phase was composed of solvent A (acetonitrile with 0.1% formic acid) and solvent B (water with 0.1% formic acid). Linear gradients of solvents A and B were used, as follows: 0 min, 8% A; 14 min, 48% A; 16 min, 100% A; 17 min, 100% A; 17.5 min, 8% A; 24 min, 8% A. The flow rate was 200 µL/min and the injection volume was 1 µL. Collected urine samples were centrifuged at 13,000 rpm for 5 min before analysis and directly injected in the UPLC. Quality control (QC) samples (n=6) were prepared mixing 100 µL of each urine sample and used to monitor the UPLC-MS performances. Sequence of injection comprising QC, control and treated samples were randomized in order to avoid any bias due to samples order.

Centroided and integrated chromatographic mass data were processed by MarkerLynx Applications Manager version 4.1 (Waters) to generate a multivariate data matrix. A method for data deconvolution, alignment and peak detection was created. The parameters used were retention-time range 2.00–17.00 min, mass range 100–650 Da and mass tolerance 0.01 Da. Noise elimination level was set to 10.00, minimum

intensity was set to 15% of base peak intensity, maximum masses per RT were set to 6 and, finally, RT tolerance was set to 0.01 min. Isotopic peaks were excluded from analysis. A list of the ion intensities of each peak detected was generated, using retention time and the *m/z* data pairs as the identifier for each ion. The resulting three-dimensional matrix contained arbitrarily assigned peak index (retention time-*m/z* pairs), sample names (observations), and ion intensity information (variables). After the exclusion of the variables having more than 30% of missing data in both groups under investigation and log-transformation, the obtained data set composed of 483 time x mass variables was normalized by Median Fold Change normalization and mean centred.

1.2.4. ^{1}H-NMR 24-h urine analysis

Sample preparation was performed as described in (Beneduci et al., 2011), with minor modifications. Frozen urine samples were thawed in a fuming hood for 30 min and then 1 mL of urine was transferred into a 1.5 mL eppendorf vial. The pH value was adjusted to $1.2 \leq pH \leq 2$ by adding 3 M HCl (120 ± 80 µL) and the sample was centrifuged at 13,000 rpm for 10 min. To 700 µL of supernatant, 70 µL of 2 mM sodium 3-trimethylsilylpropionate-2,2,3,3,-d4 (TSP) in D_2O were added. Finally, 700 µL were transferred into an NMR tube and the pH was monitored by inspection of the chemical shift of the citrate signal and sometimes adjusted by adding 5 µL of 1 M NaOH or HCl. 2D-experiments were performed on a urine sample three times more concentrated, obtained by pooling several samples and partially evaporating the solvent.

All ^{1}H-NMR spectra were acquired on a Bruker Avance DMX600 MHz spectrometer equipped with a 5 mm TXI xyz gradient inverse probe at room temperature. 1D ^{1}H-NMR spectra were acquired with the NOESYGPPR1D pulse sequence and the following parameters: 64 scans; 32k data points; spectral width, 8389.26 Hz; relaxation delay, 2 s; mixing time, 50 ms. The ^{1}H-^{1}H NOESY spectrum was recorded with the NOESYGPPRTP pulse sequence, with a spectral window of 13 ppm in both dimensions, 2048×512 data points, 1.2 s relaxation delay, 0.6 s mixing time, and 256 scans. Prior to Fourier transformation, the FIDs were zero-filled to 64K points and an exponential line-broadening factor of 0.3 Hz was applied. All spectra were processed using ACD/NMR Manager 12.01 (Advanced Chemistry Development Inc.). Spectra were referenced to 0.0 ppm using the resonance of TSP and manually

corrected for phase and baseline distortions. Intelligent bucketing was applied to the region between 0.6 ppm and 9.5 ppm excluding the regions where resveratrol derivatives (6.24-7.50 ppm, 5.10-5.22 ppm, 4.10-4.26 ppm, 3.56-3.96 ppm, 2.74-2.82 ppm) and water (4.70-4.95 ppm) resonate. Total sum normalization was applied to compensate for differences in overall concentration between individual urine samples. The obtained data set composed of 229 variables was mean centered and Pareto scaled.

1.2.5. Statistical data analysis

Data modelling was performed by applying multivariate techniques based on projection. Specifically, Principal Component Analysis (PCA) was used for exploratory data analysis and for highlighting the presence of outliers while Projection to Latent Structures by partial least squares regression (PLS) was applied to investigate the relationships between the metabolite content of the urines collected during the experiment and the time of treatment and type of diet. To perform an efficacy data modelling able to extract the whole information contained into the collected data, a design matrix supporting an interaction model including time, treatment and time x treatment effects, was explicitly considered. The measured variables and the design matrix were used as X-block and Y-block, respectively, in the PLS regression. N-fold full cross-validation with different values of N (N = 6,7,8) and permutation test on the responses (1000 random permutations) were performed, in order to avoid over-fitting and prove the robustness of the obtained models. The number of components of the PLS models was estimated on the basis of the first maximum of Q2 calculated by 7-fold full cross-validation ($Q2_{7\text{-fold CV}}$) under the constraint to pass the permutation test on the responses. To better interpret the obtained model, a new method for rotating the PLS model, called post-transformation of PLS2 (ptPLS2), was applied (Stocchero and Paris, 2016). The main advantage to use the post-transformation of the PLS model is the possibility to obtain a new model where the structured variation of the X-block discovered by PLS is decomposed into two blocks, corresponding to the variations correlated (predictive part of the model) and orthogonal (non-predictive part) to the Y-block. The post-transformed model maintains the same power in prediction of the PLS model but simplifies model interpretation because the dimension of the predictive latent space is usually lower than that of the whole latent space discovered by PLS.

Recently, stability selection was introduced in metabolomics to avoid false

discoveries due to overtraining (Wehrens et al., 2011). The central idea of stability selection is that real differences or effects should be present consistently, and therefore should be found even under perturbation of the data by subsampling or bootstrapping. Thus, stability selection by Monte-Carlo subsampling using PLS VIP-based as regression technique (Wehrens et al., 2011) was used for identifying putative markers. Specifically, 200 random subsamples were extracted by Monte Carlo sampling of the collected urine samples (with prior probability of 0.70), and then PLS VIP-based applied to each subsample, obtaining a set of 200 regression models. Within this set of PLS VIP-based models, variables related to the effects of time and/or treatment were identified as the most frequently selected variables. The threshold of the VIP score to use in variable selection within PLS VIP-based was estimated by maximizing the $Q2_{7\text{-fold CV}}$. As a result, a small number of metabolites changing during the experiment was extracted and the behavior of each single metabolite was studied by linear mixed-effects model for longitudinal studies (Chong and Jun, 2005).

PCA was performed using SIMCA 13 (Umetrics, Umea, Sweden) while the platform R 3.0.2 (R Foundation for Statistical Computing) was used for statistical data analysis on single variable, to build the ptPLS2 model and to perform Monte-Carlo stability selection.

1.2.6. Focus on the effects of P. cuspidatum supplementation on rat aging

Data regarding urine samples collected at day 0 of the experiment (beginning) and at day 49th of the supplementation period (end) were isolated from the dataset described in Paragraph 1.2.3., and used to compare aging-related composition changes of urine collected from control animals and treated ones. Using SIMCA 13 (Umetrics, Umea, Sweden), OPLS-DA models comparing control urine samples at day 0 and day 49th, treated urine samples at day 0 and day 49th, and control and treated urine at day 49th were created. N-fold full cross-validation and permutation test on the responses were performed using the same software, as previously described. Descriptive variables were selected on the basis of their significance value ($p<0.05$) and on the basis of their VIP-value (VIP>2). Only significant variables that were detectable in both the OPLS-DA comprising controls and treated animals separately were considered as descriptive and further tentatively identified, as described in the previous sections. The urinary excretion of N-Methyl-2-pyridone-5-carboxamide and phenylacetylglycine, that were

identified as aging markers from the obtained multivariate models and were previously reported as markers of aging in rats (Slominska et al., 2004, Zhang et al., 2012), was monitored in both treated and control groups throughout the supplementation period, extracting the respective AUC values from the dataset and normalizing the data with urinary creatinine. The plots obtained from the two groups were finally compared.

1.2.7. Targeted analysis of allantoin and 8-OHdG in 24-h urine samples

Allantoin and 8-OHdG were quantified in urine samples from both treated and control rats using appropriate HPLC-MS/MS methods. A Varian 212 HPLC system equipped with a Varian MS 500 IT detector was used for HPLC-ion trap mass spectrometry. A Phenomenex Kinetex EVO C-18 column (3 mm x 100 mm, 5 μm) was used as stationary phase. The detector was equipped with an ESI source and was operating in positive resolution mode. For allantoin quantification, the operating parameters used were as follows: nebulizing gas, nitrogen; nebulizing pressure, 35.0 psi; needle voltage, 4500 V; capillary voltage, 600.0 V; drying gas temperature, 350 °C; drying gas pressure, 10.0 psi. The mobile phase was composed of solvent A (acetonitrile with 0.1% formic acid) and solvent B (water with 0.1% formic acid). Linear gradients of A and B were used, as follows: 0 min, 15% A; 7 min, 100% A; 7.06 min, 15% A; 10 min, 15% A. The flow rate was 200 μL/min and the injection volume was 10 μL. An MS^n experiment was performed, monitoring the fragmentation of allantoin precursor ion ($[M+H]^+$, *m/z* 159) in the product ion mass range 65-169 Da. Allantoin was finally quantified on the basis of its major fragment (*m/z* 116) using a standard titration curve obtained by eluting 0.3 - 1 μg/mL allantoin solutions in water ($y = 97216x + 51629$; $R^2 = 0.9833$). LOD and LOQ were 0.1 and 0.5 ng/mL, respectively.

For 8-OHdG quantification, the operating parameters used were as follows: nebulizing gas, nitrogen; nebulizing pressure, 20.0 psi; needle voltage, 4500 V; capillary voltage, 600.0 V; drying gas temperature, 280 °C; drying gas pressure, 15.0 psi. The mobile phase was composed of solvent A (acetonitrile with 0.5% formic acid) and solvent B (water with 0.1% formic acid). Linear gradients of A and B were used, as follows: 0 min, 10% A; 1 min, 10% A; 10 min, 60% A; 12 min, 10% A; 16 min, 10% A. The flow rate was 200 μL/min and the injection volume was 10 μL. An MS^n experiment was performed, monitoring the fragmentation of 8-OHdG precursor ion ($[M+H]^+$, *m/z* 284) in the product ion mass range 155-175 Da. 8-OHdG was finally

quantified on the basis of its major fragment (*m/z* 168) using a standard titration curve obtained by eluting 3 - 100 ng/mL 8-OHdG solutions in water (y = 48.853x + 1002.5; R2 = 0.9981). LOD and LOQ were 1 and 5 ng/mL, respectively.

Before analyses, urine samples were centrifuged at 13,000 rpm for 5 minutes and supernatants were directly injected in the instrument.

2. *Vaccinium macrocarpon* (Cranberry)

2.1. Materials

The dry cranberry extract used in animal experiments and the supplement used in the human trial were purchased from a local market. The powder content of each sachet used in the human trial was 500 mg, 180 mg of which was dry cranberry extract and 100 mg was quercetin. Standard PAC-A2 (Extrasynthese, France), Sephadex LH-20 and epigallocatechin gallate were purchased from Sigma Aldrich. HPLC-grade acetonitrile and formic acid were purchased from Sigma Aldrich. Deionized water used in HPLC and UPLC analysis was filtered through a Milli-Q system equipped with a 0.22 μm cut-off filter (Millipore).

2.2. Methods

2.2.1. Animal experiment

2.2.1.1. Profiling of PACs in cranberry extract

30 mg of dry cranberry extract were suspended in 5 mL of an acetone/water (70/30% v/v) mixture and were extracted using an ultrasound bath for 15 minutes. Sample was centrifuged at 3,500 rpm for 10 minutes and liquid was collected in a flask. The solid residue was re-extracted with a further amount of 5 mL of solvent and sonicated for further 15 minutes. Extraction was repeated 4 times. Liquids were collected in round bottom flask and volume was reduced under vacuum at 30°C to 5 mL. Liquid was then transferred to a volumetric flask and volume was adjusted to 25 mL with methanol.

Analyses of PAC-A and PAC-B were performed by HPLC-MS. The chromatographic system was composed by a Varian 212 binary pump, coupled to a Varian 500-MS Ion Trap mass spectrometer (MS). A Tosoh TSKgel Amide-80 column (3,5 μm, 2.1 x 150 mm) was used as stationary phase. 0.5% formic acid in acetonitrile (A) and 2% formic acid in water (B) were used as mobile phase. Gradient elution was as follows: starting with 90% A, then in 20 min to 80% A, isocratic conditions (80% A) until 25 min, then to 35% A in 45 min and isocratic (35% A) until 51 min. Finally, column was left to riequilibrate to the initial conditions for 9 minutes. Flow rate was 200 μL/min and injected volume was 10 μL. The MS parameters were as follows: spray chamber temperature, 50°C; nebulizer gas pressure, 25 psi; drying gas pressure, 25 psi; drying gas temperature, 385°C; needle voltage, ± 4500 V; spray shield voltage, 600 V. Mass spectra were acquired in negative mode in the spectral range 150-2000 Da. For PAC-A, $[M-H]^-$ ions at *m/z* 575, 863 and 1151 were monitored for dimers, trimers and tetramers, respectively. For PAC-B, $[M-H]^-$ ions at *m/z* 577, 865 and 1153 were monitored for dimers, trimers and tetramers, respectively. Being other trimeric or tetrameric procyanidins not commercially available, PAC-A2 was used as standard compound for quantitative purposes. Calibration curve was built in the range 1-20 μg/mL, and all samples and calibration solutions were analysed in triplicate. The obtained linear curve had function $y = 0.6915x$ ($R^2 = 0.9989$), showing a good linear response. Limit of detection (LOD = 0.45 μg/mL) and limit of quantification (LOQ = 0.7 μg/mL) were determined following USP methods. For LOD, samples with known concentration of PAC-A2 were analysed and minimum concentration at which analyte could be reliably detected was established. On the other hand, LOQ was established by visual evaluation.

2.2.1.2. Animal procedures

All experimental protocols were approved by the Animal Care and Use Ethics Committee of the University of Padova (number 3112017PR) under license from the Italian Ministry of Health and they were in compliance with the National and European guidelines for handling and use of experimental animals. In the first experiment (Figure 18), twelve healthy Sprague-Dawley rats (six males and six females) of 7 ± 2 weeks of age and weighing 173.0 ± 3.1 g, were used. Animals were fed standard laboratory diet and had free access to water during the experiments. Rats were maintained in a

temperature- and photoperiod- controlled room (12-hrs light/dark cycle). Rats were divided randomly in a cranberry treated group (three males and three females) and a control group (three males and three females). No differences were observed between control and treated groups at the beginning of the experiment. The treated group received by intra-gastric gavage a daily dose of 100 mg/kg body weight of cranberry extract in 2 mL of water for a total of 35 days. The control group received daily an identical volume of water by intra-gastric gavage. Rats were housed individually in metabolic cages and 24-hrs urine output was collected and stored at -80 °C to avoid chemical degradation. Urine samples were collected on days 0, 7, 14, 21 and 35 during the experiment and further subjected to UPLC-ESI-QTOF analysis.

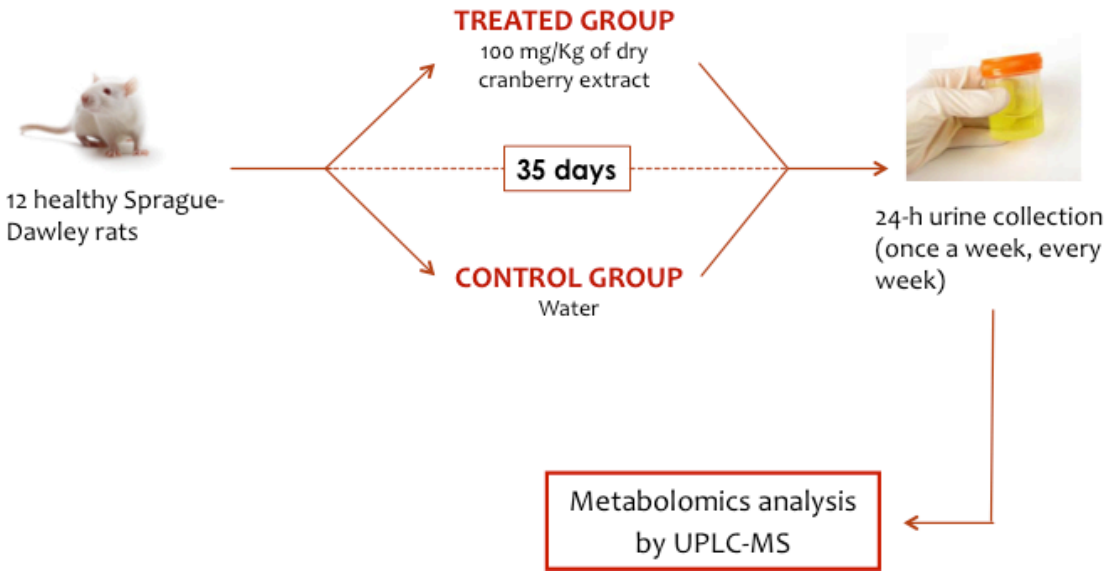

Figure 18. Scheme of cranberry longitudinal experiment.

A second experiment was performed (Figure 19), involving six healthy Sprague-Dawley rats (three males and three females), 6 ± 1 weeks of age and weighing 125 ± 7.4 g. They were orally given a single dose of 100 mg/Kg of 15% PACs cranberry extract suspended in 1 mL of water by gavage. Before treatment, animals were individually positioned in metabolic cages to collect 24-h control urine. After cranberry administration, urinary outputs at 2, 4, 6, 8 and 24 hours were collected following the same procedure. Urine samples were then stored at -80 °C until used for UPLC-ESI-QTOF and HPLC-MS/MS analyses and for adhesion studies, to avoid chemical degradation.

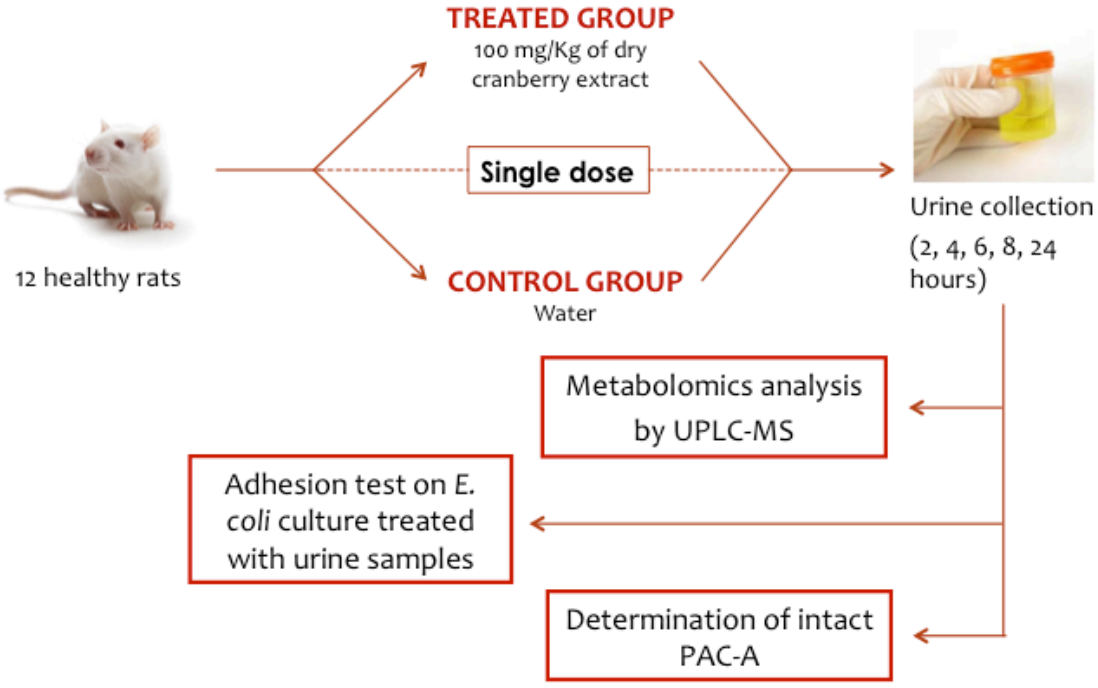

Figure 19. Scheme of the "single intake" cranberry experiment.

2.2.1.3. Profiling of 24-h urine by UPLC-ESI-QTOF

To obtain a metabolic profiling of urine, a UPLC-HRMS full-scan method was used. An Agilent 1290 Infinity UPLC system equipped with a Waters Xevo G2 Q-TOF MS was employed. The detector was equipped with an ESI ionisation source and was operating in both positive and negative resolution mode. Instrument settings and chromatographic conditions were the same reported in Paragraph 1.2.3. Collected urine samples were centrifuged at 13,000 rpm for 10 minutes prior to analysis and directly injected in the UPLC. Quality control samples (QC, n=6) were prepared mixing 100 µL of every collected urine sample and they were centrifuged at 13,000 rpm for 10 minutes. Sequence of injection comprising pool, control and treated samples were randomized in order to avoid any bias due to samples order.

2.2.1.4. Multivariate data analysis

Centroided and integrated chromatographic mass data were processed by MarkerLynx Applications Manager version 4.1 (Waters) to generate a multivariate data matrix. An appropriate method for data deconvolution, alignment and peak detection

was used, as previously described in Paragraph 1.2.3. Data modelling was further performed using SIMCA 13 software (Umetrics), applying multivariate techniques based on projection. PCA was used for exploratory data analysis and for identification of outliers. PLS-DA was applied to investigate the relationships between urine composition and cranberry administration. The measured variables and the matrix were used as X-block and Y-block, respectively, in the PLS regression. N-fold full cross-validation with different values of N (N = 6,7,8) and permutation test on the responses (999 random permutations) were performed. Biomarkers were identified as previously reported in *P. cuspidatum* protocol.

2.2.1.5. Profiling of urinary outputs at 2, 4, 8 and 24 hours after cranberry administration

To obtain a metabolic profiling of urine collected at 2, 4, 8 and 24 hours after cranberry administration, UPLC-ESI-QTOF full-scan method was used. The instrumentation employed was the same described for the profiling of 24-h urine, as well as the settings of the ESI-QTOF mass detector. An Agilent Zorbax Rapid Resolution High Definition (RRHD) SB-C18 column (2.1 mm x 50 mm, 1.8 μm) was used as stationary phase and the mobile phase was composed of solvent A (acetonitrile with 0.1% formic acid) and solvent B (water with 0.1% formic acid). Linear gradients of solvents A and B were used, as follows: 0 min, 2% A; 1 min, 2% A; 8 min, 55% A; 10 min, 55% A; 10.5 min, 98% A; 11.5 min, 98% A; 12 min, 2% A and isocratic for 1 minute. The flow rate was 300 μL/min and the injection volume was 1 μL. As for 24-h urine analysis, samples were pre-treated in the same way and QC samples (n=5) were prepared and randomly injected in the UPLC.

Data extraction was performed as previously described, using MarkerLynx Applications Manager version 4.1 (Waters) and setting time-range between 1.00–10.00 min; the obtained matrix was then processed using SIMCA 13 software.

2.2.1.6. HPLC-MS/MS determination of oligomeric PAC-A in treated animal's urine

Urine samples were purified prior to analysis to isolate PACs from lower molecular weight polyphenols and increase sensitivity of mass spectrometric analysis. 1

mL of urine samples were added with 10 μL of a 10 μg/mL epigallocatechin gallate solution (equivalent to 100 ng of epigallocatechin gallate), used as internal standard (ISTD). Samples were loaded on a 20 x 3 cm glass column pre-packed with 400 mg of Sephadex LH-20, which was left to equilibrate in 70% MeOH in water for 30 min prior to sample loading. Loaded resin was then washed with 4 mL of 70% MeOH in water to elute low molecular weight polyphenols. Subsequently, the resin was washed with 5 mL of 70% acetone in water to elute PACs. Acetone fraction was evaporated under vacuum to dryness and residue was dissolved with 100 μL of methanol for analysis. Calibration curves using different amount of ISTD and PAC-A2 were obtained, namely adding to 1 mL of urine 100 ng of ISTD and 2, 4, 8, 10, 20 ng of PAC-A2. Urine samples with added ISTD were purified through Sephadex as described and final solutions used to build a calibration curve. Calibration curve (y = quantity of ISTD/quantity of PAC; x = area ISTD/area PAC) was the following: $y = 0.3683x$ ($R^2 = 0.9991$). LOD and LOQ were 0.2 and 0.4 ng/mL, respectively, and they were established using USP methods, as previously described.

An Agilent 1260 Infinity HPLC binary pump coupled to a Varian 320-MS TQD MS was employed. The detector was equipped with an ESI ionisation source and was operating in negative mode. The MS conditions were as follows: spray chamber temperature, 50°C; nebulizer gas pressure, 25 psi; drying gas pressure, 25 psi; drying gas temperature, 385°C; needle voltage, ±4500 V; spray shield voltage, 600 V. Mass spectra were acquired in negative mode in the spectral range 150-2000 Da. MRM traces were used for quantitation purposes. For PAC-A dimer, the *m/z* transition 575-285 was monitored, corresponding to the fragmentation of $[M-H]^-$ parent ion. *m/z* transitions monitored for trimers and tetramers were 863-289 and 1151-285, respectively, corresponding to the fragmentations of $[M-H]^-$ parent ions. A Tosoh TSKgel Amide-80 column (2.1 mm x 150 mm, 3.5 μm) was used as stationary phase. The mobile phase was composed of solvent A (0.1% formic acid in water) and solvent B (0.1% formic acid in acetonitrile). Linear gradients of solvents A and B were used, as follows: 0 min, 8% A; 14 min, 48% A; 16 min, 100% A; 17 min, 100% A; 17.5 min, 8% A; 24 min, 8% A. The flow rate was 200 μL/min and the injection volume was 10 μL.

2.2.1.7. Microbiology and in vitro adhesion assays

A freshly isolated uropathogenic P-fimbriated *E. coli* from a woman with urinary tract infection (UTIs) was obtained from University Hospital of Padova. The microbe was characterized by biochemical and molecular tests and then used in the adhesion assays. A single colony was inoculated in trypticase soy broth at 37 °C with shaking at 200 r.p.m. After 16 hours the microbes were collected by centrifugation, resuspended in fresh sterile trypticase soy broth and *E. coli* concentration adjusted to of 10^7 CFU/mL. Then bacteria were incubated in urine samples, both from control or after consumption of cranberry extract, at 10^5 CFU/mL final concentration for four hours at 37 °C. Bacteria were then harvested from the urines by centrifugation (2,500 rpm x 10 min), suspended in DMEM at a concentration of 5 x 10^8 CFU/ml and quantified by vital count assay seeding on LB agar plates. The remaining microbes were added to human intestinal epithelial cells (HT-29 cells, from ATCC) confluent monolayers (MOI 1:10) cultured in DMEM supplemented with 10% heat inactivated faetal calf serum. Tissue cultures were incubated with *E. coli* at 37 °C. After 30 minutes the culture medium was removed and monolayers were carefully washed three times with 2 ml of warm sterile DMEM to remove non adhering microbes. Following the last washing step, to quantify the adhering *E. coli* to HT-29 cells, monolayers were detached, collected and lysed. Living bacteria were enumerated by vital count assay. Serial dilutions were seeded on LB agar plates, incubated at 37 °C for 24 hours and CFU enumerated.

Adhesion data were given as mean ± standard error of the mean (SEM), and one-way analysis of variance followed by Bonferroni multicomparison tests was used to compare data using GraphPad Prism 3.03 software (GraphPad, San Diego, CA). A p-value of <0.05 was considered statistically significant.

2.2.2. Human pilot trial

2.2.2.1. Phytochemical composition of the cranberry-containing product

Five hundred milligrams of supplement were suspended in 15 mL of an acetone/water (70/30% v/v) mixture and were extracted using an ultrasound bath for 10 minutes. The extraction protocol was the same previously described in Paragraph 2.2.1.1.

Analyses of PAC-A and PAC-B were performed by HPLC-MS^n, as previously described. In this case, the PAC-A2 calibration curve was: $y = 0.7143x + 0.012$ ($R^2 = 0.9988$).

For flavonoids analysis, an Agilent 1260 HPLC system coupled to a DAD and to a Varian 500-MS IonTrap detector was used. An Agilent XDB C-8 (3.5 µm, 3 x 150 mm) column was used as stationary phase. For elution, acetonitrile (A) and water with 0.1 % formic acid (B) were used. Gradient started with 90% B and in 20 minutes decreased to 10% B, then isocratic conditions were kept up to 25 minutes. After the column separation, eluate was splitted to DAD and to MS detectors. DAD traces were collected at wavelength of 280 and 350 nm, UV spectra were acquired in the range 190-400 nm. Quercetin was used as reference standard for aglycones, while rutin was used as reference compound for glycosylated derivatives. Calibration curves were built in the range 1-1000 µg/mL, and all samples and calibration solutions were analysed in triplicate. The obtained linear curves were $y = 0.7143x + 0.012$ ($R^2 = 0.9988$) for quercetin, and $y = 0.4143x + 0.007$ ($R^2 = 0.9998$) for rutin. Both analytes showed a good linear response in the considered concentration range. Limits of detection and quantification for both the analytes were LOD = 0.5 µg/mL and LOQ = 1.5 µg/mL and were determined following USP method. Peaks were identified on the basis of MS fragmentation patterns. MS spectra were acquired in the range 50-2000 Da in negative ion mode using tdds® utility, which allowed the observation of fragmentation pathways.

For quercetin determination, the same HPLC-MS/MS system was used but an Agilent Poroshell EC 120 C-18 (3.5 µm, 2.1× 50 mm) was used as stationary phase. Mixture of 0.1% formic acid and acetonitrile were used as mobile phase, with the following gradient: 0 min, 10% A; 6 min, 80% A; 8 min, 80% A; 10 min, 10% A; 13 min, 10% A. The flow rate was 200 µL/min and the injection volume was 10 µL. For quantitative purposes, quercetin was used as reference standard. Calibration curve was built in the range 1.4–1400 ng/mL, and all samples and calibration solutions were analysed in triplicate. The obtained linear curve was: y = 134,300x +124 (R^2 =0.9991), showing a good linear response. Limit of detection (LOD = 1.5 ng/mL) and limit of quantification (LOQ = 5 ng/mL) were determined following USP method.

2.2.2.2. Human pilot trial methodology

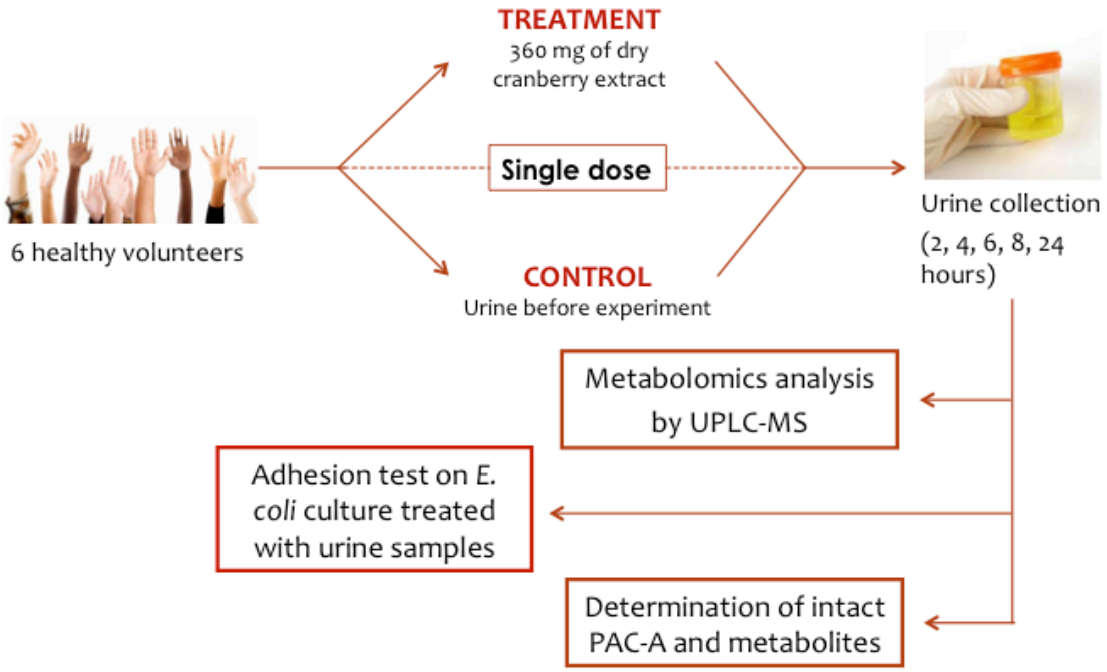

Figure 20. Scheme of the cranberry experiment involving human volunteers.

The scheme of the experiment is reported in Figure 20. Six healthy adult volunteers (four women and two men, 31±8 years, BMI 22.8±1.8) were enrolled for the study and informed consent was obtained. The *in vivo* procedures were conducted at the University of Trieste, Italy. The protocol was conducted in compliance with the Declaration of Helsinki and the International Conference on Harmonization Guidelines and each participant signed an informed consent form. All subjects were non-smoking, normally active and with no history of urinary tract infections in the last 12 months. No medications were taken during the study (wash out period: 7 days). They were required to maintain a low-polyphenol diet for 48 h before laboratory visit, free of green vegetables, fruits, fruit juices and red wine, to reduce as much as possible the amounts of polyphenols and related metabolites excreted in urines. Nothing except water could be consumed for 8 h prior to laboratory arrival. Volunteers took orally two sachets of product, corresponding to 360 mg of dried cranberry extract and 200 mg of quercetin, dispersed in 100 mL of tap water. Urine samples were collected 1 h before supplement consumption (control sample) and 2, 4, 6, 8 and 24 h after cranberry intake. Urine samples were immediately centrifuged at 5,000 rpm for 10 minutes, sampled in 50 mL vials and stored at -80 °C until analysis.

2.2.2.3. UPLC–MS analysis of urine samples

For untargeted analysis, an UPLC-ESI-QTOF full-scan method was used, as previously described in Paragraph 2.2.1.5. The stationary phase used was an Agilent Zorbax Rapid Resolution High Definition (RRHD) SB-C18 column (2.1 mm x 50 mm, 1.8 μm) and the mobile phase was composed of solvent A (acetonitrile with 0.1% formic acid) and solvent B (water with 0.1% formic acid). Linear gradients of solvents A and B were used, as previously reported. Quality control samples (QC, n=6) were used to monitor the instrument performance. They were prepared mixing 100 μL of each urine sample and centrifuged at 13,000 rpm for 10 minutes. Sequence of injection comprising pool, control and treated samples was randomized in order to avoid any bias due to samples order.

Data extraction was performed using MarkerLynx Applications Manager version 4.1 (Waters), using the same protocol described in the animal experiment.

2.2.2.4. Multivariate data analysis

After extraction, data were mean-centered, Pareto scaled and log-transformed for further PCA and PLS-DA analyses. These latters were performed using SIMCA 13 (Umetrics, Umea, Sweden) platform. N-fold full cross-validation (N = 7) and permutation test on the responses (300 random permutations) were also performed, in order to avoid over-fitting and prove the robustness of the obtained models. Finally, biomarkers were identified as previously described.

2.2.2.5. HPLC-MS/MS determination of oligomeric PAC-A in urine after cranberry consumption

Urine samples were purified prior to analysis, in order to isolate PACs from lower molecular weight polyphenols and increase sensitivity of mass spectrometric analysis. The protocol used was the same described in Paragraph 2.2.1.6. The calibration curve used to quantify PAC-A by HPLC-MS/MS (y = quantity of ISTD/quantity of PAC; x = area ISTD/area PAC) was the following: $y = 0.3841x + 0.0122$ ($R^2 = 0.999$). LOD and LOQ were 0.2 and 0.4 ng/mL, respectively, and they were established using USP method.

2.2.2.6. *HPLC-MS/MS determination of PAC-A degradation products in urine after cranberry consumption*

Three microbial degradation products of cranberry PACs, namely 5-(3',4'-dihydroxyphenyl)-γ-valerolactone, 5-(4'-hydroxyphenyl)-γ-valerolactone-4'-O-glucuronide and 5-(4'-Hydroxyphenyl)-γ-valerolactone-4'-O-sulfate, were selected from the results of untargeted metabolomics and comparing literature data (Feliciano et al., 2016, Urpi-Sarda et al., 2009), and they were monitored in urines collected after cranberry consumption. An appropriate chromatographic method was developed, and an Agilent 1260 Infinity HPLC binary pump coupled to a Varian 320-MS TQD MS was employed. The detector was equipped with an ESI ionization source and was operating in negative mode. The MS conditions were as follows: spray chamber temperature, 50 °C; nebulizer gas pressure, 25 psi; drying gas pressure, 25 psi; drying gas temperature, 385 °C; needle voltage, ±4000 V; spray shield voltage, 600 V. Fragmentation traces were used for the detection of the metabolites. *m/z* transitions 207→163, 363→191 and 271→191 were monitored respectively for 5-(3',4'-dihydroxyphenyl)-γ-valerolactone, 5-(4'-hydroxyphenyl)-γ-valerolactone-4'-O-glucuronide and 5-(4'-hydroxyphenyl)-γ-valerolactone-4'-O-sulfate. An Agilent Poroshell EC 120 C-18 column (2.1 mm x 100 mm, 2.7 μm) was used as stationary phase. The mobile phase was composed of solvent A (water with 2% formic acid) and solvent B (acetonitrile with 0.1% formic acid). Linear gradients of solvents A and B were used, as follows: 0 min, 10% B; 12 min, 85% B; 14 min, 85% B; 15 min, 10% B; 17 min, 10% B. The flow rate was 250 μL/min and the injection volume was 10 μL. AUCs of the monitored compounds were normalized to urinary creatinine, in order to overcome different urine dilutions among volunteers. Due to the lack of standards, information regarding the concentration of the monitored compounds could not be obtained.

2.2.2.7. *Determination of quercetin, quercetin-sulfate and quercetin-glucuronide in urine after cranberry consumption*

The same urine samples used for the previous analyses were used to determine the amount of quercetin absorbed from cranberry extract after supplement consumption and two quercetin derivatives formed after metabolism, namely quercetin-sulfate and

quercetin-glucuronide. The MS-chromatographic method used was the same previously described for PAC-A degradation products operating in negative ion mode. Quercetin was determined monitoring the *m/z* transition 301 → 150, while SRM traces 381 → 150 and 477 → 150 were monitored for quercetin-sulfate and quercetin-glucuronide, respectively. For quantitative purposes, quercetin was used as reference standard. Calibration curve was built in the range 0.01-10 μg/mL, and all samples and calibration solutions were analysed in triplicate. The obtained linear curve was: $y = 136640x + 1211$ ($R^2 = 0.9982$), showing a good linear response. Limit of detection (LOD = 1.2 ng/mL) and limit of quantification (LOQ = 5 ng/mL) were determined following USP method.

2.2.2.8. Microbiology and in vitro adhesion assay

The protocol used to assess the *in vitro* anti-adhesive activity of urine samples against uropathogenic *E. coli* was the same described in Paragraph 2.2.1.7.

3. Green coffee (*Coffea canephora*) bean extract

3.1. Materials

The supplement containing a standardized dry GCBE (*Coffea canephora*) was purchased from a local market. The names of product and supplier are note reported to avoid any conflict of interests. The powder extract used in the experiment was a homogeneous batch and it was formulated in gelatin capsules, each containing 200 mg of product. Standard chlorogenic acid, allantoin, and 8-OHdG were purchased from Sigma Aldrich (Milan, Italy). HPLC-grade acetonitrile and formic acid were purchased from Sigma Aldrich (Milan, Italy), as well as deuterated methanol used in NMR analysis. Deionized water used in HPLC and UPLC analyses was filtered through a Milli-Q system equipped with a 0.22 μm cut-off filter (Millipore).

3.2. Methods

3.2.1. Chemical characterization of dry GCBE

Chemical characterization of dry GCBE was performed by ^{1}H-NMR analysis and by HPLC-DAD-MS^{n}. For NMR exploratory analysis of GCBE, a Bruker Avance III spectrometer operating at 400 MHz was used. Briefly, 150 mg of dried extract were weighted in Eppendorf tube and 1 mL of deuterated methanol was added. The suspension was sonicated for 5 minutes then the tube was centrifuged at 13,000 rpm. The supernatant was transferred to a NMR tube and used for the ^{1}H-NMR analysis. For the chromatographic analysis, the system was composed of an Agilent 1260 chromatographic system with 1260 autosampler, column oven and a 1260 DAD. Out of the column a "T" union was fitted, splitting the flow identically to the diode array and to a Varian 500-MS ESI-Ion Trap MS. An Agilent Eclipse XDB-C18 column (3.5 µm, 3.0 x 150 mm) was used as stationary phase. Acetonitrile (A) and 0.1% formic acid in water (B) were used as mobile phase. Gradient elution was as follows: 5 min, 10% A; 30 min, 100% A; 100% A isocratic up to 35 min. Re-equilibration time was 5 min. Flow rate was 125 µL/min and injected volume was 10 µL. The MS parameters were as follows: spray chamber temperature, 50°C; nebulizer gas pressure, 25 psi; drying gas pressure, 25 psi; drying gas temperature, 350°C; needle voltage, ± 4500 V; spray shield voltage, 600 V. Mass spectra were acquired both in negative (for phenols characterization) and positive (for caffeine and trigonelline characterization) mode in the spectral range 150-2000 Da. Compounds were identified studying their fragmentation spectra obtained using the tdds® utility, and comparing the spectra with literature (Clifford et al., 2003, Clifford et al., 2005, Clifford et al., 2006, Clifford et al., 2008). For quantitative purposes, a DAD detector was used and chlorogenic acid and caffeine were used as standard compounds. Calibration curves were built in the range 1-100 µg/mL for chlorogenic acid (at 330 nm) and 2.5-85 µg/mL for caffeine (at 254 nm), and all calibration solutions were analyzed in triplicate. The obtained linear curves were: $y = 35.61\ x + 0.052$ ($R^2 = 0.9998$) and $y = 5.23\ x + 0.011$ ($R^2 = 0.9998$) for chlorogenic acid and caffeine, respectively. Limit of detection (LOD) and limit of quantification (LOQ) were determined following US Pharmacopeia methods. LOD = 0.5 µg/mL and 1.5 µg/mL and LOQ = 1.5 µg/mL and 5.0 µg/mL, for chlorogenic acid and caffeine respectively.

3.2.2. Human pilot trial methodology

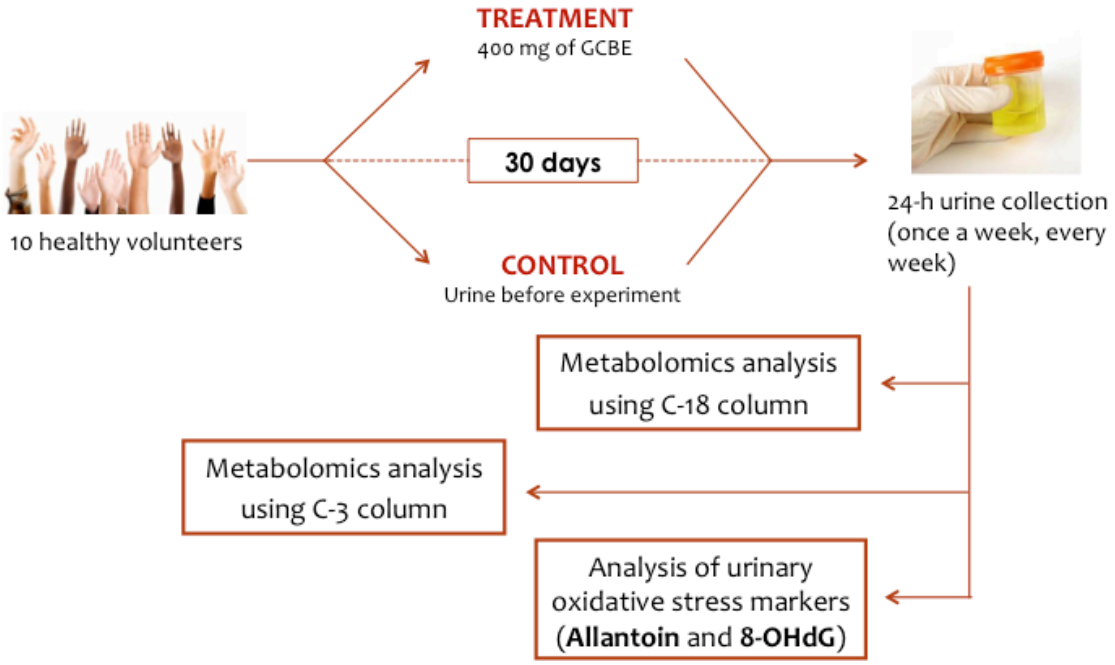

Figure 21. Scheme of the GCBE experiment involving human volunteers.

Ten healthy adult volunteers (five women and five men, 31±10 years, BMI 23.2±2.6) were enrolled for the study and informed consent was obtained. The protocol (Figure 21) was conducted in compliance with the Declaration of Helsinki and the International Conference on Harmonization Guidelines. All subjects were non-smoking and normally active. No medication was taken during the study (wash out period: 7 days). They were required to maintain a low-polyphenol diet for 7 days before product consumption, free of green vegetables, fruits, fruit juices and red wine, to reduce as much as possible the amounts of polyphenols and related metabolites excreted in urines. One day before the beginning of the experiment volunteers collected control urine, and nothing except water could be consumed for 8 h prior to GCBE consumption. Then, volunteers took daily 400 mg of dry GCBE (2 capsules) each day for 30 days and they collected 24-h urine once a week during the experiment (5 harvesting days, considering also the first day of supplementation). The dose was established on the basis of the doses of green coffee extract that are commonly introduced in food supplements. Urine was centrifuged at 5,000 rpm for 10 minutes, sampled in 50 mL vials and stored at -80 °C until analysis. The body weight of volunteers was monitored before the starting of the experiment and during treatment.

3.2.3. UPLC-QTOF analysis of 24-h urine output using C-18 stationary phase

To obtain a metabolite profiling of urine samples, an Agilent 1290 Infinity UPLC system equipped with a Waters Xevo G2 Q-TOF MS was employed. The detector was equipped with an ESI ionization source and was operating both in positive and negative modes. An Agilent Zorbax Rapid Resolution High Definition (RRHD) SB-C18 column (2.1 mm x 50 mm, 1.8 μm) was used as stationary phase. The mobile phase was composed of solvent A (acetonitrile with 0.1% formic acid) and solvent B (water with 0.1% formic acid). Instrument settings and chromatographic method were the same previously described in Paragraph 2.2.1.5. Quality control samples (QC, n=12) were used to monitor the instrument performance. They were prepared mixing 100 μL of each urine sample and they were centrifuged at 13,000 rpm for 10 minutes. Sequence of injection comprising pool, control and treated samples was randomized to avoid any bias due to samples order.

3.2.4. LC–MS analysis of 24-h urine output using C-3 stationary phase

A specific LC-ESI-MS method was developed on a C-3 stationary phase to better separate polar and smaller molecular weight metabolites. An Agilent 1260 HPLC system equipped with a Varian 500-MS IonTrap MS was employed. The detector was equipped with an ESI ionization source and was operating in positive mode. Needle voltage was adjusted to 4.5 kV, spray shield voltage to 600 V and capillary voltage to 750 V. The nebulizer gas pressure was 50 psi and drying gas (400 °C) pressure was 400 psi. Centroided data were collected in the mass range 50 – 1200 Da. MS^n spectra were acquired using the tdds® utility.

An Agilent Zorbax RRHD 300SB-C3 column (2.1 mm x 100 mm, 1.8 μm) was used as stationary phase. The mobile phase was composed of solvent A (acetonitrile with 0.1% formic acid) and solvent B (water with 1% formic acid) and the gradient used was: 0 min, 2% A; 1 min, 2% A; 20 min, 90% A; 23 min, 90% A; 25 min, 2% A. The flow rate was 150 μL/min and the injection volume was 2 μL. Pre-processing of urine samples was the same previously described and QC samples (n=12) were used to monitor instrument performance.

3.2.5. Statistical data analysis

Centroided and integrated UPLC-MS data were processed by MarkerLynx Applications Manager version 4.1 (Waters) to generate a multivariate data matrix. Method for data deconvolution, alignment and peak detection was the same described for the previous experiment, with slight modifications. The parameters used were retention-time range 1–10 min, mass range 50–1200 Da, mass tolerance 0.01 Da. Noise elimination level was set to 7.00, minimum intensity was set to 15% of base peak intensity, maximum masses per retention time (RT) was set to 6 and, finally, RT tolerance was set to 0.01 min. Isotopic peaks were excluded from analysis. Data were mean-centered, Pareto scaled and log-transformed before PCA and PLS-DA. Using SIMCA 13 (Umetrics, Umea, Sweden) platform, N-fold full cross-validation (N = 7) and permutation test on the responses (500 random permutations) were performed. Identification of biomarkers was performed as previously described.

Data obtained from LC–MS analysis using C-3 column were converted using ACD Spectrus 2014 software and then processed using MZmine Software v. 2.0. Chromatogram deconvolution, alignment of peaks, peak integration, isotopic grouping and normalization were performed. Variables having more than 30% of missing data in both groups were excluded and a list of the ion intensities of each peak detected was generated, using retention time and the *m/z* data pairs as the identifier for each ion. Data were mean-centered, Pareto scaled and log-transformed before PCA and PLS-DA, using SIMCA 13 (Umetrics, Umea, Sweden) platform. N-fold full cross-validation and permutation test on the responses were performed using the same software, as previously described. Biomarkers were identified studying their MS^n spectra and comparing fragmentation patterns with literature data.

3.2.6. Targeted analysis of allantoin and 8-OHdG in 24-h urine samples

Allantoin and 8-OHdG were quantified in urine samples using an Agilent 1260 HPLC system equipped with a Varian 320 TQD MS detector. The stationary phase was a Phenomenex Kinetex EVO C-18 column (2.1 mm x 100 mm, 5 μm). The detector was equipped with an ESI source and was operating in positive mode. The operating parameters used were as follows: nebulizing gas (N_2) pressure, 50.0 psi; needle voltage, 4.5 kV; capillary voltage, 600.0 V; drying gas temperature, 380 °C; drying gas pressure,

25.0 psi. The mobile phase was composed of solvent A (acetonitrile with 0.1% formic acid) and solvent B (water with 0.1% formic acid). Linear gradients of A and B were used, as follows: 0 min, 5% A; 1 min, 5% A; 8 min, 90% A; 10 min, 90% A; 11 min, 5% A and isocratic for 1 minute. The flow rate was 200 µL/min and the injection volume was 10 µL. For quantitative purposes, the fragmentation of allantoin $[M+H]^+$ ion was monitored (*m/z* 159 → 116) and a standard titration curve obtained eluting 1 - 100 ng/mL allantoin solutions in water ($y = 6234.3x$; $R^2 = 0.9923$) was used. Limit of detection (LOD = 1 ng/mL) and limit of quantification (LOQ = 5 ng/mL) were determined following USP guidelines. For 8-OHdG quantification, the fragmentation of 8-OHdG $[M+H]^+$ ion was monitored (*m/z* 284 → 168) and a standard titration curve obtained eluting 1 - 100 ng/mL 8-OHdG solutions in water ($y = 53429x$; $R^2 = 0.9981$) was used. Limit of detection (LOD = 0.3 ng/mL) and limit of quantification (LOQ = 1 ng/mL) were determined following USP guidelines. Before analyses, urine samples were centrifuged at 13,000 rpm for 5 minutes and supernatants were directly injected in the instrument.

RESULTS AND DISCUSSION

1. *Polygonum cuspidatum*

1.1. Animal weight and urinary output

As reported in Table 2**,** no significant differences were observed either in body weight or in 24-h urine volume in the treated *vs* control group during the experiment.

Table 2. Variations of body weight and 24-h urine volume of control and treated rats during the experiment. Values are reported as means ± SD.

	Body weight (g)		Urine volume (mL)	
Day	**Control**	**Treated**	**Control**	**Treated**
0	108.5 ± 1.2	107.5 ± 2.0	5.5 ± 0.7	6.4 ± 1.4
7	162.8 ± 12.9	164.8 ± 14.4	9.3 ± 2.8	11.4 ± 4.6
14	205.8 ± 21.2	208.6 ± 27.1	12.3 ± 3.7	10.1 ± 1.8
21	250.3 ± 34.5	248.0 ± 43.1	12.2 ± 2.3	13.5 ± 3.1
28	283.8 ± 38.1	287.7 ± 42.3	10.8 ± 1.4	13.4 ± 1.8
35	309.0 ± 53.9	303.5 ± 61.7	13.8 ± 3.8	12.7 ± 1.9
49	332.0 ± 66.0	340.3 ± 69.6	15.8 ± 8.0	12.9 ± 1.9

1.2. UPLC-HRMS measurements on 24-h urine samples

Exemplificative chromatograms obtained from UPLC-MS analysis of 24-h urine samples are reported in Figure 22. A first exploratory data analysis by PCA revealed no presence of outliers, while PLS-DA did not detect differences in the metabolite content of urine at day 0 between the two groups of rats.

As a first step of data analysis, we searched for expected metabolites directly related to the resveratrol metabolism in the treated group. Significant variables were tentatively identified as resveratrol phase II metabolites, namely resveratrol-glucuronide ($[M+H]^+$ *m/z* 405.1180 and the fragment at *m/z* 229.0866), resveratrol-sulfate ($[M+H]^+$ *m/z* 309.0414 and the fragment at *m/z* 229.0866) and dihydroresveratrol-glucuronide ($[M+H]^+$ *m/z* 407.1344 and the fragment at *m/z* 231.1022), a metabolite derived from

the action of gut microbiota and phase II metabolic processing in the liver (Andres-Lacueva et al., 2012). No significant traces of un-metabolized resveratrol were detected in rat urine samples.

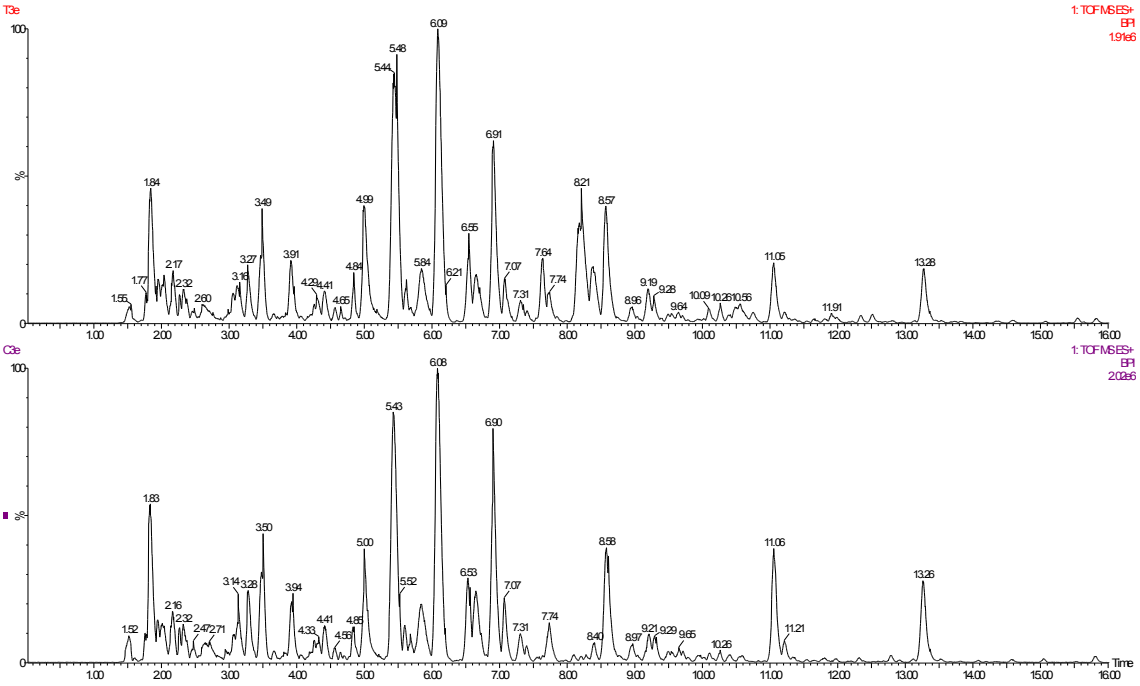

Figure 22. Typical base peak intensity (BPI) chromatograms obtained from UPLC-HRMS analysis of rat urine from both treated (upper panel) and control rats (lower panel).

After the exclusion from the model of these resveratrol metabolites, data modeling was performed by ptPLS2. The obtained model highlighted a clear effect of both time and treatment on the urine composition. The interaction term time x treatment was insignificant ($Q2_{7\text{-fold}}$=0.003). The model showed 2 parallel and 3 orthogonal components. Specifically, the model showed R2=0.89 and $Q2_{7\text{-fold}}$=0.76 for time while for the treatment resulted R2=0.89 and $Q2_{7\text{-fold}}$=0.68. Figure 23 reports the score scatter plot of the model, where the evolution of the urine composition during the experiment can be explained by considering two main effects, one related to the dietary intervention and one related to the time passing. By Monte-Carlo stability selection, a reduced set of 34 measured variables was detected as relevant in the explanation of the effects of time and treatment in the metabolite content of the collected urine. These were tentatively identified comparing the exact m/z value and fragmentation patterns with web-available databases and interpreting their MS^e spectra.

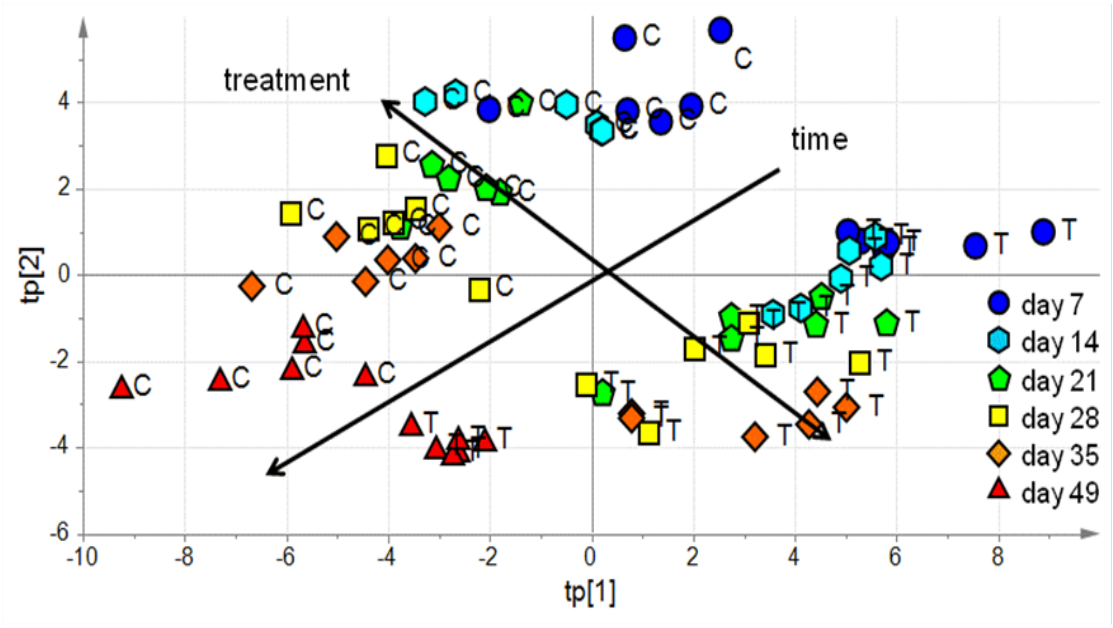

Figure 23. Score scatter plot of the ptPLS2 model for UPLC-HRMS data. The plot shows modifications of the urine composition both due to treatment and to time passing. Symbols of different shapes represent metabolic changes in urine along time.

Hypoxanthine, indole-3-carboxylic acid, 6-hydroxymelatonin, tetrahydrocortisol, 17-beta-methylestra-1,3,5(10)-trien-3-ol, sebacic acid, 3-oxo-5beta-chol-6-en-24-oic acid, 11-dehydrocorticosterone and 19-hydroxytestosterone predominantly contributed to the observed urinary metabolite differences related to *P. cuspidatum* extract supplementation (Table 3). The most significant variables related to time passing, thus potentially related to animal aging, are reported in Table 4.

Table 3. Significant variables (p-value < 0.05) related to treatment with P. cuspidatum, obtained from the ptPLS2 VIP-based model for UPLC-HRMS data (T>C means higher amounts in Treated than in Control, while T<C means higher amounts in Control than in Treated).

Retention Time (min)	*m/z*	Putative identification	Compound ID (Database)	Relative amount
2.26	137.0460	Hypoxanthine	HMDB00157 (HMDB)	T < C
6.92	162.0554	Indole-3-carboxylic acid	HMDB03320 (HMDB)	T < C
8.58	249.1242	6-Hydroxymelatonin	HMDB04081 (HMDB)	T > C
11.17	271.2060	17-beta-methylestra-1,3,5(10)-trien-3-ol	70515 (Metlin)	T > C
11.19	733.4891	Tetrahydrocortisol ($[2M+H]^+$)	HMDB00949 (HMDB)	T < C
11.34	225.1102	Sebacic acid ($[M+Na]^+$)	HMDB00792 (HMDB)	T < C
12.77	355.2634	3-oxo-5beta-chol-6-en-24-oic acid ($[M+H-H_2O]^+$)	84685 (Metlin)	T > C
12.80	345.2064	11-Dehydrocorticosterone	HMDB04029 (HMDB)	T < C
13.17	305.2116	19-Hydroxytestosterone	HMDB06769 (HMDB)	T < C

Table 4. Significant variables (p-value < 0.05) related to time passing during the experiment, obtained from the ptPLS2 VIP-based model for UPLC-HRMS data (↑ means increased amounts over time, while ↓ means decreased amounts over time).

Retention Time (min)	*m/z*	Putative identification	Compound ID (Database)	Time effect
3.08	413.1239	Unknown	-	↑
4.45	318.1555	Isoleucyl-Tryptophan	HMDB28918 (HMDB)	↑
4.65	372.2385	Unknown	-	↑
5.80	260.1501	Unknown	-	↑
7.06	242.1757	(±)-Hexanoylcarnitine ($[M+H-H_2O]^+$)	85174 (Metlin)	↑
8.85	409.1832	Unknown	-	↓
10.53	435.1285	Unknown	-	↓
13.39	410.2693	Unknown	-	↑
13.50	488.2987	Glycocholic acid ($[M+Na]^+$)	HMDB00138 (HMDB)	↑

1.3. ^{1}H-NMR measurements on 24-h urine samples

Exemplificative ^{1}H-NMR spectra in which metabolites responsible of time and treatment effects are highlighted are reported in Figures 24A and 24B.

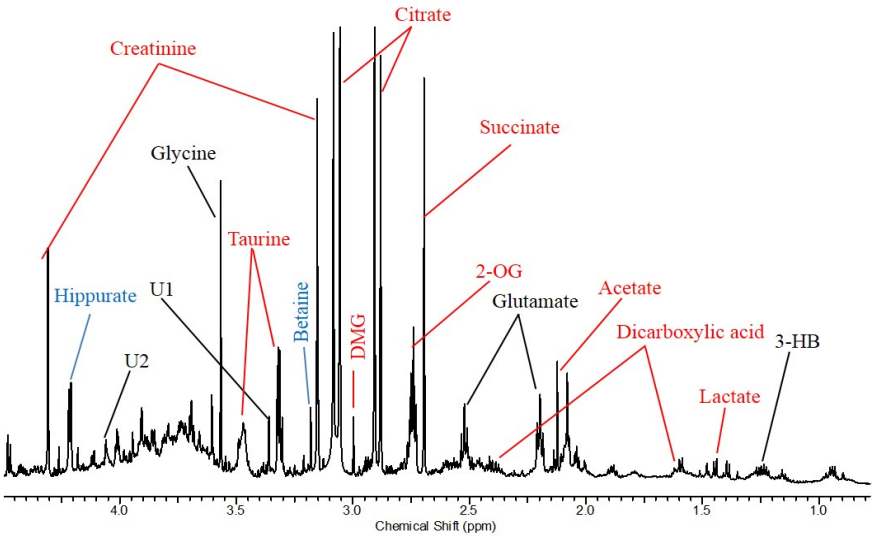

Figure 24A. Typical 1D ^{1}H-NMR spectrum of rat urine with enlargements of the aliphatic (0.6 – 4.5 ppm, above panel) regions. The resonances according to the time (red), treatment (black) and both effect (blue) effect were assigned.

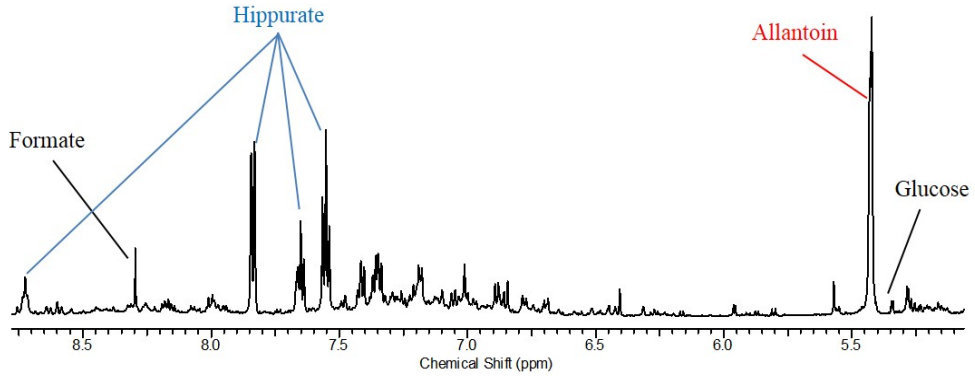

Figure 24B. Typical 1D ^{1}H-NMR spectrum of rat urine with enlargements of aromatic (5.5–9.5 ppm, lower panel) regions. The resonances according to the time (red), treatment (black) and both effect (blue) effect were assigned.

In the 1D spectra of treated rats urine, the resonances of resveratrol metabolites are evident (Figure 25). The NOESY spectrum confirms the presence of resveratrol-glucuronide and dihydroresveratrol-glucuronide (Figure 26).

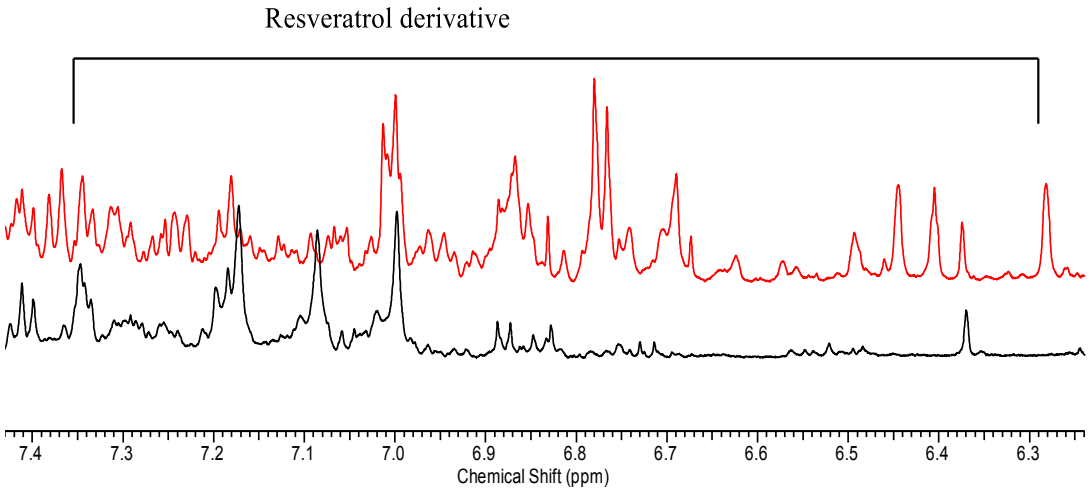

Figure 25. Representative 600 MHz ^{1}H-NMR spectra of rat urine before (black) and after (red) oral administration of P. cuspidatum. In the aromatic region (6.20 – 7.40 ppm) the presence of resveratrol derivatives in the treated spectrum is evident.

PCA analysis revealed no outliers or differences in the metabolite content of the urine collected at the beginning of the experiment. Data modeling performed by ptPLS2 highlighted a clear effect of both time and treatment on the urine composition, as observed for UPLC-MS dataset. The interaction term time x treatment was insignificant

($Q2_{7\text{-fold}}$ = -0.02). The model showed 2 parallel and 1 orthogonal components, R2 = 0.87 and $Q2_{7\text{-fold}}$ = 0.81 for time and R2 = 0.60 and $Q2_{7\text{-fold}}$ = 0.28 for treatment. Figure 27 reports the score scatter plot of the model. It is possible to observe that two main effects, one related to the time passing and one related to the dietary intervention, concur to determine the evolution of the urine composition during the experiment.

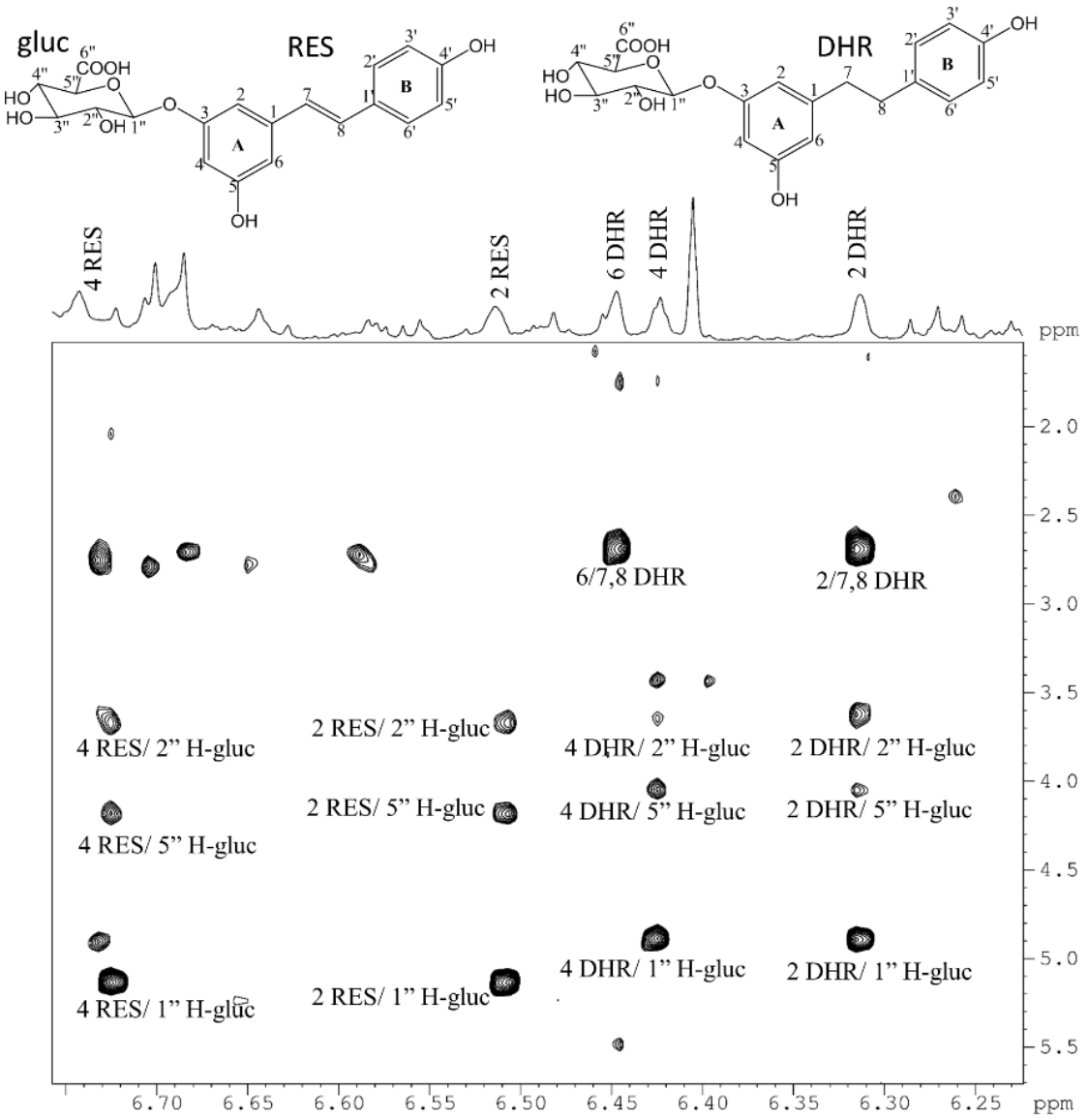

Figure 26. Portion of a NOESY spectrum in which NOE correlations of resveratrol (RES) and dihydroresveratrol (DHR) with glucuronic acid (glu) are shown.

Monte-Carlo stability selection allowed us to select a reduced set of 21 bins. The bins related to the treatment effect are reported in Table 5 while those explaining the aging effect are reported in Table 6. The metabolites were identified with the help of an online database (HMDB), literature (Van Dorsten et al., 2006), 2D-NMR spectra, or

spiking.

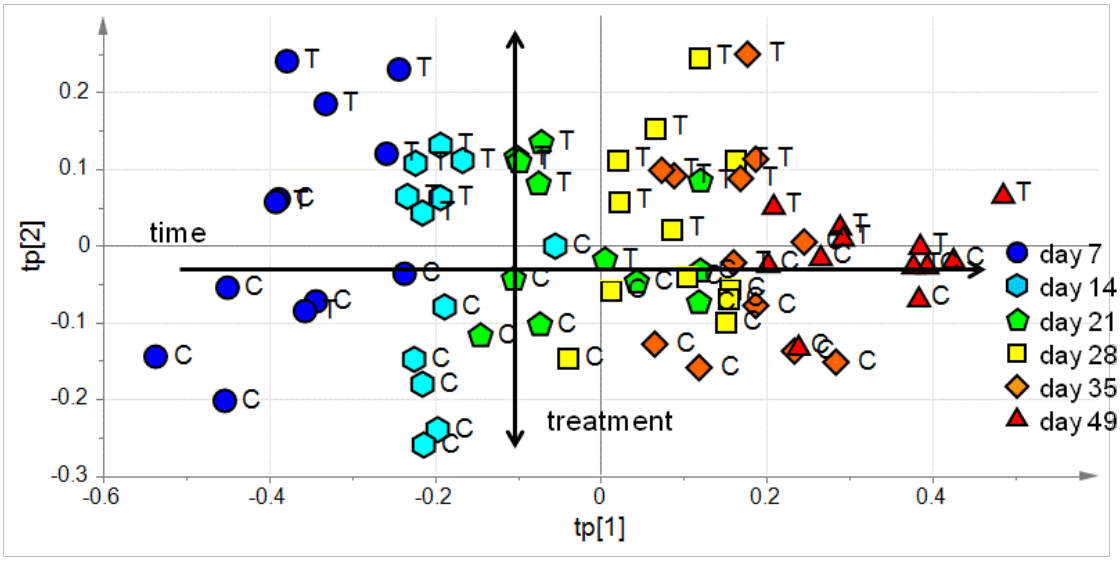

Figure 27. Score scatter plot of the ptPLS2 model for ^{1}H-NMR data set. The plot shows modifications of the urine composition both due to treatment and to aging. Symbols of different shapes represent metabolic changing in urine along time.

Table 5. Significant variables (p-value<0.05) related to treatment with P. cuspidatum, obtained from the ptPLS2 VIP-based model for the ^{1}H-NMR data (T>C means higher amounts in Treated than in Control, while T<C means higher amounts in Control than in Treated).

Bin	Chemical shift (ppm)	Metabolite	Treated vs. Control
[1.22- 1.28]	1.23 (d)	3-Hydroxybutyrate	↑
[2.46- 2.51]	2.48 (t)	Dicarboxilic acid	↓
[3.20- 3.24]	3.22 (s)	Glucose	↓
[3.30- 3.34]	3.32 (s)	Unknown	↑
[3.52- 3.56]	3.56 (s)	Glycine	↑
[4.00-4.04]	4.02 (m)	Glutamate	↑
[5.22- 5.26]	5.25 (d)	Glucose/Glucuronate	↑
[8.25- 8.29]	8.26 (s)	Formate	↑
[8.75- 8.79]	8.76 (t)	Hippurate	↑

Table 6. Significant variables (p-value<0.05) related to rat aging, obtained from the ptPLS2 VIP-based model for ^{1}H-NMR data (↑ means increased amounts over time, while ↓ means decreased amounts over time).

Bin	Chemical shift (ppm)	Metabolite	Time effect
[1.40-1.44]	1.42 (d)	Lactate	↑
[2.07-2.11]	2.10 (s)	Acetate	↑

[2.27-2.31]	2.28 (brs)	Dicarboxylic acid	↓
[2.65-2.69]	2.68 (s)	Succinate	↓
[2.69-2.73]	2.71 (t)	2-Oxoglutarate	↓
[2.82-2.86]	2.86 (d)	Citrate	↓
[2.94-2.97]	2.95 (s)	Dimethyl glycine	↑
[3.11-3.14]	3.13 (s)	Creatinine	↑
[3.20-3.24]	3.22 (s)	Glucose	↑
[3.25-3.30]	3.28 (t)/ 3.29 (s)	Taurine/Betaine	↑
[3.41-3.46]	3.44 (t)	Taurine	↑
[8.75- 8.79]	8.76 (t)	Hippurate	↓

1.4. Focus on the effects of *P. cuspidatum* supplementation on rat aging

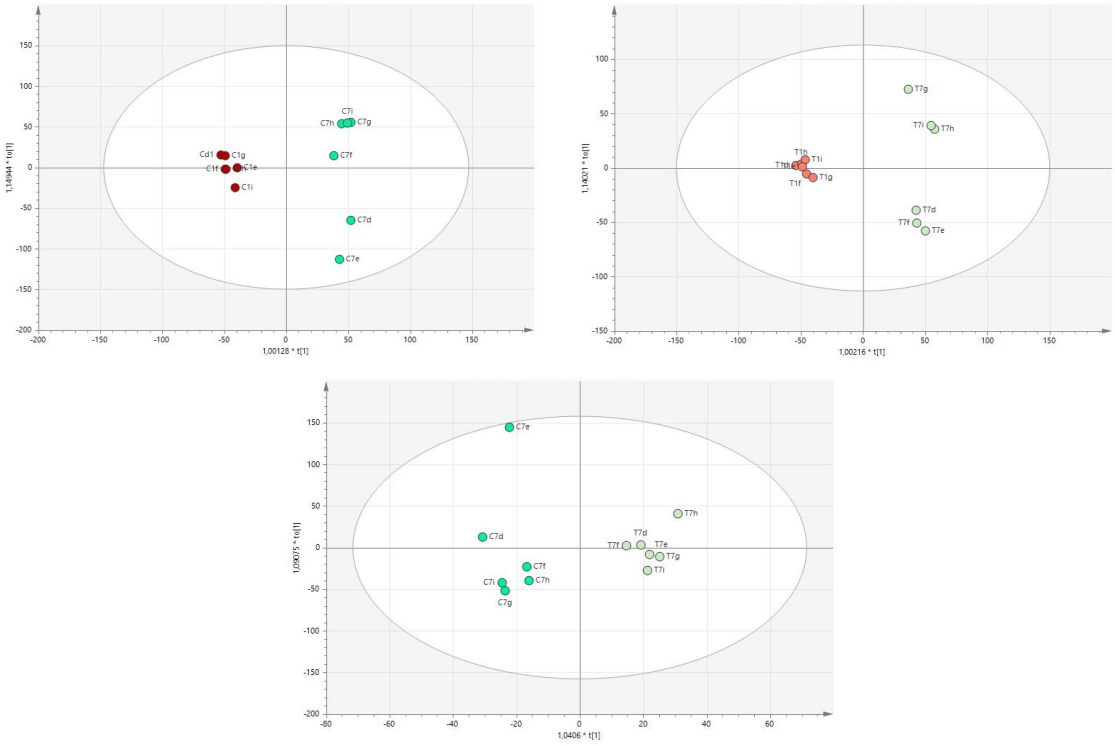

Figure 28. Score scatter plots of the OPLS-DA models of urine samples collected from control (upper left) and treated rats (upper right), respectively, at the first and last weeks of treatment. The OPLS-DA plot in the lower panel compares urine samples collected at the last week of treatment from both control and treated animals. C1: control rats, 1st week of experiment; C7: control rats, 7th week of experiment; T1: treated rats, 1st week of experiment; T7: treated rats, 7th week of experiment.

Data regarding urine collected at the beginning of the experiment and at the last week (49th day) were selected from UPLC-MS dataset, and they were compared by multivariate analysis. OPLS-DA models comparing only control (R2 = 0.75 and $Q2_{7\text{-fold}}$

= 0.50) and only treated urine samples (R2 = 0.78 and $Q2_{7\text{-fold}}$ = 0.44) were built, and significant descriptors of time-passing were selected and further identified. A third OPLS-DA model was finally built to compare urinary output collected from both treated and control rats at the end of the experiment (R2 = 0.54 and $Q2_{7\text{-fold}}$ = 0.38).

As shown in Figure 28, all the models indicated changes of urine composition related to animal aging and differences between urine samples collected from the two groups at the end of supplementation period, as well as between treated and control animals at the last week. From each model, different sets of variables describing time effects were selected, but only significant variables that were detectable in both the OPLS-DA comprising controls and treated animals separately were considered as descriptive and further identified (Table 7).

Table 7. Significant (p-value<0.05) variables descriptive for rat aging selected from OPLS-DA models of urine samples collected from control and treated rats, respectively, at the first and last days of treatment.

Retention Time (min)	*m/z*	Putative identification	Compound ID (HMDB)	Time effect, control (%)*	Time effect, treated (%)*
3.13	153.0660	N-Methyl-2-pyridone-5-carboxamide	HMDB 0004193	+146	+102
3.30	220.1182	Panthotenic acid	HMDB0000210	-77	-78
3.50	297.1450	Tetradecanedioic acid ($[M+K]^+$)	HMDB0000872	-64	-63
5.00	206.0454	Xanthurenic acid	HMDB0000881	-106	-105
5.41	190.0501	Kynurenic acid	HMDB0000715	+281	+282
5.80	260.1500	3-Hydroxysebacic acid ($[M+ACN+H]^+$)	HMDB0000350	+2835	+3565
5.83	180.0660	Hippuric acid	HMDB0000714	-62	-69
5.84	123.0442	Benzoic acid	HMDB0001870	-79	-80
6.64	194.0821	Phenylacetylglycine	HMDB0000821	+96	+39
7.30	162.0554	4,6-Dihydroxyquinoline	HMDB0004077	+262	+150
11.17	733.4890	Tetrahydrocortisol ($[2M+H]^+$)	HMDB0000949	+60799	+6187

Values are reported as % obtained comparing peak AUC at the end of the experiment to peak AUC at the beginning of the experiment. Positive values indicate an increase, negative values a decrease.

Some of the identified variables were already described by other authors as putative markers of aging. Most importantly, blood amounts of N-methyl-2-pyridone-5-carboxamide (2PY), a major catabolite of nicotinamide, a component of NAD, were reported to increase both in rats and humans with aging. The results reported by Slominska and collaborators show that plasma 2PY concentration in healthy young rats (2 months) was 0.55 ± 0.07 μmol/L, while in older rats (24 months) it was 0.84 ± 0.15 μmol/L, although data regarding urinary excretion of the metabolite were not reported

(Slominska et al., 2004). Considering these data, and due to a different % increase in the excretion of 2PY between control and treated rats in our experiment (Table 7), the excretion of the metabolite was monitored throughout experimental period, by extracting peak AUC from the dataset. The obtained results showed an increased age-related excretion of the metabolite (Figure 29), and different urinary amounts between control and treated animals were observed from the 4th week of treatment. However, this difference resulted to be significant only at the last week of experiment, being mean AUC 2PY/AUC creatinine values 53.8 and 35.7, in control and treated urine samples respectively.

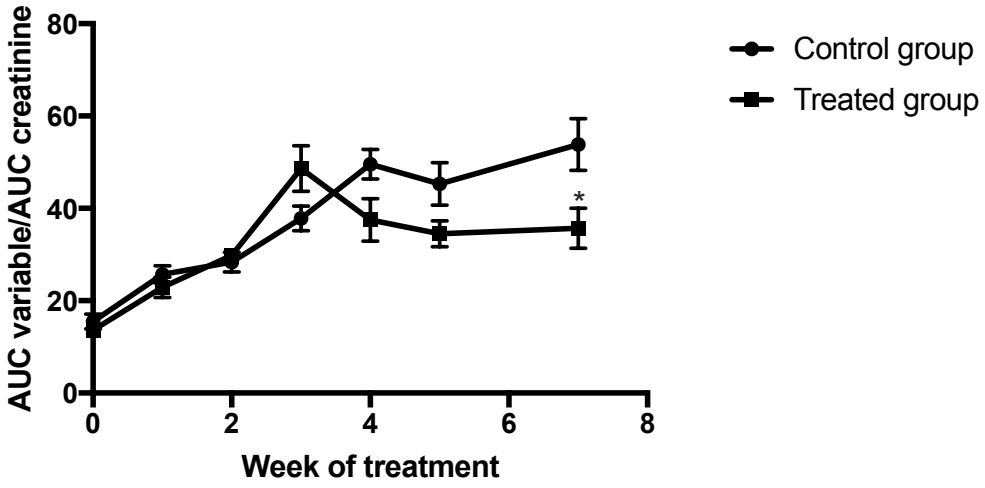

Figure 29. Urinary excretion profiles of 2PY throughout experimental period. The values are reported in the graph as means ± SD.

Similarly, urinary excretion of phenylacetylglycine was monitored throughout experimental period. This metabolite, as hippuric and benzoic acids, derives from gut microbiota metabolism, and their variation in urine correlates with a modification of microbial activity with aging of animals (Zhang et al., 2012). As observed for 2PY, an increasing trend in the excretion of phenylacetylglycine was observed with animal aging (Figure 30), as previously described by Zhang and coll. (Zhang et al., 2012). However, from the 4th week of treatment, differences between control and treated rats were detectable, and significant lower amounts of the metabolite in urine were detected in treated urine at the end of the experiment (AUC phenylacetylglycine/AUC creatinine values were 110.3 and 70.8, in control and treated urine samples respectively).

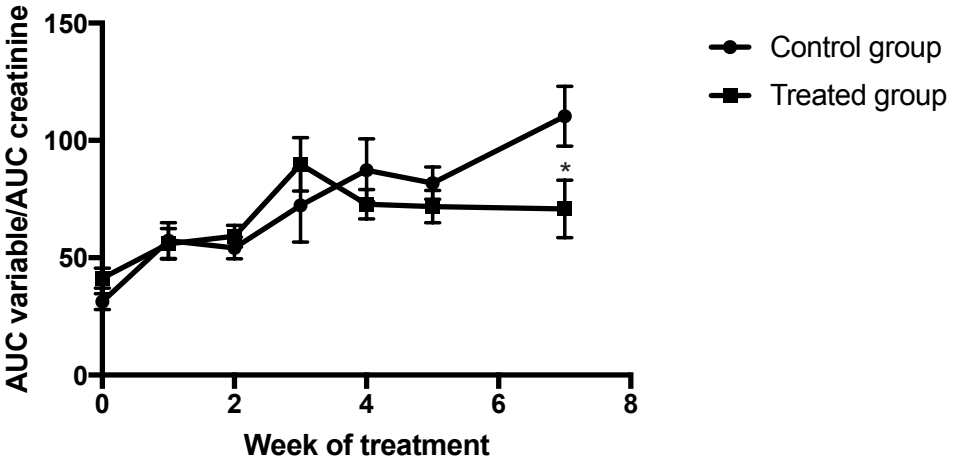

Figure 30. Urinary excretion profiles of phenylacetylglycine throughout experimental period. The values are reported in the graph as means ± SD.

1.5. Quantification of allantoin and 8-OHdG in 24-h urine samples

The amounts of the two oxidative stress markers in collected urine samples, allantoin and 8-OHdG, were assessed monitoring their major fragments at the beginning and at the end of the experiment (day 49) with a specific HPLC-MS/MS method ($[M+H]^+$ at *m/z* 159/116 for allantoin and $[M+H]^+$ at *m/z* 284/168 for 8-OHdG). Data are summarized in Table 8 and in Figure 31.

Table 8. Urinary variations of 8-OHdG and allantoin from the beginning of the experiment (day 0) to the end (day 49). Results obtained from rats supplemented with *P. cuspidatum* extract (treated) are compared to results obtained from the control group (control). Values are represented as means ± SEM. p-values calculated in unpaired t test. $p < 0.05$ (*), $p < 0.001$ (***).

8-OHdG	**Day 0**	**Day 49**	**t-test p-value**
Control	9.54 ± 0.49 ng/mL	10.35 ± 1.05 ng/mL	0.47
Treated	10.83 ± 0.54 ng/mL	8.64 ± 0.92 ng/mL	0.05*

Allantoin	**Day 0**	**Day 49**	**t-test p-value**
Control	1.75 ± 0.08 µg/mL	1.01 ± 0.18 µg/mL	0.02*
Treated	1.54 ± 0.06 µg/mL	0.41 ± 0.05 µg/mL	<0.0001***

The content of 8-OHdG in the urine weakly decreased for the treated rats (t-test p-value = 0.05) while it did not change for the control rats (t-test p-value = 0.47). At the beginning of the experiment, the urinary concentration of 8-OHdG was 10.83 ± 0.54

ng/mL for the treated rats and it weakly decreased to 8.64 ± 0.92 ng/mL at the 49th day of treatment. Allantoin concentration significantly decreased for both control and treated rats (t-test p-value = 0.02 and test p-value < 0.001, respectively). Specifically, for control rats the allantoin concentration decreased from 1.75 ± 0.08 µg/mL to 1.01 ± 0.18 µg/mL while for treated rats from 1.54 ± 0.06 µg/mL to 0.41 ± 0.05 µg/mL. Overall, the reduction of the concentration of these two markers was more relevant for treated rats than control rats, suggesting a reduction of oxidative stress related to supplementation with *P. cuspidatum*.

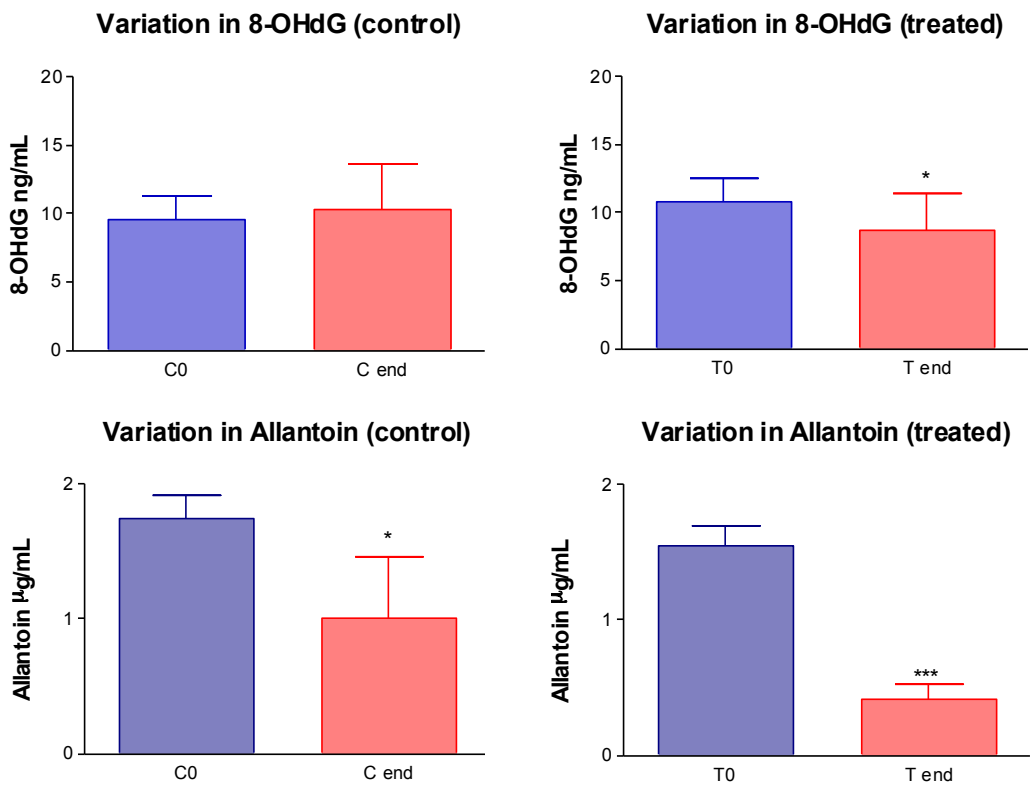

Figure 31. Urinary variations of 8-OHdG (upper panel) and allantoin (lower panel) from the beginning of the experiment to the end. Results obtained from rats treated with P. cuspidatum extract (T0 and Tend) are compared to results obtained from the control group (C0 and Cend). Values are represented as means ± SEM. p-values calculated in unpaired t test. $p < 0.05$ (*), $p < 0.001$ (***).

1.6. Discussion

Differences in the treated *vs* control animals were observed using both UPLC-HRMS and ^{1}H-NMR platforms. The ptPLS2 models revealed both treatment and time-related modifications, showing a valuable application of metabolomics to both

nutraceutical and aging studies. Nevertheless, the two analytical techniques revealed different metabolites. From the UPLC-HRMS dataset, decreased levels of hypoxantine and indole-3-carboxylic acid were observed and were correlated to treatment. Hypoxanthine is normally detected in urine and blood, but increased levels could be related to oxidative stress (Gerritsen et al., 1997, Saiki et al., 2001). Also increased urinary levels of indole-3-carboxylic acid, a tryptophan metabolite normally detected in urine (Byrd et al., 1974), can be related to oxidative stress and were reported in diet-induced hyperlipidemic rats (Miao et al., 2014). These data suggest that supplementation with *P. cuspidatum* extract reduces oxidative stress in healthy rats. In order to confirm this observation, measurements of specific oxidative stress markers, namely allantoin and 8-OHdG, were performed. Allantoin is formed from the stepwise degradation of uric acid due to the reaction with oxidative species (Kim et al., 2009) and is present in urine of healthy subjects. Its level is increased with increasing oxidative stress in the body (Tolun et al., 2010). 8-OHdG is formed by the 8-hydroxylation of the guanine base by reactive oxygen species, and its a product of mitochondrial and nuclear DNA oxidative damage (Zhang et al., 2013). The oxidized nucleoside is enzymatically cleaved from the DNA chains, is released in the bloodstream, and is eliminated in the urine (Zhang et al., 2013). This biomarker is normally present in urine of healthy people, and variations of its urinary levels suggest alterations of the oxidative status. Thus the observed reduction of the urinary levels of both these metabolites in the treated group supports an *in vivo* antioxidant effect of *P. cuspidatum* supplementation.

6-hydroxymelatonin (a hydroxylated hepatic metabolite of melatonin, mainly excreted in urine) increased in urine from treated group. Previous studies reported that melatonin and its metabolites exert both immunomodulatory and antioxidant activities (Ozkan et al., 2012, Reiter et al., 2008). Its meaning in the *P. cuspidatum* mode of action needs to be further investigated in depth.

Another series of metabolites related to treatment were identified as steroid derivatives. Tetrahydrocortisol, 17-beta-methylestra-1,3,5(10)-trien-3-ol, 11-dehydrocorticosterone and 19-hydroxytestosterone, a metabolite derived from androgen and estrogen metabolisms (Watanabe et al., 1994), were detected in lower amounts in treated rat urine. A biliary acid derivative was also identified, 3-oxo-5beta-chol-6-en-24-oic acid, and its urinary amount was increased in the treated group.

Tetrahydrocortisol is a urinary metabolite of cortisol (Pavlovic et al., 2013) and its urinary levels can be increased by ACTH administration (Gomez-Sanchez et al., 1988).

This preliminary observation suggests a role for *P. cuspidatum* extract as stimulant of corticosurrenal hormones, thus being related to anti-stress or "adaptogenic" activity as Ginseng or similar herbal products (Nocerino et al., 2000). The role of resveratrol on cortisol biosynthesis was previously investigated in vitro showing that the compound is able to stimulate cortisol biosynthesis by activating SIRT-dependent deacetylation of P450scc (Li et al., 2012). The change in sterol and corticosterol levels may be related to some of the health promoting effects of resveratrol.

The amounts of sebacic acid were decreased in urine after treatment. This metabolite is a medium chain dicarboxylic acid normally detected in urine. Sebacic acid and dodecanedioic acid are naturally occurring substances formed by cytochrome P-450-mediated ω-oxidation of fatty acids in the cytosol. The levels of urinary medium chain dicarboxylic acid can raise when the fatty acid utilization is increased beyond the capacity of mitochondrial β-oxidation such as during starvation or diabetes, and it can be observed also during treatments with drugs that are able to inhibit fatty acid β-oxidation (as valproic acid) (Clarke, 2005). This result indicates that *P. cuspidatum* supplementation may have a role on energetic metabolism in rats. Furthermore, the indication that the decreased levels of dicarboxylic acids in urine are in general associated with starvation may be interpreted as an indirect confirm of the known effects of resveratrol on decreasing blood glucose and increasing lipolysis and fatty acid oxidation (Szkudelska and Szkudelski, 2010). In this case, the UPLC-HRMS data are in agreement with the ^{1}H-NMR data, that revealed the glucose and dicarboxylic acid decrement related to *P. cuspidatum* supplementation.

^{1}H-NMR showed the increase of 3-hydroxybutyrate (3-HB) in treated group. This metabolite is synthesized in the liver from acetyl-CoA, and can be used as an energy source by the brain when blood glucose is low. The increase of 3-HB is normally detected in ketosis thus indicating a glucose shortage, thus this effect could be considered as related to the possible reduction of blood glucose induced by resveratrol administration, as reported by other authors (Szkudelska and Szkudelski, 2010). Increased amount of hippurate in treated group was revealed. This observation is in agreement with literature data that reported the increased urinary level of hippuric acid due to consumption of phenolic compounds (for example from tea, wine, fruit juices) (Daykin et al., 2005, Krupp et al., 2012). The increased urinary excretion of hippurate should also be related to interaction of the treatment with gut microbiota. In fact, in a previously published paper hippuric acid excretion was not detected in volunteers

without colon, meaning that it was formed by metabolisation inside the colon (Olthof et al., 2003).

Changes in urine composition were also related to time passing, as observed by both UPLC-MS and NMR. Considering the UPLC-HRMS data set, several variables related to aging were detected but only few of them were identified. Among them, (±)-hexanoylcarnitine was found increasing in urine over time, as previously described, due to an age-related gradual decline in kidney function leading to alterations in carnitine and acylcarnitines homeostasis (Lee et al., 2014). Furthermore, an increasing tendency of urinary medium-chain acylcarnitines due to aging was reported (Lee et al., 2014). Other two metabolites related to rat aging were identified from the UPLC-HRMS data set as isoleucyl-tryptophan and glycocholic acid, but further studies are needed to assess their role in aging processes. Many aging-related metabolites were identified by ^{1}H-NMR as lactate, acetate, 2-oxoglutarate, citrate, succinate and glucose, accordingly to previously published results (Bell et al., 1991, Wu et al., 2008). Furthermore, the increasing amounts of urinary creatinine observed with aging may be related to the greater output from the growing muscles of the larger rats and to the age-related increasing of glomerular filtration rate (Bell et al., 1991). Dimethyl glycine and hippurate are related to the gut microbiota activity, and in previously published papers they were considered as age-related urinary metabolites (Zhang et al., 2012). Taurine has been reported as a marker of liver function and its increased urinary amounts may be related to a decreased liver function related to aging (Schnackenberg et al., 2007). To explore more in depth the effects of aging on urine composition, statistical models were built considering only samples collected at the beginning and at the end of the supplementation period. Among descriptive markers, phenylacetylglycine, 3-hydroxysebacic acid, hippuric and benzoic acids were correlated to the results obtained from previous ^{1}H-NMR analysis, and more specifically, to the markers related to gut microbiota activity. Amounts of N-Methyl-2-pyridone-5-carboxamide, a major catabolite of nicotinamide and an aging marker previously described by other authors (Slominska et al., 2004), were found to be increased in urine with aging of rats, but differences between control and treated groups were observed. The increasing trend of excretion of this marker with animal aging was observed to be lower in treated rats compared to controls, indicating a possible protective effect of *P. cuspidatum* on age-dependent DNA damage. In fact, N-methyl-2-pyridone-5-carboxamide is produced from the metabolism of NAD, which is a substrate for the poly(ADP-ribosyl)ation

reaction catalyzed by poly(ADP-ribose) polymerase (PARP-1), aimed to DNA repairing. In case of oxidative DNA damage caused by aging, the activation of PARP-1 is induced, and consequently the use of NAD as substrate is increased (Slominska et al., 2004). The observed decrease in the excretion of N-methyl-2-pyridone-5-carboxamide in animals treated with *P. cuspidatum* can be related to its anti-oxidant activity and to the consequent scavenging activity against ROS, thus preventing DNA damaging.

A similar trend was observed for another marker, namely phenylacetylglycine, and also in this case significant lower amounts in urine from treated rats were detected at the 49th day of supplementation. This metabolite was already reported as aging marker by Zhang and coll. (Zhang et al., 2012), whose observed that, in urine of rats undergoing caloric restriction, its amounts were significantly lower (processed AUC normalized and logarithm transformed were 25.98±10.79 in control rats and 15.27±13.39 in rats undergoing caloric restriction). Thus, the reduced excretion of phenylacetylglycine observed in the group supplemented with *P. cuspidatum* in our experiment can be linked to the caloric restriction mimetic role of resveratrol and to the consequent decrease of blood glucose and increase of lipolysis and fatty acid oxidation (Szkudelska and Szkudelski, 2010), as we observed with untargeted analysis. However, although these metabolic activities could be linked to the "anti-aging" effects of resveratrol, an in depth investigation on the involvement of phenylacetylglycine is needed.

In conclusion, UPLC-MS and NMR showed their complementarity yielding two different patterns of metabolites describing the changes ascribed to *P.cuspidatum* supplementation and to time passing, being this latter somehow a representation of aging processes. The UPLC-HRMS data allowed the exploration of different patterns of metabolites during the experiment. The metabolites observed in the untargeted metabolomics data and the decreased levels of urinary oxidative stress markers are indicative of *in vivo* antioxidant effect of *P. cuspidatum* in healthy rats. However, no oxidized resveratrol or oxidized resveratrol metabolites were detected, suggesting a negligible role of its "direct" antioxidant activity. Moreover, UPLC-HRMS approach allowed the identification of steroid derivatives as markers of treatment. On the other hand, urinary changes observed with ^{1}H-NMR measurements were related to hippuric acid increase, as previously reported for other polyphenol supplementation, and to some metabolites that suggest a relationship between *P. cuspidatum* treatment and energy metabolism such as glucose levels and fatty acid oxidation.

2. *Vaccinium macrocarpon* (Cranberry)

2.1. Supplementation of healthy rats with a standardized dry cranberry extract

2.1.1. Profiling of PACs in cranberry extract

The total PAC-A content was 11.3 ± 1.3% w/w of dry cranberry extract, whereas the total content of PAC-B was 4.3 ± 0.4% w/w. PAC-A dimers constituted the 4.5 ± 0.7% w/w of dry extract, trimers were 3.6 ± 0.2% w/w and tetramers 3.2 ± 0.2% w/w. PAC-B dimers constituted the 1.3 ± 0.3% w/w of dry extract, trimers were 1.8 ± 0.1% and tetramers 1.2 ± 0.1% w/w.

2.1.2. Profiling of 24-h urine by UPLC-ESI-QTOF

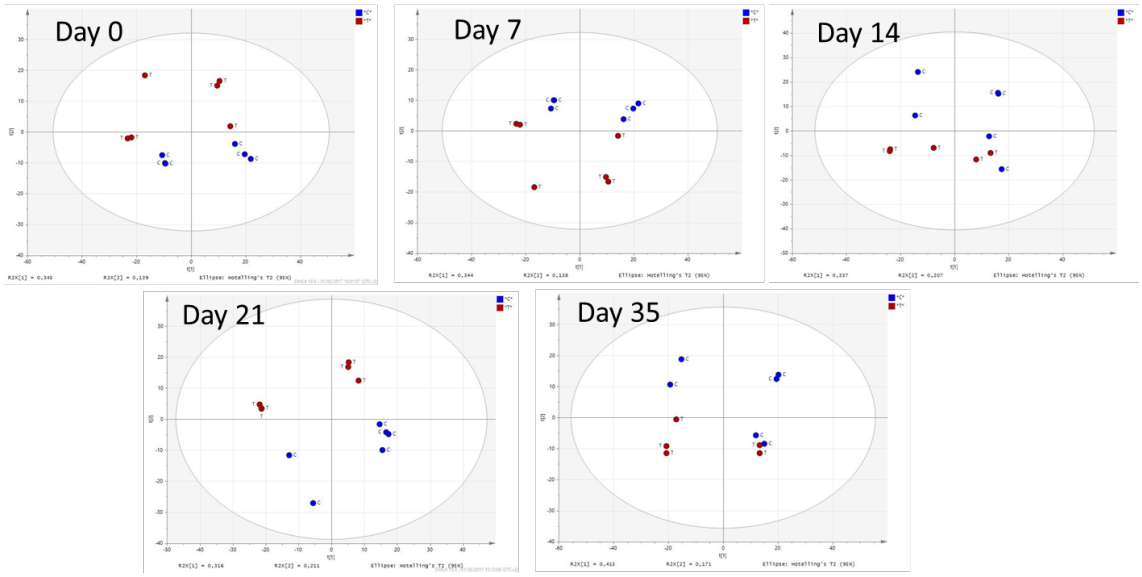

Figure 32. Exemplificative score scatter plots obtained from the PCA of UPLC-MS data recorded in negative ion mode. The plots show cranberry extract treated group (red dots) and control group (blue dots) at day 0, 7, 14, 21 and 35.

24-h urine samples collected during the 35 days of cranberry supplementation were analyzed by UPLC coupled with ESI-QTOF-MS, and urinary metabolite profiles of both treated and control animals were obtained. Mass spectrometric data were

acquired both in positive and negative ion modes, in order to consider the largest number of metabolites, and two different datasets were obtained and used for multivariate analysis. Exploratory data analysis by PCA on urine samples collected at days 0, 7, 14, 21 and 35 resulted in partial grouping of treated versus controls (Figure 32), supporting the changes of urine composition after oral administration of cranberry extract.

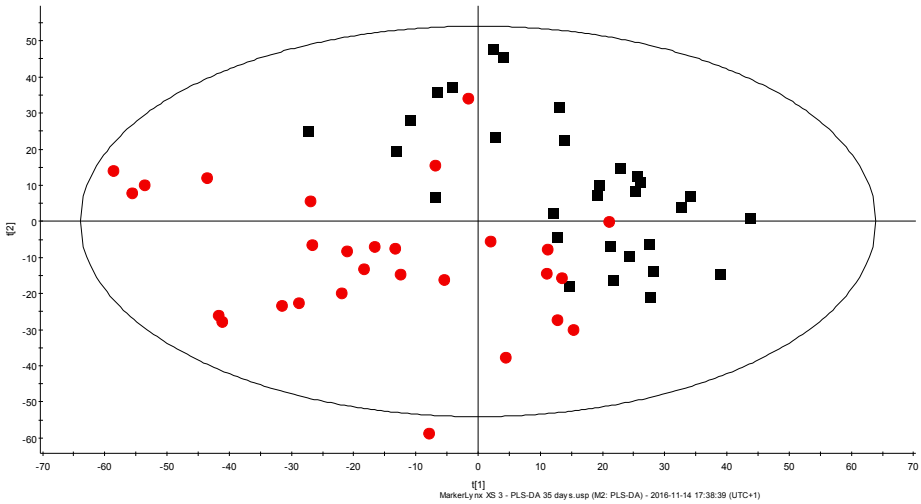

Figure 33. Score scatter plot obtained from PLS-DA modeling of "positive" dataset. The plot shows cranberry extract treated group (red dots) and control group (black squares).

Data modeling was subsequently performed by Partial Least Squares Discriminant Analysis (PLS-DA). The PLS-DA model for the "positive ion mode" dataset could explain 71% of the data variance using 3 components and the variance predicted was 36%. Y-axis intercepts after permutation test were R2 = (0.0, 0.408) and Q2 = (0.0, 0.216). On the other hand, the PLS-DA model built from the "negative ion mode" dataset could explain 80% of the data variance using 3 components and the variance predicted was 53%. Y-axis intercepts after permutation test were R2 = (0.0, 0.468) and Q2 = (0.0, 0.308). Representative PLS-DA score scatter plots for the positive and negative datasets are reported in Figure 33 and 34, respectively. The plots show that urine samples collected during treatment and controls are grouped in two clusters, although they partially overlap.

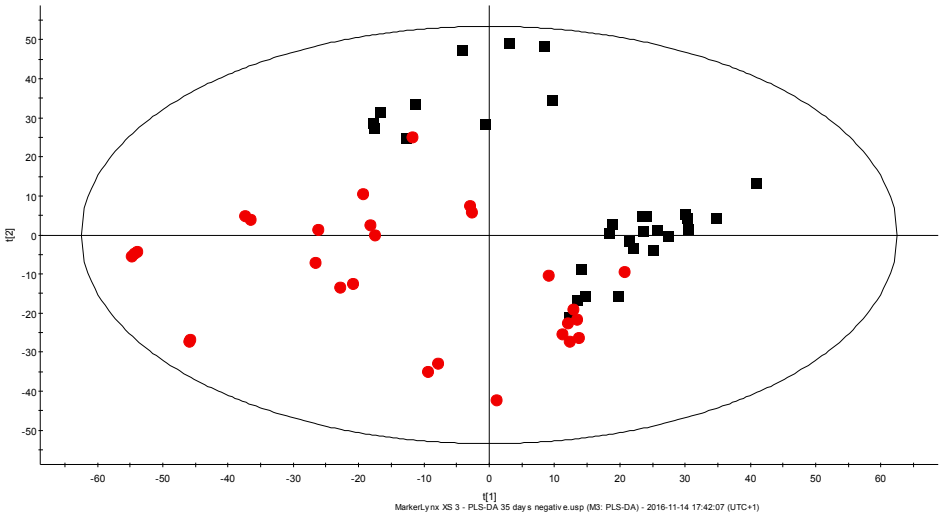

Figure 34. Score scatter plot obtained from PLS-DA modeling of "negative" dataset. The plot shows cranberry treated group (red dots) and control group (black squares).

Time x mass variables contributing to group separation were selected on the basis of their variable importance on projection (VIP) value. Only variables bearing VIP values > 2.0 were considered significant in differentiating the two groups and were subsequently putatively identified. The selected variables are listed in Table 9A and 9B.

Table 9A. Variables related to treatment with cranberry extract, obtained from the PLS-DA model for UPLC-MS data acquired in positive ion mode.

R.T. (min)	Measured HR *m/z*	Significant fragments, *m/z*	VIP	Amount T *vs* C[#]	p-value	Putative identification	Compound ID (Database)
2.2	146.0687	112.3876	2.3	↑	0.890	Unknown	-
3.3	271.1205	166.0743, 138.0784, 114.0430	2.0	↑	0.042*	Unknown	-
2.3	282.1004	150.0538, 114.0426	2.2	↑	0.001*	1-Methyladenosine	HMDB03331 (HMDB)
5.5	297.1261	286.1209, 279.1148, 126.0316	2.4	↑	0.021*	Desmosflavone	HMDB38518 (HMDB)
6.4	338.0716	162.0314, 134.0363	5.4	↑	0.002*	2,8-Dihydroxyquinoline-beta-D-glucuronide	HMDB11658 (HMDB)
6.7	340.0869	164.0474, 113.0001	4.6	↑	0.290	5-Hydroxy-6-methoxyindole glucuronide	HMDB10363 (HMDB)
7.0	431.0875	255.0444, 199.0519	4.3	↑	0.015*	Daidzein 4'-*O*-glucuronide	HMDB41717 (HMDB)

7.6	447.0835	271.0399, 91.0316	2.9	↑	0.044*	Genistein 5-*O*-glucuronide	HMDB41738 (HMDB)
8.0	146.0364	128.0260, 85.0284	3.0	↑	0.221	2-Keto-glutaramic acid	HMDB01552 (HMDB)
9.6	347.2061	121.0778, 105.0467, 91.0317	2.1	↑	0.050*	Corticosterone	HMDB01547 (HMDB)
10.3	701.5128	373.2208, 333.2260	2.0	↑	0.900	Unknown	-
5.3	154.0266	127.0155, 92.0268, 84.0586	3.2	↓	0.755	Unknown	-
6.3	206.0224	178.0267, 160.0156, 132.0208	4.3	↓	0.235	Xanthurenic acid	HMDB00881 (HMDB)
6.5	190.0268	162.0315, 144.0206, 116.0261	3.2	↓	0.664	Kynurenic acid	HMDB00715 (HMDB)
7.3	162.0316	144.0204, 134.0365	2.7	↓	0.006*	2,8-Dihydroxyquinoline	66378 (Metlin)
7.5	164.0470	146.0360, 118.0411	4.4	↓	0.008*	5-Hydroxy-6-methoxyindole	144618 (Chemspider)
8.7	255.0448	199.0528, 181.0418, 136.9998	4.2	↓	0.023*	Daidzein	HMDB03312 (HMDB)
8.7	285.0568	270.0324, 153.0461	2.5	↓	0.030*	Unknown	-
9.6	271.0402	152.9947, 91.0318	4.2	↓	0.035*	Genistein	HMDB03217 (HMDB)
10.1	373.2597	355.2486, 213.1415, 159.0931, 145.0775	2.7	↓	0.096	Prostaglandin derivative	-
10.2	371.2441	353.2316, 211.1254, 145.0772	2.8	↓	0.020*	Prostaglandin derivative	-

*Significant level < 0.05, calculated using ANOVA.
#The level of biomarkers in treated (T) and control (C) urine samples was evaluated by their normalized area. ↑: higher amounts in treated group compared to control; ↓: lower amounts in treated group compared to control.

Table 9B. Variables related to treatment with cranberry extract, obtained from the PLS-DA model for UPLC-MS data acquired in negative ion mode.

R.T. (min)	Measured HR *m/z*	Significant fragments, *m/z*	VIP	Amount T *vs* C#	p-value	Putative identification	Compound ID (Database)
2.2	190.9951	161.9964, 144.9897, 110.9843	2.4	↑	0.900	Citric acid	HMDB00094 (HMDB)
5.4	188.9616	109.0049, 96.9363	2.9	↑	0.020*	Catechol sulfate	HMDB61713 (HMDB)
5.9	172.9663	160.0156, 151.9870, 93.0109	4.6	↑	0.600	Unknown	-
6.3	289.0184	209.0586, 135.0208, 112.9998	4.4	↑	<0.001*	4-Hydroxy-5-(3'-hydroxyphenyl)-valeric acid-3'-*O*-sulfate	HMDB59975 (HMDB)

6.7	241.9892	162.0311, 134.0120, 112.9997	2.2	↑	0.200	Unknown	-
6.7	178.0257	134.0360, 77.0181	2.0	↑	0.080	Hippuric acid	HMDB00714 (HMDB)
7.0	271.0058	191.0469, 147.0563, 96.9358	2.2	↑	<0.001*	5-(Hydroxyphenyl)-gamma-valerolactone-*O*-sulfate	HMDB59993 (HMDB)
7.0	461.1758	443.1646, 253.0284	5.4	↑	0.050*	Unknown	-
7.1	283.0612	121.0044, 102.9793	2.2	↑	0.020*	2-*O*-Benzoyl-D-glucose	HMDB34618 (HMDB)
7.7	332.9892	265.0974, 223.0852, 137.0355	4.6	↑	0.070	Unknown	-
7.8	297.0778	121.0407, 102.9792	3.9	↑	0.700	Benzoyl glucuronide	HMDB10324 (HMDB)
8.1	187.0727	123.9825, 96.9358	4.3	↑	0.200	Azelaic acid	HMDB00784 (HMDB)
6.4	211.9783	132.0203, 79.9341	7.7	↓	0.031*	Indoxyl Sulfate	HMDB00682 (HMDB)
8.7	253.0283	223.0167, 208.0289, 90.9950	5.0	↓	0.170	Daidzein	HMDB03312 (HMDB)
9.5	269.0239	159.0196, 133.0039	5.4	↓	0.060	Genistein	HMDB03217 (HMDB)
9.7	297.0931	145.0407, 107.0256	4.0	↓	0.150	Enterolactone	HMDB06101 (HMDB)
10.1	453.2759	409.2518, 325.1675	3.2	↓	0.080	Unknown	-

*Significant level < 0.05, calculated using ANOVA.
#The level of biomarkers in treated (T) and control (C) urine samples was evaluated by their normalized area. ↑: higher amounts in treated group compared to control; ↓: lower amounts in treated group compared to control.

Among the time x mass variables related to dietary intervention, none of them was identified as intact PAC-A, suggesting that only negligible amounts of such compounds are present in urine of the treated animals. However, two compounds, increased in urine after cranberry supplementation, were putatively identified as 4-hydroxy-5-(3'-hydroxyphenyl)-valeric acid-3'-O-sulfate and 5-(hydroxyphenyl)-gamma-valerolactone-O-sulfate, which can be related to the intestinal metabolism of PACs (Monagas et al., 2010). Other variables related to treatment were putatively identified as glucuronide derivatives of isoflavones, namely daidzein 4'-O-glucuronide and genistein 5-O-glucuronide, whose urinary amounts were significantly increased after cranberry

supplementation. Conversely, lower amounts of free genistein and daidzein (introduced with the standard diet) were detected in treated rat urine as compared to controls. Genistein and daidzein were provided mainly by soy from dietary sources, as confirmed by HPLC-MS/MS analysis of fodder (Figure 35).

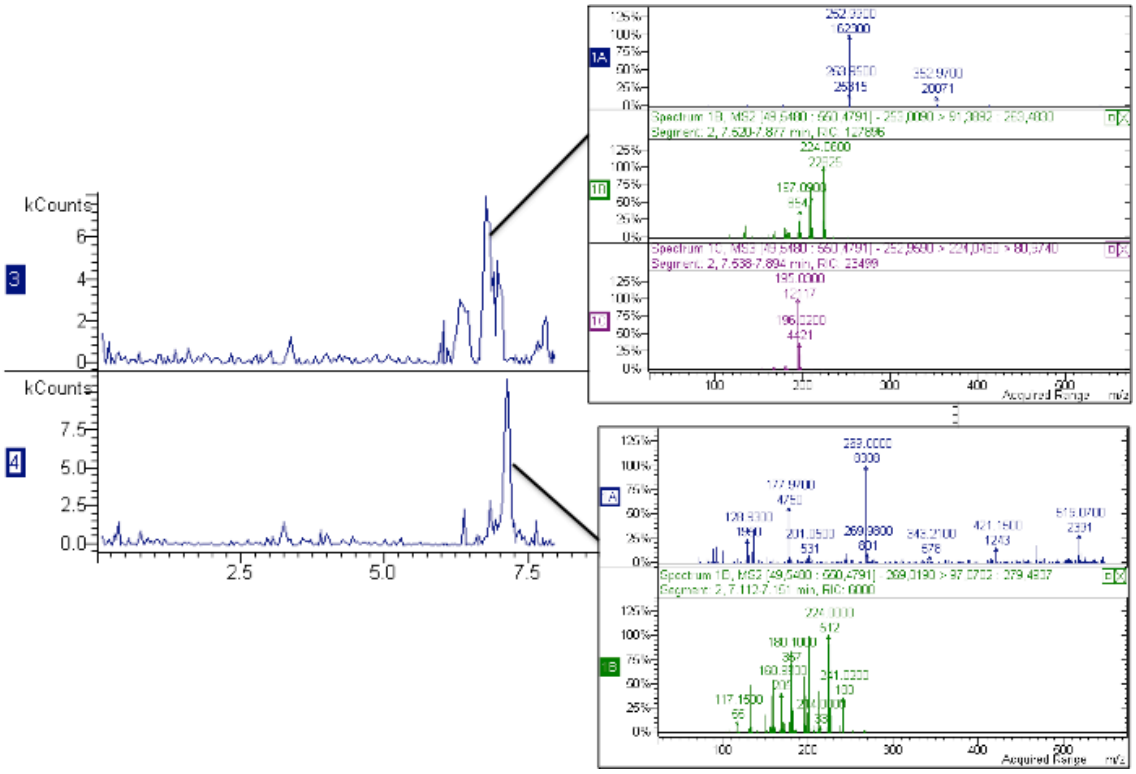

Figure 35. Selected Ion Monitoring chromatograms of daidzein (m/z 253, upper panel) and genistein (m/z 269, lower panel) in fodder. Respective MS/MS spectra are reported.

The same trend was observed for other two markers, namely 5-hydroxy-6-methoxyindole and 2,8-dihydroxyquinoline, a quinoline derivative found in urine of rats fed with fodder containing corn (Inagami et al., 1965). These data regarding induction of glucuronidation are in agreement with a previously published paper that demonstrated glucuronidation induction in ex vivo experiment (Bártíková et al., 2014). Catechol sulfate, benzoyl glucuronide (Pimpão et al., 2015) and hippuric acid (Lees et al., 2013) are considered biomarkers of polyphenols intake formed by intestinal microbiota, and they have been reported in urine. Our data showed a significant increased amount of the first and the last metabolite after treatment, while values were not statistically significant for benzoyl glucuronide.

Urinary amounts of tryptophan metabolites, namely xanthurenic and kynurenic acids and indoxyl sulfate, were influenced by treatment. Indoxyl sulfate, derived from

tryptophan metabolisation by colonic bacteria (Wikoff et al., 2009), showed significant decrease suggesting an influence of cranberry consumption on intestinal microbial activity.

2.1.3. Anti-adhesive properties of urine from animals treated with cranberry extracts

In order to study the anti-adhesive effects of urine samples after a single intake of cranberry, 6 healthy Sprague-Dawley rats were fed with a 100 mg/kg dose of cranberry extract (containing 15% total PACs) and urinary outputs were collected at 2, 4, 8 and 24 hours after treatment. Results showed a time dependent ability to decrease bacterial adherence to epithelial cells (Figure 36). The adherence of uropathogenic P-fimbriated *E. coli* incubated with urine samples collected at 2 and 4 hours after cranberry intake was not significantly changed compared to control urine. However, urine samples collected 8 hours after cranberry ingestion caused a significant reduction of *E. coli* adherence to HT-29 cells. A 47% reduction in *E. coli* binding was still evident by incubating bacteria in urine collected 24 hours after cranberry consumption.

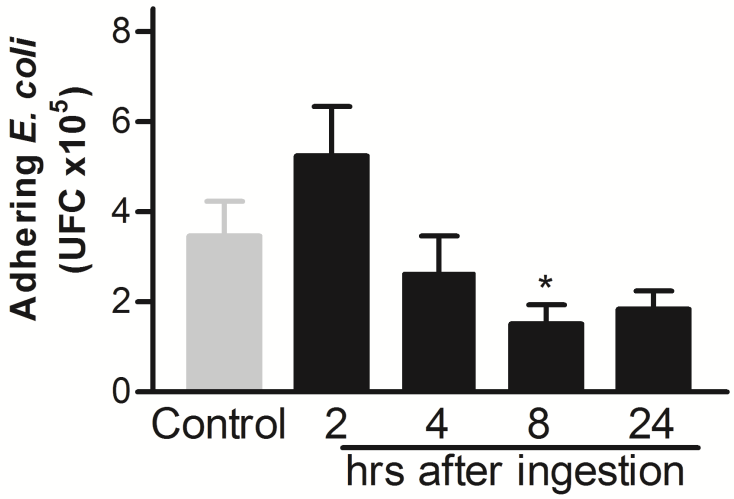

Figure 36. Histogram representing the adhering ability of uropathogenic *E. coli* to HT-29 epithelial cells after incubation in rat urine samples collected at 2, 4, 8 and 24 hours following oral treatment with 100 mg/kg cranberry extract or from untreated animals (control). Significance was calculated using t-test. The asterisk indicates a p-value <0.05.

2.1.4. Metabolomic profiling of urinary output at 2, 4, 8 and 24 hours after a single dose of cranberry

In order to evaluate the changes of urinary composition after a single intake of cranberry (100 mg/kg dose), the urinary outputs collected at 2, 4, 8 and 24 hours after treatment were analyzed by UPLC-QTOF. Control urine samples were collected from the same rats before treatment. Exploratory PCA analysis revealed limited differences, as reported in Figure 37 (R2 = 0.306; Q2 = 0.202). Considering the significant anti-adhesive activity measured for the 8 hours samples, data modeling was performed by PLS-DA comparing control samples *vs* 8 hours collection (Figure 37). The resulting model could explain 99% of the data variance using 3 components and the variance predicted was 73%. Y-axis intercepts after permutation test were R2 = (0.0, 0.992) and Q2 = (0.0, 0.333).

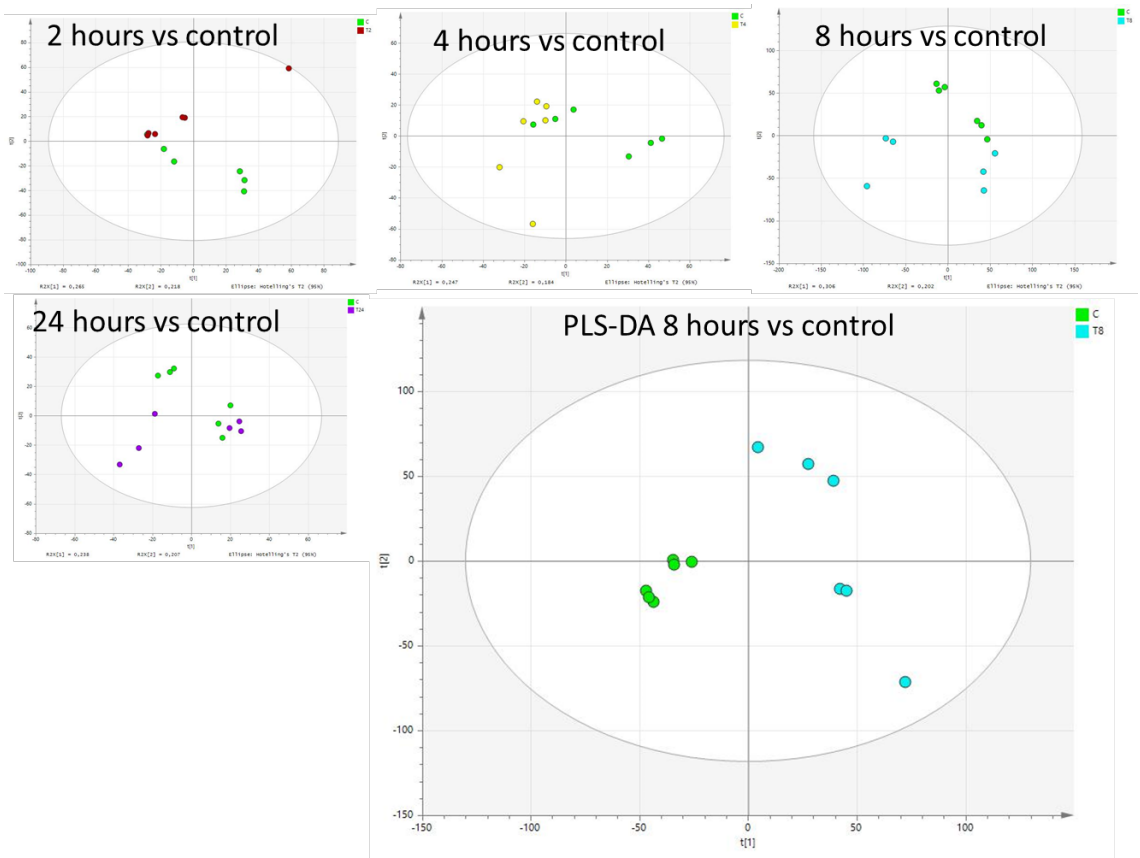

Figure 37. PCA exploratory plots obtained from urine analysis at 2, 4, 8 and 24 hours after cranberry administration to rats (T) compared to control (C). The PLS-DA score plot obtained with 8 hours data of treated group *versus* control is also reported.

Variables contributing to differentiate urine at 8 hours after treatment from control were identified as intestinal degradation products of PACs (Monagas et al., 2010), specifically vanillic acid 4-sulfate, epicatechin, 5-(hydroxyphenyl)-gamma-valerolactone-O-sulfate, 5-(3'-hydroxyphenyl)-gamma-valerolactone, 4-hydroxy-5-(3'-hydroxyphenyl)-valeric acid-3'-O-sulfate and 5-(3',4'-dihydroxyphenyl)-gamma-valerolactone (Table 10). None of the significant variables for the 8 hours samples was identified as intact PAC.

Table 10. Significant variables discriminating for urine samples collected at 8 hours after treatment with cranberry extract. Data were obtained from the PLS-DA model for UPLC-MS data acquired in negative ion mode.

VIP	Measured HR *m/z*	Significant fragments, *m/z*	R.T. (min)	Amount T *vs* C[#]	p-value	Putative identification	Compound ID (Database)
8.9	461.1816	285.0399, 267.0293, 135.0082	5.3	↑	0.002*	Kaempferol glucuronide	HMDB29500 (HMDB)
8.1	417.1140	241.0825 121.0290	6.3	↑	0.002*	Equol glucuronide	HMDB41732/41732(HMDB)
8.0	445.0734	269.0215	7.6	↑	0.002*	Genistein glucuronide	HMDB41738/41739 (HMDB)
7.9	429.0734	223.0162	4.3	↑	0.002*	Daidzein glucuronide	HMDB41717/41718 (HMDB)
4.4	160.0391	142.0496	4.0	↑	<0.001*	4,6-Dihydroxyquinoline	HMDB04077 (HMDB)
3.0	271.0058	191.0469, 147.0563, 96.9358	7.0	↑	<0.001*	5-(Hydroxyphenyl)-gamma-valerolactone-*O*-sulphate	HMDB59993 (HMDB)
2.3	191.0335	147.0583, 96.8655	4.6	↑	<0.001*	5-(3'-Hydroxyphenyl)-gamma-valerolactone	HMDB62066 (HMDB)
1.8	289.0184	209.0586, 135.0208, 112.9998	6.3	↑	<0.003*	4-Hydroxy-5-(3'-hydroxyphenyl)-valeric acid-3'-*O*-sulphate	HMDB59975 (HMDB)
1.7	247.0265	167.0606, 123.9969, 108.0111	3.0	↑	<0.001*	Vanillic acid 4-sulfate	HMDB41788 (HMDB)
1.1	289.1045	203.1114, 123.9971, 109.0549,	6.2	↑	0.002*	Epicatechin	HMDB01871 (HMDB)

0.6	207.0568	189.0504, 106.9703	4.8	↑	<0.001*	5-(3',4'-Dihydroxyphenyl)-gamma-valerolactone	HMDB29185 (HMDB)

*Significant level < 0.05, calculated using ANOVA.
#The level of biomarkers in treated (T) and control (C) urine samples was evaluated by their normalized area. ↑: higher amounts in the treated group compared to control; ↓: lower amounts in the treated group compared to control.

2.1.5. Quantification of PAC-A in urinary output at 2, 4, 6, 8 and 24 hours after single dose of cranberry

In order to evaluate the amounts of intact PAC-A in urinary outputs at 2, 4, 6, 8 and 24 hours after treatment, a targeted HPLC-MS/MS method was used. The chromatographic method allowed the detection of PAC-A dimers, trimers and tetramers in urine (a representative chromatogram is reported in Figure 38).

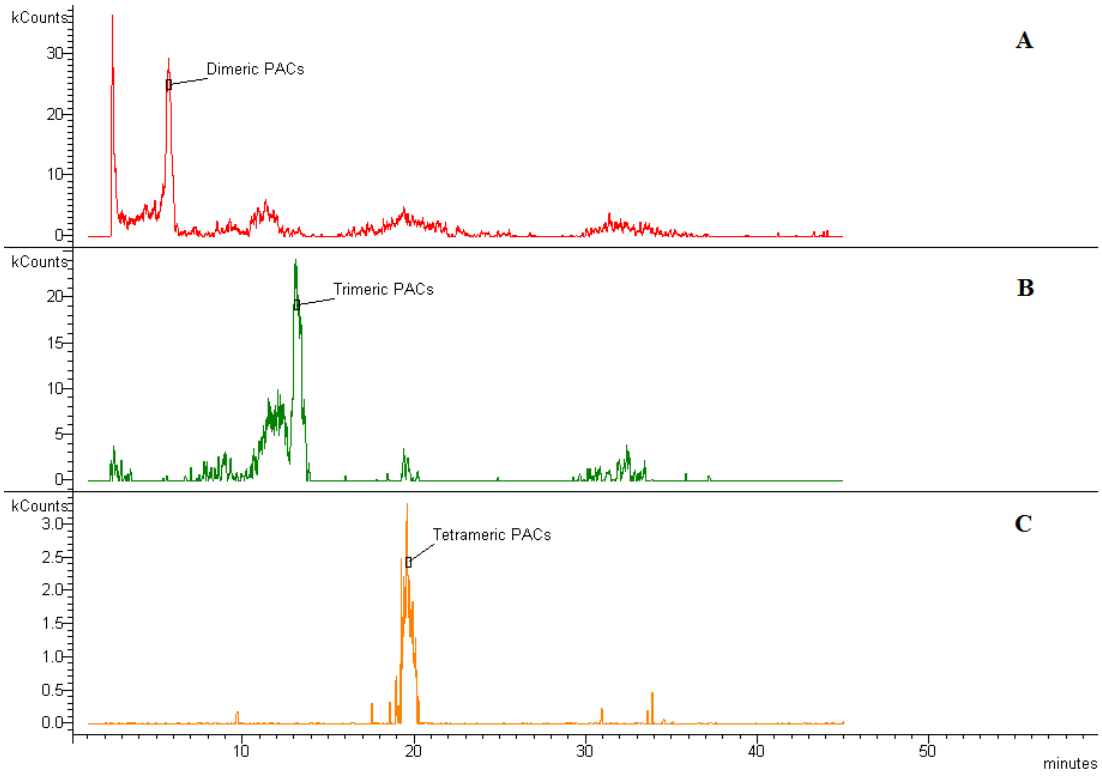

Figure 38. Multi Reaction Monitoring traces extracted from the analysis of rat urine spiked with cranberry extract. Track A shows dimeric PAC-A (m/z transition 575 > 285), track B shows trimeric PAC-A (m/z transition 863 > 289) and track C shows tetrameric PAC-A (m/z transition 1151 > 285).

Because of the lack of reference standards for trimeric and larger oligomeric PAC-A, the only available standard PAC-A dimer (PAC-A2) was used for the

quantification of dimers and an estimation of the amount of other oligomeric derivatives. Before HPLC-MS/MS analysis, urine was purified from low molecular weight polyphenols (Wallace and Giusti, 2010), in order to increase mass spectrometric sensitivity in PACs detection; the method allowed us to detect PAC-A2 down to 0.2 ng/mL in urine. Measurements on urine samples collected 24 hours after the administration of cranberry extract resulted in an average PAC-A2 concentration of 1.58 ± 0.44 ng/mL. The highest concentration of intact PAC-A2, 4.04 ± 2.87 ng/mL, was found at 4 hours after cranberry administration while in the control group, PAC-A was not detectable. Figure 39 summarizes the results. No other PAC-A or PAC-B were revealed.

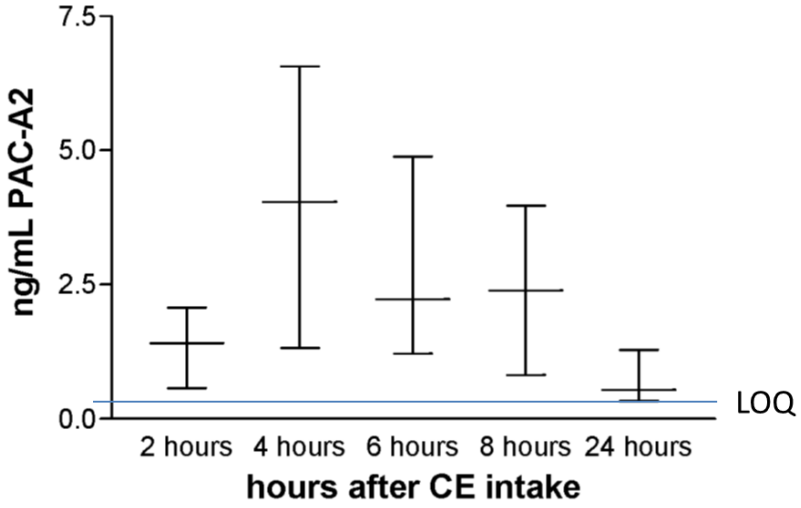

Figure 39. Urinary PAC-A2 amounts at 2, 4, 6, 8 and 24 h after cranberry extract administration to rats. Values are reported as means ± SD, LOQ is indicated in figure.

2.1.6. Discussion

In this study, the effects of supplementation of healthy rats with a cranberry extract containing 15% PACs were observed by monitoring the changes of urinary metabolome. In a first experiment, healthy rats were orally supplemented with 100 mg/kg of cranberry extract daily (11.3 mg/kg PAC-A; 4.3 mg/kg PAC-B) for 35 days and 24-h urinary outputs were collected weekly. The metabolic composition of urine was explored by a UPLC-QTOF metabolomic approach. We observed changes in urine composition after treatment using both unsupervised and supervised techniques and markers related to treatment were identified. Significant induction of glucuronidation

was observed, as demonstrated by increased amounts of isoflavone glucuronides and decreased amounts of aglyconic isoflavones in urine samples. These findings are in agreement with a previously published paper (Bártíková et al., 2014), which describes the treatment of Wistar rats with cranberry extracts in doses of 0.5 mg for 14 days or 1.5 mg of proanthocyanidins/kg/day for 1 day. Results showed that both cranberry dosages significantly enhanced microsomal UDP-glucuronosyl transferase activity, and long-term consumption of a regular dose had more pronounced effects on enzymatic activity than a short-term overdose (Bártíková et al., 2014). Thus, our data confirm that the induced glucuronidation activity should be further investigated, considering the large use of cranberry in food supplements and because of the possible use by subjects during other pharmacological treatments.

Changes in metabolites related to tryptophan, such as xanthurenic and kynurenic acids and indoxyl sulfate (this latter related to colonic bacteria catabolism) were also observed, suggesting a role of cranberry constituents on microbiota activity.

Increased levels of cranberry-derived metabolites were also detected, namely 4-hydroxy-5-(3'-hydroxyphenyl)-valeric acid-3'-O-sulfate and 5-(hydroxyphenyl)-gamma-valerolactone-O-sulfate. Conversely, none of the variables describing the effect of treatment were identified as intact PAC-A.

In a second experiment, rats were fed with a single dose of cranberry extract and urine samples were collected after 2, 4, 8 and 24 hours. These samples were used to perform adhesion assays, by treating uropathogenic E. coli, showing the highest activity 8 hour after cranberry ingestion. In order to establish the role of intact PAC-A on activity, samples were analyzed using a specific targeted LC-MS/MS method. Urinary PAC-A2 levels were measured in the collected urine samples (at 2, 4, 8 and 24 hours after cranberry administration) of the treated group and the results showed levels in the range of ng/mL (the highest concentration detected was 4.04 ± 2.87 ng/mL at 4 hours after cranberry administration). The LC-MS/MS results indicated negligible quantities of unmodified compound detectable in urine. Those levels are far from the concentration used in previous *in vitro* tests demonstrating the anti-adhesive properties of PAC-A. Foo and collaborators described the anti-adhesive effects of some PAC-A oligomers isolated from cranberry using an *in vitro* model and the activity was observed with concentrations higher than 0.3 mg/mL (Foo et al., 2000). Our data show that a single administration of 100 mg/kg of extract (15 mg/kg of PACs) yielded in a maximum amount of 4.04 ± 2.87 ng/mL 4 hours after cranberry intake. This amount is

six orders of magnitude lower than the previously published data (Foo et al., 2000). Gupta and collaborators observed a dose dependent anti-adhesive activity of cranberry in an *in vitro* model in the range of 5 to 74 μg/mL, still much higher than the values we measured (Gupta et al., 2007). In a previously published paper, female Fischer-344 rats were treated for 10 months with cranberry extract via gavage (1 g/kg body weight, 1 gavage/day, five days a week) and urine samples were collected at 18, 25, 42, 48 hours after cranberry administration (1 gavage) (Rajbhandari et al., 2011). The authors reported that intact PAC-A2 was detected at ng/mL, although the exact concentration was not specified (Rajbhandari et al., 2011).

In our experiment, an untargeted metabolomics approach revealed slight differences among urine samples collected at different times after cranberry administration. Furthermore, the results of adhesion assays, performed by treating uropathogenic *E. coli* with the same urine samples, showed the highest activity 8 hour after cranberry ingestion. Significant differences in the composition of urine samples collected at 8 hours with respect to control samples were observed. Among the identified metabolites, kaempferol glucuronide, equol glucuronide, daidzein and genistein glucuronides were the most discriminant ones, confirming the induction of glucuronidation observed in the first dataset. Furthermore, significant descriptors related to PACs and phenolic metabolites were identified, namely vanillic acid 4-sulfate, epicatechin, 5-(hydroxyphenyl)-gamma-valerolactone-O-sulfate, 5-(3'-hydroxyphenyl)-gamma-valerolactone, 4-hydroxy-5-(3'-hydroxyphenyl)-valeric acid-3'-O-sulfate and 5-(3',4'-dihydroxyphenyl)-gamma-valerolactone. These latter metabolites derived from intestinal degradation of procyanidins (Monagas et al., 2010), showing their extensive microbial degradation prior to absorption in the intestinal lumen.

In conclusion, metabolomics was a valuable tool to explore cranberry bioactivity. The changes induced by oral consumption of cranberry extract were explored in urine considering their entire metabolic composition. An untargeted approach showed that procyanidins from cranberry are poorly absorbed by the intestine and are extensively metabolized by gut microbiota, leading to the excretion of negligible amounts of intact PAC-A; considering this, PAC-A cannot be directly related to the anti-adhesive effects of cranberry *in vivo*. Furthermore, an influence on the glucuronidation of isoflavones was observed in the treated group, supporting an induction of glucuronidation after cranberry administration. The anti-adhesive activity of urine samples collected at different times after oral cranberry administration was studied and the highest anti-

adhesive activity was observed for the sample collected 8 hours after gavage. Metabolomic analysis revealed the presence of polyphenol-derived microbial catabolites. These metabolites could play a crucial role against *E. coli* adhesion to epithelial cells and they can be, at least in part, responsible for cranberry activity.

Due to the fact that cranberry supplements are intended for a preventive activity in humans, we decided to reproduce the supplementation experiment in a small number of healthy human volunteers. This further trial was intended also to obtain more detailed information about the absorption, metabolism and excretion of cranberry phytoconstituents in humans and about their bioactivity.

2.2. Supplementation of healthy volunteers with a standardized dry cranberry extract

2.2.1. Phytochemical analysis of cranberry extract and urine collection

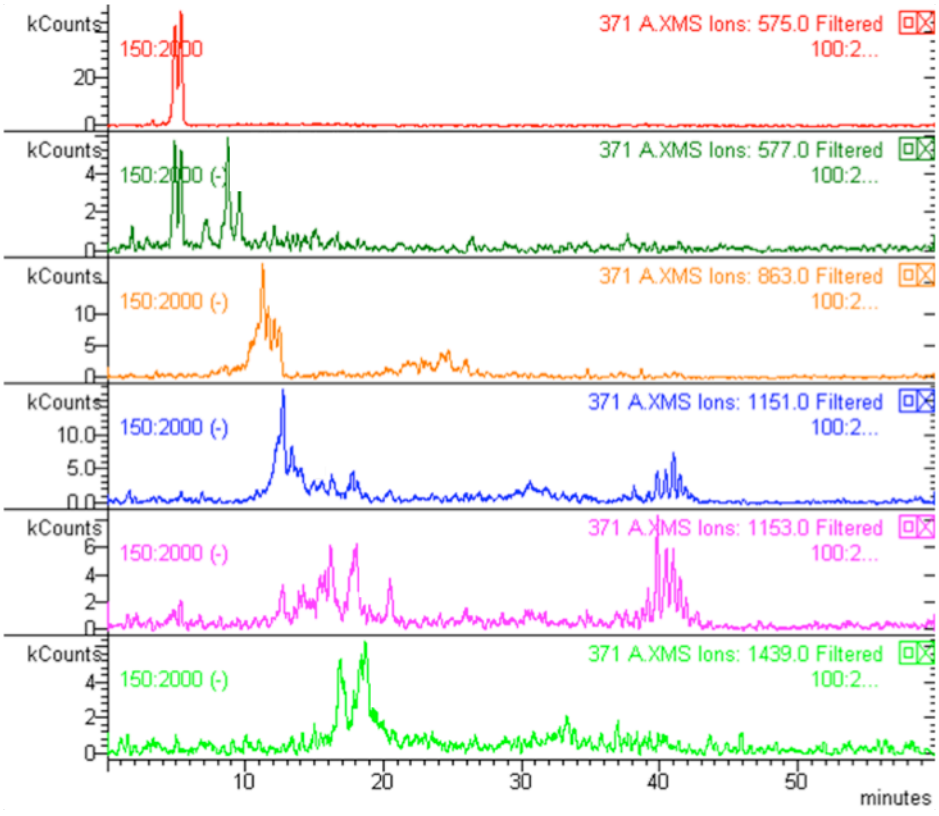

Figure 40. Selected Reaction Monitoring traces of PACs in cranberry extract. Red: dimeric PAC-A; dark green: dimeric PAC-B; orange: trimeric PAC-A; blue: tetrameric PAC-A; violet: tetrameric PAC-B; light green: pentameric PAC-A.

The phytochemical analysis revealed the presence of PAC-A and flavonoid derivatives in the product. The amount of procyanidins for one supplement sachet was 105.7 ± 2.2 mg, namely 60% w/w of total cranberry extract. The relative percentage of PAC-A oligomers was 72.7 ± 3.1%, corresponding to 42.6% w/w of cranberry extract, whereas the relative amount of PAC-B oligomers was 27.3 ± 2.1%, corresponding to 14.6% w/w of extract. The characterization of PACs in the extract is reported in Tables 11 and 12, and representative chromatograms are reported in Figure 40. A- and B-type pentamers and hexamers were identified and quantified as a single molecular species, due to peak overlapping (traces not reported in the Figure 40). The total amount of quercetin aglycone for one sachet was 100 mg, but also quercetin glycosides (190 mg/sachet) and myricetin glycosides (133 mg/sachet) were present (Table 13).

Table 11. Characterization of PACs amounts in the product.

Constituents	**Amount (mg/sachet)***
Catechin	6.6±0.3
PAC Dimers and trimers	15.4±0.5
PAC Tetramers	17.9±0.1
PAC Pentamers and hexamers	15.7±0.2
PAC > Hexamers	50.1±1.1
Total PAC amount	**105.7±2.2**

*Values are reported as means ± SD

Table 12. Relative amounts of PAC-A and PAC-B in dry cranberry extract.

PAC type	**Relative % on total PAC amount***	**Amount (mg/sachet)***
A, dimers	20.9±0.3	22±0.3
B, dimers	3.9±1.4	4.1±1.0
A, trimers	18.8±0.6	19.8±1.0
Other PAC-A	33.0±2.3	34.9±1.1
Other PAC-B	23.4±0.7	24.7±1.1

*Values are reported as means ± SD

Table 13. Amount of flavonoid derivatives in used product.

Flavonoid derivative	Amount (mg/sachet)*
Myiricetin galactoside	49.7±0.5
Myiricetin pentoside	12.8±0.4
Quercetin galactoside	97.5±0.2
Quercetin pentoside	35.5±0.3
Dimethoxymyricetin hexoside	14.0±0.3
Quercetin rhamnoside	43.6±0.3
Myricetin	69.8±0.3
Methoxyquercetin pentoside	4.2±0.3
Quercetin	103.7±0.8
Quercetin-3-(6-benzoyl)-galactoside	10.8±0.2

*Values are reported as means ± SD

Urine samples were collected at selected times, namely 2, 4, 6, 8 and 24 h after cranberry consumption, and these specimens were studied for their anti-adhesive properties against uropathogenic *E.coli.*

2.2.3. Anti-adhesive activity of urine after cranberry consumption

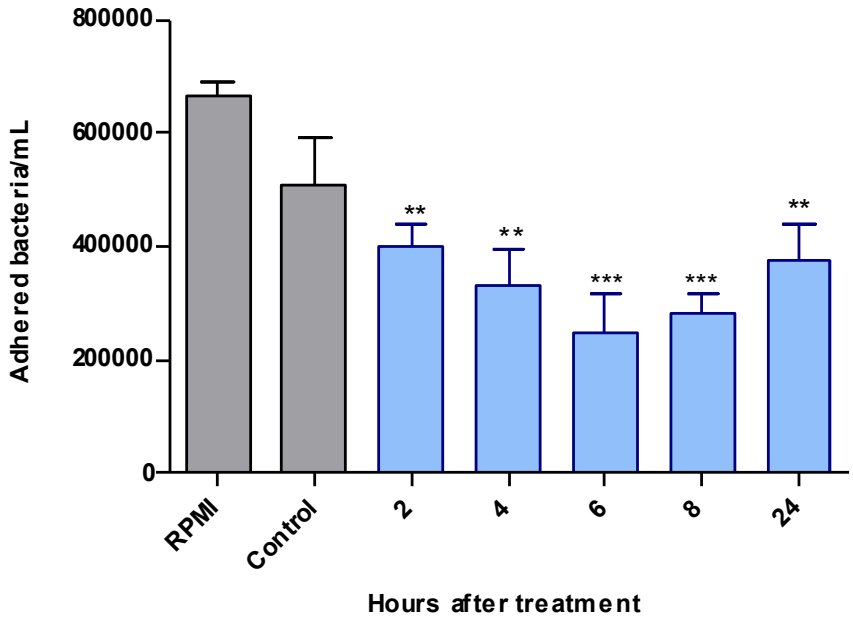

Figure 41. Histogram representing the ability of uropathogenic *E. coli* to adhere to HT-29 epithelial cells after incubation in urine samples collected at 2, 4, 6, 8 and 24 hours following oral cranberry consumption or in control samples. RPMI: untreated bacteria. ** indicates p-value < 0.01 versus RPMI, *** indicates p-value < 0.001 versus RPMI.

The urine samples were tested in anti-adhesion studies against uropathogenic *E. coli*. A time dependent capacity of urine to decrease bacterial adherence to HT-29 epithelial cells was observed (Figure 41). A slight reduction in bacterial adhesion was observed also testing control urine samples, although the anti-adhesive activity was not significant. Conversely, samples collected at 2, 4, 6, 8 and 24 hours after cranberry consumption revealed a significant inhibition of *E. coli* adhesion, being the ones collected at 6-8 hours the most active.

2.2.4. Metabolomics profile of urine after supplement consumption

Untargeted metabolomics analysis of the active urinary outputs was performed, to explore their composition. Urine samples collected after treatment were compared to the urine of same subjects collected before product consumption (controls).

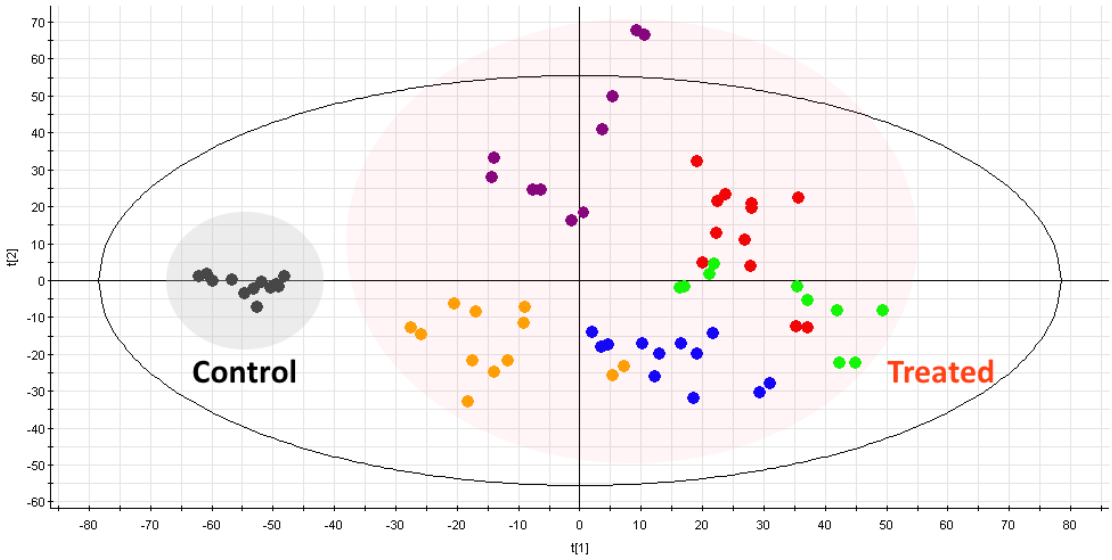

Figure 42. PLS-DA showing differences in metabolic composition of urine before and after cranberry consumption. Control urine samples are represented by black dots, treated urine samples by colored dots. Different collection times are represented by differently colored symbols in the plot: red, 2 h; green, 4 h; blue, 6 h; orange, 8 h; violet, 24 h.

The dataset used to build the multivariate models consisted of 2565 time x mass variables. Urine samples collected during the experiment were analyzed by an explorative PCA, that revealed no presence of outliers and a tight grouping of QC samples in a segregated cluster, indicating the robustness of the metabolic profiling platform. Nevertheless, the same model did not show any distinction between urine

samples collected before and after supplement consumption (data not shown). Thus, data were further analyzed by a supervised PLS-DA. The obtained model was composed by 3 principal components, and R2 and $Q2_{7\text{-fold CV}}$ were respectively 0.51 and 0.38. The score plot of the obtained model (Figure 42) shows a grouping of control and treated urine samples in two distinct clusters, due to differences in metabolic composition related to treatment. This first result clearly shows a significant modification of urinary output after product administration. Furthermore, the same PLS-DA model shows that, within the "treated" cluster, urine samples collected at different times after cranberry consumption are distinctly grouped, meaning that metabolic composition of urinary output changed through time after supplement intake. To better evaluate the differences among these samples, a second PLS-DA model was built, excluding controls. The resulting plot (Figure 43), composed by 2 orthogonal components (R2 = 0.82; $Q2_{7\text{-fold CV}}$ = 0.20), shows that urine samples collected at 6, 8 and 24 h after cranberry consumption form three separate clusters, while samples at 2 and 4 h are partially superimposed, due to negligible variations in their metabolic composition.

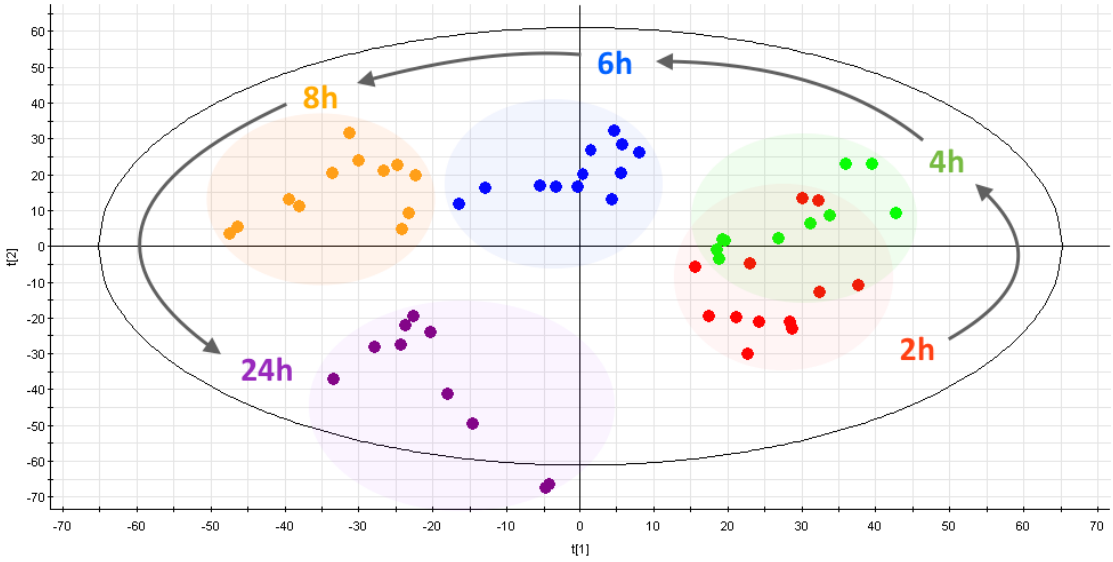

Figure 43. PLS-DA showing differences in metabolic composition of urine samples collected at 2, 4, 6, 8 and 24 hours after cranberry consumption. Control samples were not included in the model. Different collection times are represented by differently colored symbols in the plot: red, 2 h; green, 4 h; blue, 6 h; orange, 8 h; violet, 24 h.

Time x mass variables related to treatment and contributing to the differentiation of the groups at 6, 8 and 24 hours were selected based on their VIP value, and only

variables with VIP > 1 were considered. None of them was identified as intact PAC-A, PAC-B or their phase II metabolites, suggesting that only negligible amounts of such compounds were excreted with the urine after treatment. Nevertheless, many variables were identified as intestinal degradation products of PACs or other polyphenols (Mena et al., 2017, Monagas et al., 2010), as reported in Table 14. Specifically, the amounts of propionic acid, valeric acid and valerolactone derivatives and benzoic acid were found increased in 6 and 8 hours' urine compared to 2 and 4 hours urine, along with O-methoxycatechol-O-sulphate and vanillin 4-sulphate, whose could be more generally referred to polyphenols intake (Neveu et al., 2010, Van Der Hooft et al., 2012). In 24 hours urine, increased levels of vanillic acid and its glycine-conjugated derivative and 3-hydroxyhippuric acid, also related to intestinal degradation of PACs (Monagas et al., 2010), were detected. Based on these results we could observe that, after cranberry consumption, PACs are extensively metabolized by intestinal microbiota and metabolites are excreted with the urine, thus reaching the lower urinary tract.

Table 14. Significant (p-value < 0.05) ariables related to treatment with cranberry extract at 6, 8 and 24 hours after supplement consumption

6 hours					
VIP	**R.T. (min)**	**$[M-H]^-$ (*m/z*)**	**Amount *vs* 2-4 h***	**Tentative identification**	**Database ID (HMDB)**
4.85	3.19	181.0490	↑	3,4-Dihydroxyphenylpropionic acid	HMDB00423
4.04	3.18	121.0287	↑	Benzoic acid	HMDB01870
2.17	5.25	369.1188	↑	4-Hydroxy-5-(phenyl)-valeric acid-O-glucuronide	HMDB59980
1.41	3.88	207.0654	↑	5-(3',4'-Dihydroxyphenyl)-γ-valerolactone	HMDB29185
1.40	4.48	165.0544	↑	3-(3-Hydroxyphenyl)propanoic acid	HMDB00375
8 hours					
6.27	4.00	203.0012	↑	O-methoxycatechol-O-sulphate	HMDB60013
3.79	3.63	273.0072	↑	4-Hydroxy-5-(phenyl)-valeric acid-O-sulphate	HMDB59981
2.63	3.62	193.0497	↑	3-Hydroxyphenyl-valeric acid	HMDB41666
2.36	3.12	230.9960	↑	Vanillin 4-sulphate	HMDB41789
1.25	7.26	363.2164	↑	5-(4'-Hydroxyphenyl)-gamma-valerolactone-4'-O-glucuronide	HMDB59992

1.24	3.75	289.0334	↑	4-Hydroxy-5-(3'-hydroxyphenyl)-valeric acid-3'-O-sulphate	HMDB59975
24 hours					
10.99	3.17	224.0559	↑	Vanilloylglycine	HMDB60026
2.60	2.94	167.0339	↑	Vanillic acid	HMDB00484
2.33	4.41	194.0451	↑	3-Hydroxyhippuric acid	HMDB06116

[#]The levels of biomarkers were evaluated by their normalized area. Significant level < 0.05, calculated using ANOVA. ↑: higher amounts compared to 2-4 h urine samples.

2.2.5. Quantification of PAC-A in urine after consumption of cranberry extract

Due to its supposed anti-adhesive activity, the amounts of intact PAC-A were monitored in urinary output after cranberry consumption, using a specific HPLC-MS/MS method. The method, using TQD mass spectrometry, allowed sufficient sensitivity with a LOD of PAC-A2 at 0.2 ng/mL. Before analysis, urine samples were purified using a Sephadex LH 20 resin, using acetone to elute PACs and using epigallocatechin gallate as internal standard. This procedure allowed the increase of the signal of procyanidins in mass spectrometric analysis, due to the reduction of noise generated by other constituents of the extract. Despite the high sensitivity of the method, PAC-A2 was not detected in urine, and its level was lower than LOD in all the collected samples. PAC-A2 could be detected in urine samples only after a second independent experiment, in which the same six volunteers enrolled in the first experiment took the same oral dose (360 mg) of cranberry extract, following the same procedure described above; urinary output was finally collected after an overnight (8 hours from supplement consumption). In this case, the average PAC-A2 concentration in urine was 0.40 ± 0.10 ng/mL, although an important inter-individual variability was observed. Intact PAC-A2 amounts were higher and detectable in these overnight urine samples because no other collections were previously performed, unlike the previous experiment. Representative chromatograms are reported in Figure 44.

Overall, the results show that, after an oral intake of a single dose of dry cranberry extract, only negligible amounts of intact PAC-A reached the urine.

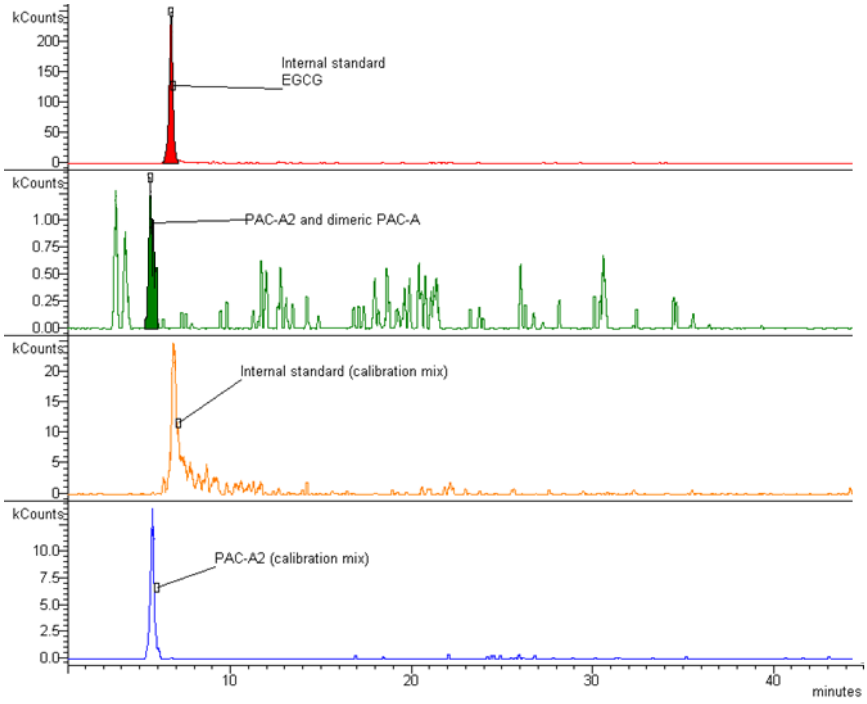

Figure 44. Comparison of chromatograms obtained from the analysis of PAC-A2 in urine samples collected at 8 hours (overnight) after cranberry consumption and chromatograms obtained from the analysis of a standard solution (calibration mix). Red and orange traces represents internal standard (epigallocatechin gallate) in samples collected after treatment and standard solution, respectively. Green and blue traces represents PAC-A2 in samples collected after treatment and standard solution, respectively.

2.2.6. HPLC-MS/MS determination of PAC-A degradation products in urine after treatment

Using a specific HPLC-TQD-MS/MS method, three metabolites deriving from microbial degradation of PACs were monitored in urine samples collected after cranberry consumption. The first two were 5-(3',4'-dihydroxyphenyl)-γ-valerolactone and 5-(4'-hydroxyphenyl)-γ-valerolactone-4'-O-glucuronide. Such compounds were selected from the discriminant variables for 6 and 8 hours urine samples in the untargeted analysis, respectively. Furthermore, also the sulfated derivative of 5-(4'-hydroxyphenyl)-γ-valerolactone was monitored, since Feliciano and coll. reported the detection of the same metabolite in human urine after consumption of cranberry juice (Feliciano et al., 2016).

Despite it was not feasible to perform a quantitative measurement, due to the absence of commercially available standards, an estimation of the compound was

obtained determining the area of peaks normalized on the creatinine amount in each urine sample. The analyses showed a time-dependent excretion of the metabolites, with a peak 6-8 hours after cranberry consumption (Figure 45). Moreover, the three metabolites could be still detected in urine samples collected 24 hours following cranberry consumption. Conversely, in control samples the three compounds were not detectable.

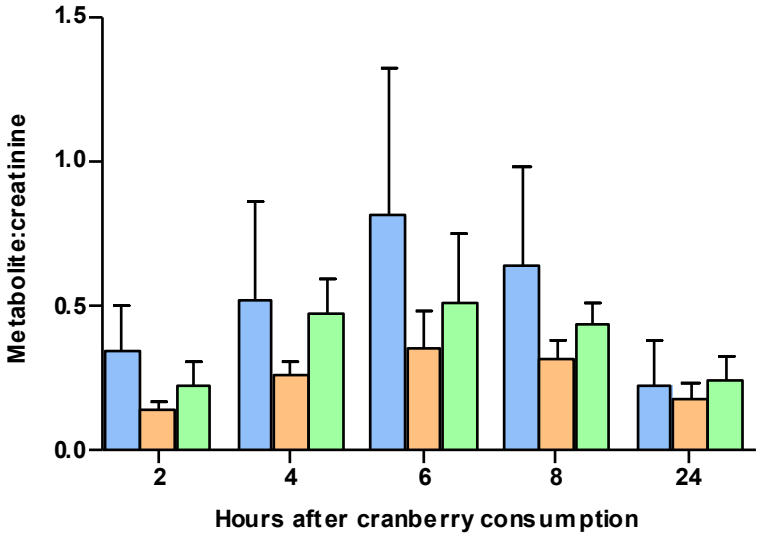

Figure 45. Urinary excretion of three selected PACs metabolites monitored by HPLC-MS/MS. Blue: 5-(4'-Hydroxyphenyl)-γ-valerolactone-O-sulfate; orange: 5-(4'-hydroxyphenyl)-γ-valerolactone-4'-O-glucuronide; green: 5-(3',4'-dihydroxyphenyl)-γ-valerolactone

2.2.7. Determination of quercetin, quercetin-sulfate and quercetin-glucuronide in urine after cranberry consumption

Quercetin and its sulfated and glucuronidated metabolites were monitored in urine samples using a specific HPLC-TQD-MS/MS method. After cranberry consumption, urinary amounts of un-metabolized quercetin were found to be low, i.e. C_{max} was 0.14 ± 0.10 μg/mL at 4 hours after supplement consumption (Figure 46). On the other hand, amounts of quercetin metabolites were found to be higher: C_{max} of sulfate derivative was 3.36 ± 1.31 μg/mL, C_{max} of glucuronidated was 0.46 ± 0.11 μg/mL, both at 4 hours after supplement intake. Results showed that quercetin is absorbed from cranberry after consumption of dry extract, but it is extensively metabolized mainly by phase II reaction and conjugated derivatives can be found at relatively high concentrations in

urinary output.

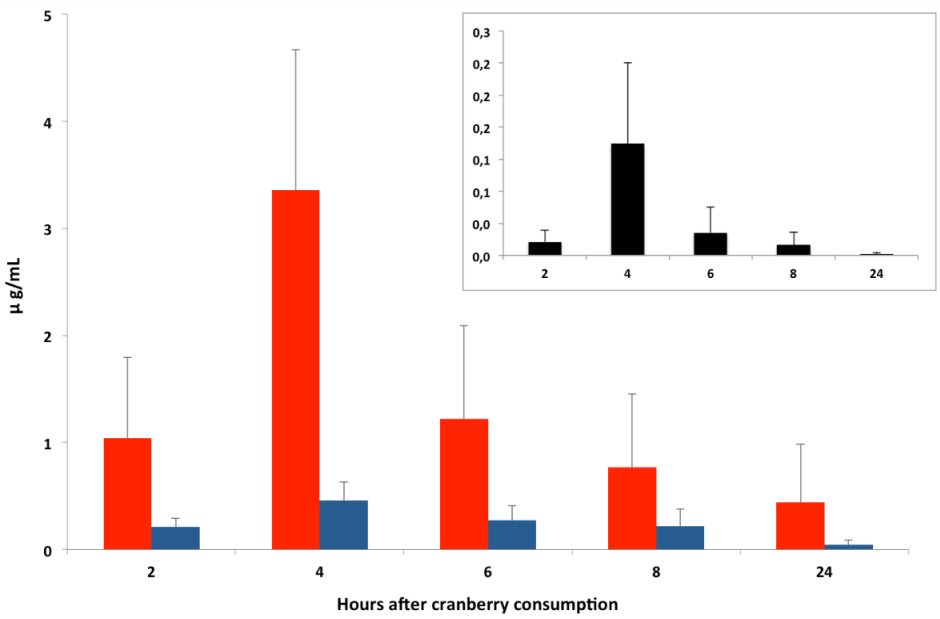

Figure 46. Urinary excretion of quercetin and two related metabolites, quercetin sulfate (red) and quercetin glucuronide (blue). Urinary levels of un-metabolized quercetin are reported in the box.

2.2.8. Discussion

The use of cranberry in the treatment of UTIs has become popular during the last years and cranberry activity has been attributed to its high content of A-type PACs, that could inhibit the adherence of uropathogenic bacteria to the urinary epithelium in µM concentration range (Gupta et al., 2012, Gupta et al., 2007, Howell et al., 2005, Polewski et al., 2016). Quercetin and its derivatives have also been considered as possible useful compounds, due to the antioxidant and anti-inflammatory effects (Fan et al., 2011). Furthermore, in a recent study several flavonoids have been also considered *in silico* as potentially active compounds against β-ketoacyl acyl carrier protein synthase I, an enzyme targeting the fatty acid synthesis in bacteria (Sabbagh and Berakdar, 2015).

Metabolomics offer the opportunity to explore the effects of complex mixtures in living organisms. Considering the cranberry extract, the putative active compounds (PAC-A) present limited intestinal absorption and extensive metabolism by gut microbiota (De Llano et al., 2015, Feliciano et al., 2016, Monagas et al., 2010). Consequently, several authors pointed out the possible role exerted by microbial

degradation products of PACs (phenolic acids and valerolactones, among the others) in the anti-adhesive activity of cranberry.

In this study, six healthy adult volunteers consumed 1 g of a dry cranberry extract standardized at 42.6% w/w of PAC-A and 14.6% w/w of PAC-B, flavonoid glycosides and quercetin aglycone (200 mg/dose). Here, the significant anti-adhesive activity of urine samples collected at 2, 4, 6, 8 and 24 hours after product consumption is reported, as well as their composition changes using a metabolomics approach. The anti-adhesive activity on *E. coli* tested against H29 human intestinal epithelial cells was higher in the samples collected at 6 and 8 hours, showing significant activity compared to controls. A PLS-DA analysis allowed the observation of grouping between control samples and urine collected after treatment. The PLS-DA model was re-processed excluding controls, and a clusterization of samples collected at different times was observed. Variables describing the model were identified as PACs degradation products, probably formed in the intestinal environment due to microbial catabolism. Several valeric acid and valerolactone derivatives were detected in 6 and 8 h urine samples, namely 4-hydroxy-5-(phenyl)-valeric acid-O-glucuronide and 5-(3',4'-dihydroxyphenyl)-γ-valerolactone at 6 hours and 4-hydroxy-5-(phenyl)-valeric acid-O-sulphate, 3-hydroxyphenyl-valeric acid, 5-(4'-hydroxyphenyl)-gamma-valerolactone-4'-O-glucuronide and 4-hydroxy-5-(3'-hydroxyphenyl)-valeric acid-3'-O-sulphate at 8 hours. Previously published studies reported the urinary excretion of such valeric acid and valerolactone derivatives after cranberry consumption in humans (Feliciano et al., 2016, Monagas et al., 2010), and these are related to the intestinal degradation of epicatechin, which in turn is formed by the depolimerization of PACs (Monagas et al., 2010). Mena and coll. recently reported that 5-(3',4'-dihydroxyphenyl)-γ-valerolactone and its sulfate conjugates, representative circulating metabolites of flavan-3-ols, exhibit anti-adhesive activity against uropathogenic *E. coli* in bladder epithelial cells (Mena et al., 2017). Testing the same urine samples used in the untargeted analysis against *E. coli*, we observed the highest anti-adhesive activity between 6 and 8 h after cranberry consumption, and these data correlated with the detection of valerolactone derivatives as the most descriptive variables, among whom 5-(3',4'-dihydroxyphenyl)-γ-valerolactone at 6 h. Furthermore, using a targeted HPLC-MS/MS approach, we monitored the amounts of three valerolactone derivatives, namely 5-(3',4'-dihydroxyphenyl)-γ-valerolactone and 5-(4'-hydroxyphenyl)-γ-valerolactone-4'-O-glucuronide, that were selected from the discriminant variables for 6 and 8-hours urine

samples in the untargeted analysis, respectively, and 5-(4'-hydroxyphenyl)-γ-valerolactone. The results showed that 6 and 8 h urine samples contained the highest amounts of these products. The same samples were the ones that showed the highest anti-adhesive activity against uropathogenic bacteria. Other variables for the 6 h urine samples were 3,4-dihydroxyphenylpropionic acid and benzoic acid, while for 8 h urine were 3-(3-hydroxyphenyl)propanoic acid, O-methoxycatechol-O-sulphate and vanillin 4-sulphate. Propionate derivatives could be related, as the valeric acid and valerolactone ones, to the intestinal degradation of PACs (Mena et al., 2017), as well as benzoic acid (Mena et al., 2017), although it could derive also from the degradation of several other polyphenols, as for O-methoxycatechol-O-sulphate and vanillin 4-sulphate (Neveu et al., 2010, Van Der Hooft et al., 2012).

A significant anti-adhesive activity was observed also testing urine samples collected 24 hours after cranberry consumption. Vanillic acid, its glycine conjugate and 3-hydroxyhippuric acid were detected as the discriminant variables, and they could derive from microbial degradation of PACs, being terminal products of this catabolic process (Monagas et al., 2010). By targeted HPLC-MS/MS analysis of the same 24 h samples, we detected 5-(3',4'-dihydroxyphenyl)-γ-valerolactone, 5-(4'-hydroxyphenyl)-γ-valerolactone-4'-O-glucuronide and 5-(4'-hydroxyphenyl)-γ-valerolactone, although their amounts were lower than those observed at 6 and 8 h. The co-administration of quercetin resulted in the observation of quercetin glucuronide and sulphate derivatives in urine, but their levels appear not to be related to the anti-adhesive properties, because their maximum concentration was observed at 4 hours after oral administration of the product, non-corresponding to the higher anti-adhesive activity. Limited data are available about quercetin glucuronide activity. In a recent study, the compound resulted able to suppress ear edema induced by dimethyl benzene and peritoneal permeability induced by acetic acid in mice (Fan et al., 2011). Other authors reported significant variations of quercetin activity after glucuronidation or sulphation and suggested that different metabolites can have lower effects than the parent compound. However, at least two of the major *in vivo* metabolites of quercetin retained significant activity for the inhibition of pro-inflammatory eicosanoids, such as LTB4 and PGE2 (Loke et al., 2008).

Intact PAC-A was not detectable in any of the collected urine samples, nor by untargeted metabolomics nor performing a specific HPLC-MS/MS analysis using an appropriate chromatographic method. PAC-A2 could be detected in urine only in a

different experiment, in which the same six volunteers took orally the same dose (360 mg) of cranberry extract and they collected urine samples after an overnight (8 hours from supplement consumption). In this case, the average urinary PAC-A2 concentration was 0.40 ± 0.10 ng/mL, meaning that only negligible amounts of intact PAC-A reach the urinary tract with urine. Those levels are far from the concentration used in previous *in vitro* tests demonstrating the anti-adhesive properties of PAC-A. The finding that we obtained confirms the results of previously published papers, showing only few ng (C_{max} = 24 ng/mg creatinine) of PAC-A in urine after cranberry consumption (McKay et al., 2015), or no detection of PAC-A at all (Feliciano et al., 2016). Hence, our data indicate that the anti-adhesive activity of urine after cranberry consumption could not be related to a direct effect of PAC-A on bacteria adhering to the HT29 cells. Metabolomics data indicate that it is related to the urinary excretion of PACs degradation products formed by catabolism of gut microbiota, or at least to a synergistic effect of small concentrations of intact PAC-A and smaller molecular weight compounds formed by its degradation. As observed in the animal experiments, excretion concentrations of intact PAC-A were six orders of magnitude lower compared to the PAC-A concentrations considered active as anti-adhesive (Foo et al., 2000). Thus, the previously demonstrated anti-adhesive properties of PAC-A oligomers could not be related to the *in vivo* effect of cranberry.

In conclusion, UPLC-MS-based metabolomics proved to be a useful and powerful tool to study phytochemical bioactivity of cranberry in humans. We observed changes in urine composition mainly due to small phenolics formed by extensive microbial catabolism, with the subsequent excretion of the derived products with the urine. The negligible amount of intact PAC-A excreted with urine cannot be correlated to the cranberry activity observed in our experiment, or at least the activity of cranberry is related to the interactions between its constituents and the degradation products formed by microbial catabolism. The highest anti-adhesive activity against *E. coli* correlated with the peaks of excretion of valerolactone derivatives, indicating that these gut microbiota-derived PACs metabolites are, at least in part, responsible of the observed effects.

3. Green coffee (*Coffea canephora*) bean extract

3.1. Characterization of the phytoconstituents of dry GCBE

As preliminary analysis, the dried extract was extracted in deuterated methanol and ^{1}H-NMR was acquired (Figure 47). Signals indicating the presence of caffeic acid derivatives were detected, namely the pair of doublets at δ 7.57 and 6.28 (J=16.7 Hz) ascribable to trans double bond, the aromatic signals at δ 7.06 (d, 1.8 Hz) and the partially overlapped signals at δ 6.85 and 6.80 (Bajko et al., 2016). Signals supporting the presence of quinic acid (δ 4.20; 3.85; 2.18 and 2.00) were also detected (Bajko et al., 2016), as well as the signals ascribable to caffeine (δ 7.87 and methyl groups at 3.37, 3.55 and 3.91).

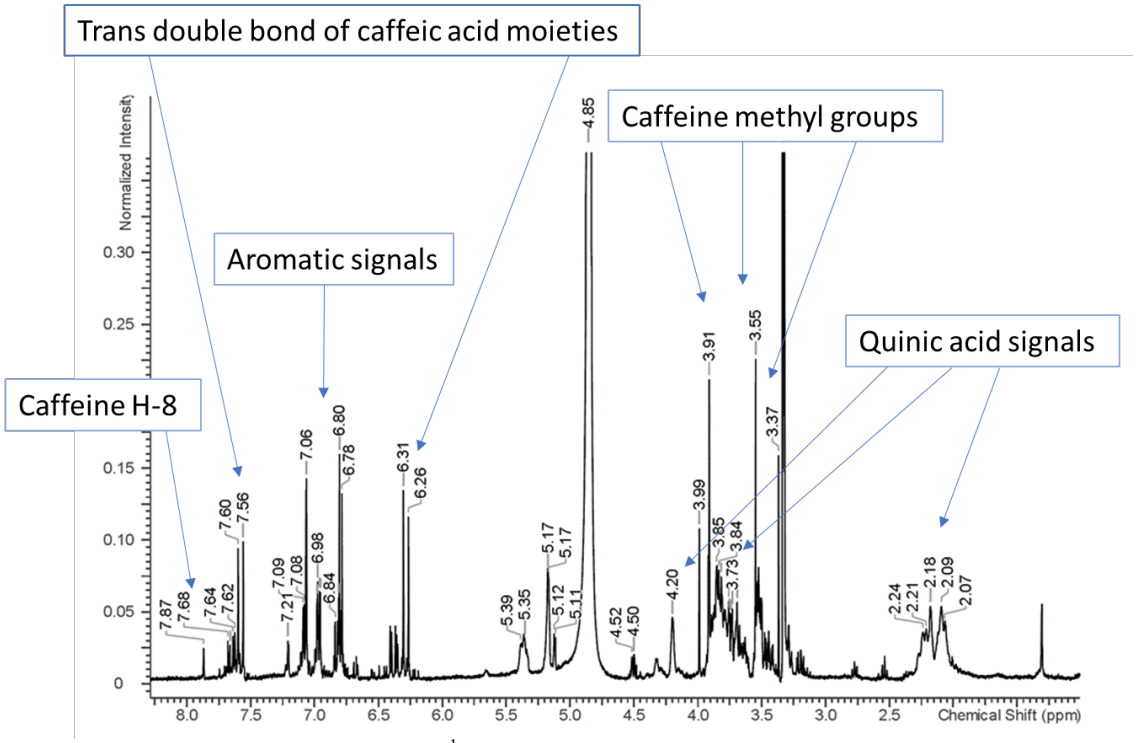

Figure 47. ^{1}H-NMR spectrum of the GCBE.

Further data were obtained using LC-DAD-ESI-MS^{n} in negative ionization mode. Twelve different phenolic compounds, mainly caffeoyl-quinic and feruloyl-quinic acids derivatives (Table 15 and Figure 48) were identified on the basis of their MS^{n} spectra and comparison with literature (Clifford et al., 2003, Clifford et al., 2005, Clifford et al., 2006, Clifford et al., 2008). Quantification was obtained using a diode array detector

and chlorogenic acid as reference compound. The most abundant constituents were 5-caffeoylquinic acid (5-CQA, 4.93± 0.50 w/w) and feruloylquinic acid (FQA, 1.059 ± 0.04 w/w), while hexahydroxydiphenoyl (HHDP)-hexoside was the less abundant (0.089 ± 0.01 w/w).

Table 15. Polyphenolic constituents of GCBE. Analysis was performed by HPLC-MS/MS in negative ion mode.

R.T. (min)	Compound	$[M-H]^-$ (*m/z*)	Fragments (*m/z*)	% (w/w)
9.3	3-CQA	353	191 85	0.593 ± 0.02
11.5	4-CQA	353	191 85	0.308 ± 0.04
11.8	5-CQA	353	173 93	4.93± 0.50
12.1	F pentoside	367	193 134 149	0.177 ± 0.01
12.7	Caffeic acid*	179	135	0.422 ± 0.06
13.5	FQA	367	191 85 111 127	1.059 ± 0.04
14.6	HHDP hexoside	481	301 257	0.089 ± 0.01
14.9	3,4-diCQA	515	353 335 191 179 173	0.520 ± 0.04
15.4	1,5-diCQA	515	353 191 179 173	0.304 ± 0.04
15.8	3,5-diCQA	515	353 191 173	0.437 ± 0.04
16.2	3-C-5-FQA	529	367 335 173 193 111 93	0.162 ± 0.01
16.8	3-F-4-CQA	529	353 367 173 93	0.150 ± 0.01
			Total amount	**9.15**

(R.T. = Retention Time; QA = quinic acid; diCQA = dicaffeoyl quinic acid; C =caffeoyl; F = feruloyl)
*: identification was performed comparing with reference compounds.

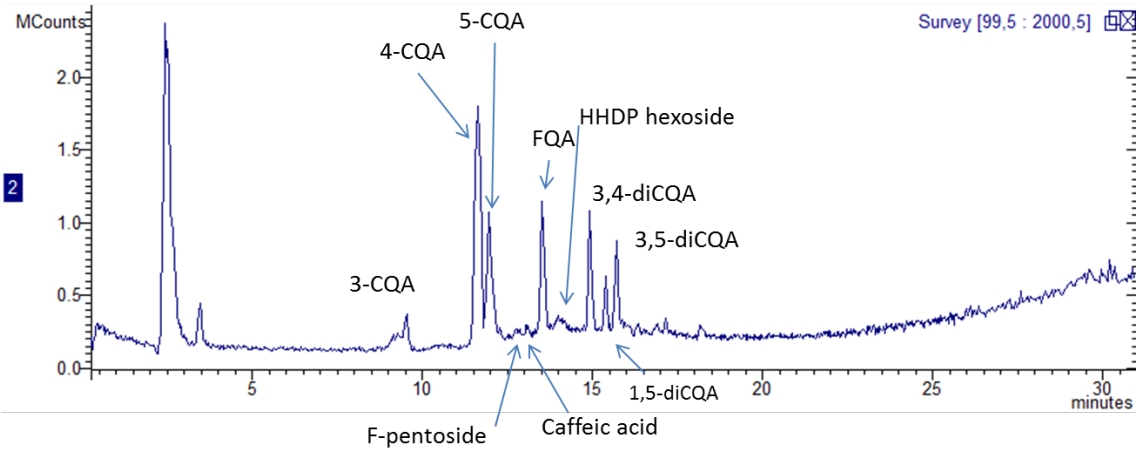

Figure 48. Representative chromatogram obtained from HPLC-MS/MS analysis of GCBE in negative ion mode.

Positive ionization mode was used to quantify caffeine and trigonelline (Table 16). Caffeine amount was 0.593 ± 0.02 % w/w, trigonelline one was 0.308 ± 0.04 % w/w.

Table 16. Amounts of trigonelline and caffeine in GCBE. Analysis was performed by HPLC-MS/MS in positive ion mode.

R.T. (min)	Compound	$[M+H]^+$ (*m/z*)	Fragments (*m/z*)	% (w/w)
2.6	Trigonelline	138	94 92	0.308 ± 0.04
12	Caffeine	195	138 110 83	0.593 ± 0.02
			Total amount	**1.01**

(R.T. = Retention Time)

3.2. UPLC-QTOF analysis of 24-h urine output using C-18 stationary phase

An untargeted approach was used to explore the changes in urine composition related to the consumption of GCBE. At first attempt, a chromatographic method using a C-18 column as stationary phase was developed. Exemplificative chromatograms are reported in Figure 49.

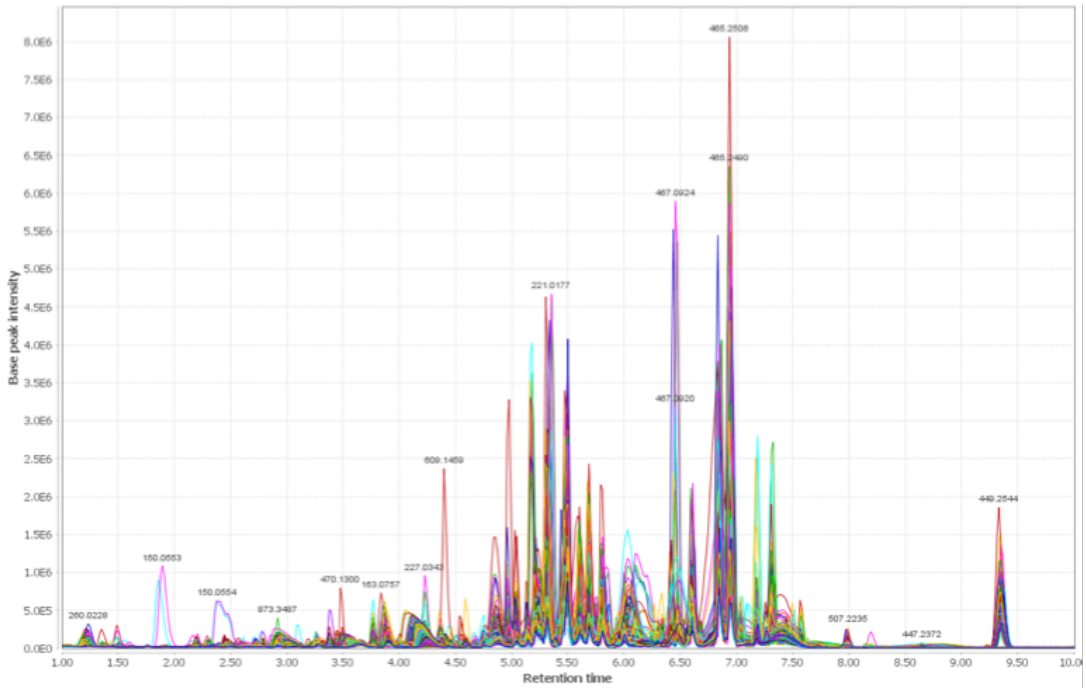

Figure 49. Exemplificative chromatograms obtained from LC-MS metabolomics profiling of urine collected after consumption of GCBE and control samples. Chromatograms were re-built using MZmine software.

At first attempt, LC-MS data were analyzed by explorative PCA, in order to detect the presence of outliers and to assess method robustness by the analysis of QC

samples. The models showed that 24-h urine samples collected from different subjects were partially grouped in different clusters. The PCA models for "positive" and "negative" datasets showed grouping of QC samples in tight clusters at the origin of the axes, confirming the robustness of the chromatographic method and of the metabolic profiling platform used (data not shown) (Vorkas et al., 2015).

The same datasets were further processed using supervised method, namely PLS-DA, using controls and urine samples collected during treatment as groups (Figures 50 and 51). The model built using data in positive acquisition mode was characterized by 3 components and R2 = 0.69 and $Q2_{7\text{-fold}}$ = 0.46. Similarly, the model built using the data acquired in negative ion mode was characterized by 3 components and R2 = 0.65 and $Q2_{7\text{-fold}}$ = 0.39. The two datasets (positive and negative) were composed by 4600 and 3000 variables, respectively, among whom significant descriptive ones for treatment were selected from loading plots depending on their VIP value. Only variables having VIP > 1 were considered. Two sets of 22 and 4 measured variables were detected as relevant in the explanation of the effects of treatment, from "positive" and "negative" datasets, respectively, and were tentatively identified based on their HR m/z value and considering their R.T. and fragmentation spectra (Table 17).

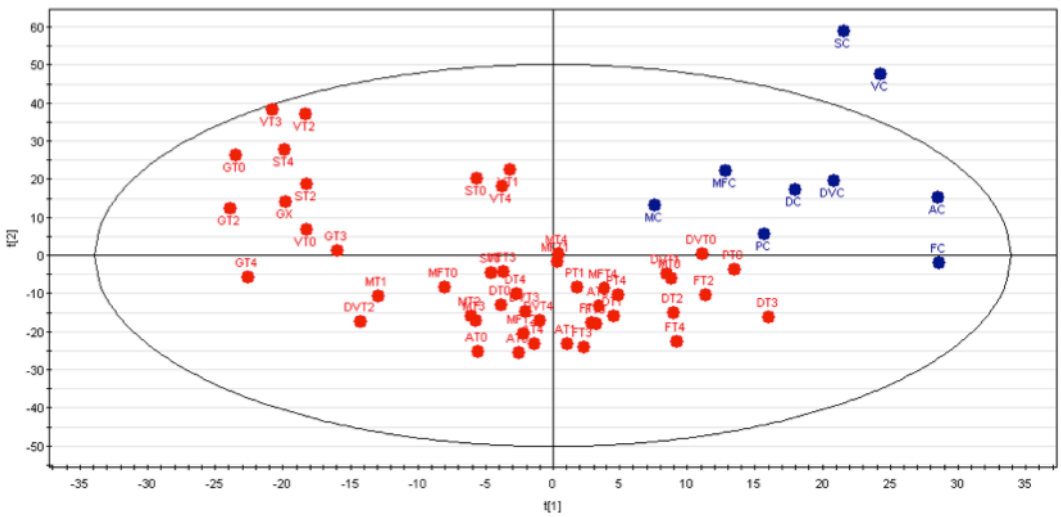

Figure 50. PLS-DA score plot obtained from UPLC-MS acquired in positive ion mode, using the C-18 stationary phase. Control (blue circles) and treated (red circles) urine samples collected during the experiment are represented in the plot. The acronyms reported in the plot represent sample names.

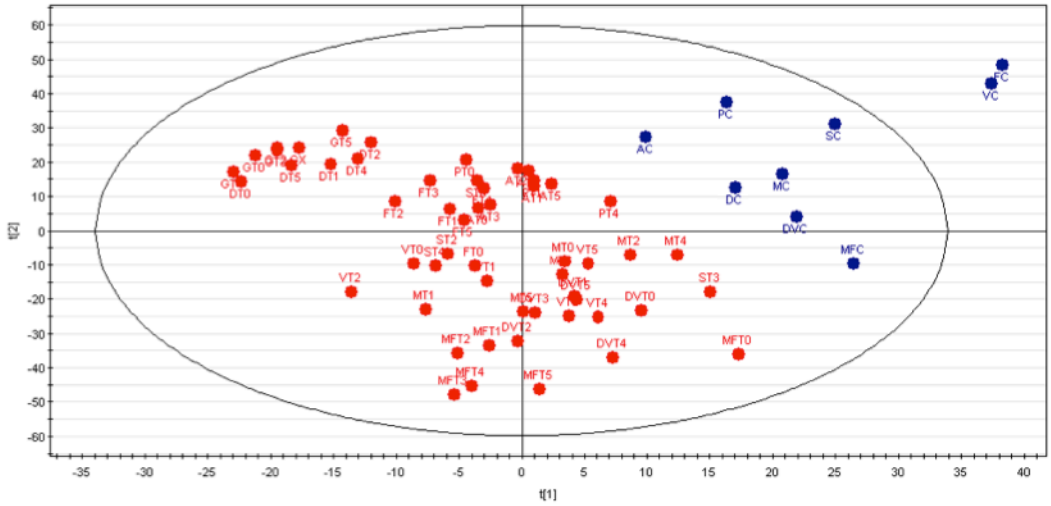

Figure 51. PLS-DA score plot obtained from UPLC-MS acquired in negative ion mode, using the C-18 stationary phase. Control (blue circles) and treated (red circles) urine samples collected during the experiment are represented in the plot. The acronyms reported in the plot represent sample names.

Benzoic acid, hippuric acid, 4-hydroxybenzoic acid, quinic acid and dihydrocaffeic acid sulfate amounts were increased in urine collected during treatment, compared to controls, and they can be considered as markers of consumption of CGA, along with isoferulic acid, p-coumaric acid, 3(3-hydroxyphenyl)propanoic acid and dihydrosinapic acid (Del Rio et al., 2010, Farah et al., 2008), whose amounts were increased in urine after supplement consumption. Significant traces of intact CGA were not present in urine after treatment, indicating that those compounds are extensively metabolized by gut microbiota and only derived catabolites could be detected. Other significant variables were tentatively identified as medium-chain (C8-C10) acyl-carnitines, whose amounts in urine were increased with intake of GCBE. Acyl carnitines are involved in the metabolism of fatty acids. Further compounds, namely 3-hydroxysuberic acid (3-hydroxyoctanedioic acid) and 3-hydroxyadipic acid (3-hydroxyhexanedioic acid) are metabolite derived from the ω-oxidation of 3-hydroxy fatty acids and the β-oxidation of longer-chain 3-hydroxy dicarboxylic acids (Tserng, 1991). They are normally found in blood and urine and their amounts are increased in ketoaciduria (Verhaeghe et al., 1992), so in conditions that may be related to starvation.

Table 17. Significant variables (p-value<0.05) related to treatment with GCBE, obtained from the PLS-DA model for the C-18 data (T>C means higher amounts in Treated than in Control, while T<C means higher amounts in Control than in Treated).

	Amount T *vs* C	**VIP**	**R.T. (min)**	**HR *m/z***	**Tentative identification (adduct ion type)**	**Database ID**
Positive						
	T > C	8.80	5.42	312.2177	2-trans,4-cis-Decadienoylcarnitine	HMDB13325
	T > C	6.30	3.60	123.0444	Benzoic acid*	HMDB01870
	T > C	6.20	5.09	286.2020	2-Octenoylcarnitine	HMDB13324
	T > C	4.50	3.60	202.0479	Hippuric acid ($[M+Na]^+$)	HMDB00714
	T > C	4.20	6.06	314.2332	9-Decenoylcarnitine	HMDB13205
	T > C	4.10	5.86	326.1968	3-Hydroxyoctanoylcarnitine ($[M+Na]^+$)	HMDB61634
	T > C	3.00	2.71	180.0884	3-Hydroxyadipic acid ($[M+NH_4]^+$)	HMDB00345
	T > C	2.70	6.24	338.2329	Decanoylcarnitine ($[M+Na]^+$)	HMDB00651
	T > C	2.50	4.42	139.0393	4-Hydroxybenzoic acid	HMDB00500
	T > C	2.40	5.27	330.2277	6-Keto-decanoylcarnitine	HMDB13202
	T > C	2.20	4.68	274.2018	Heptanoylcarnitine	HMDB13238
	T > C	2.10	2.95	195.0656	Isoferulic acid	HMDB00955
	T > C	2.00	5.73	288.2171	L-Octanoylcarnitine	HMDB00791
	T > C	1.90	5.52	444.3101	Gamma-linolenyl carnitine ($[M+Na]^+$)	HMDB06318
	T > C	1.80	4.55	302.1425	Hydroxyvalerylcarnitine ($[M+K]^+$)	HMDB13132
	T > C	1.70	5.07	374.2537	Dodecanedioylcarnitine	HMDB13327
	T > C	1.65	4.19	184.0969	3-(3-Hydroxyphenyl)propanoic acid ($[M+NH_4]^+$)	HMDB00375
	T > C	1.58	5.72	229.0502	3-Hydroxysuberic acid ($[M+K]^+$)	HMDB00325
	T > C	1.55	3.82	182.0808	*p*-Coumaric acid ($[M+NH_4]^+$)	HMDB41592
	T > C	1.50	4.36	330.2275	6-Keto-decanoylcarnitine	HMDB13202
	T > C	1.45	3.40	328.1588	3-Hydroxyhexanoyl carnitine	HMDB61633
	T > C	1.40	2.94	153.0549	4-Hydroxyphenylacetic acid	HMDB60390
Negative	T > C	2.80	4.25	227.0340	Quinic acid ($[M+Cl]^-$)	HMDB03072
	T > C	2.60	6.04	272.1290	Glutaconylcarnitine	HMDB13129
	T > C	2.32	3.43	207.0663	Dihydrosinapic acid ($[M-H_20-H]^-$	HMDB41727
	T > C	1.85	3.96	261.0064	Dihydrocaffeic acid sulfate	HMDB41721

*: identification was performed comparing with reference compounds.

3.3. UPLC-QTOF analysis of 24-h urine output using C-3 stationary phase

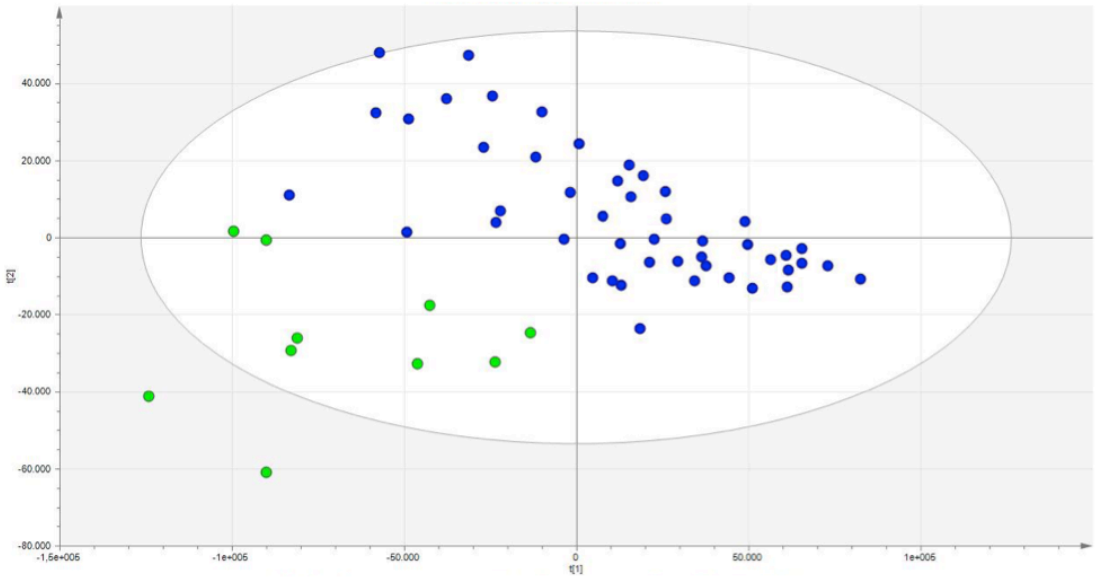

Figure 52. PLS-DA score plot obtained from HPLC-MS untargeted analysis of urine, using the C-3 stationary phase in positive ion mode. The plot was obtained using SIMCA 13 software. Control (green circles) and treated (blue circles) urine samples collected during the experiment are represented.

The same urine samples were analyzed by LC-MS using a C-3 column as stationary phase, in order to have different chromatographic behavior. Also in this case, an untargeted approach was used. Explorative PCA model did not show discrimination between "treated" samples and controls. The same model showed grouping of QC samples in tight clusters at the origin of the axes, confirming the robustness of the chromatographic method and of the metabolic profiling platform used (data not shown) (Vorkas et al., 2015).

To observe differences between control urine samples and ones collected during supplement consumption, the same dataset was processed using PLS-DA. The resulting model (characterized by 2 components and R2 = 0.69 and $Q2_{7\text{-fold}}$ = 0.32) can emphasize the differences in urine samples due to GCBE intake (the score plot is reported in Figure 52). Four variables were selected as significantly discriminating treated urine samples from controls (Table 18), and they were tentatively identified studying their fragmentation spectra and by comparison with web databases and literature data. Along with two acyl-carnitine derivatives (O-adipoylcarnitine and decanoylcarnitine), the other two variables were tentatively identified as acetone and

vanillic acid. Carnitine derivatives and acetone are related to fatty acids metabolism, while vanillic acid could be related to intestinal catabolism of CGA.

Table 18. Significant urinary variables (p-value<0.05) related to consumption of GCBE, detected by LC-MS metbolomics, using a C-3 stationary phase. Beside Retention Time (R.T., minutes), experimental *m/z* values and tentative identification, variations of the urinary amounts of each metabolite in treated urine samples (T) compared to controls (C) are reported.

Amount T *vs* C	**VIP**	**R.T. (min)**	***m/z***	**Tentative identification**	**Database ID**
T > C	3.50	7.26	76.18	Acetone*	HMDB00714
T > C	3.12	17.87	312.48	*O*-Adipoylcarnitine	HMDB13325
T > C	2.40	18.98	354.37	Decanoylcarnitine	HMDB01870
T > C	1.80	15.09	266.34	Vanillic acid	HMDB13324

*: identification was performed comparing with reference compounds.

3.4. Quantification of allantoin and 8-OHdG in 24-h urine samples

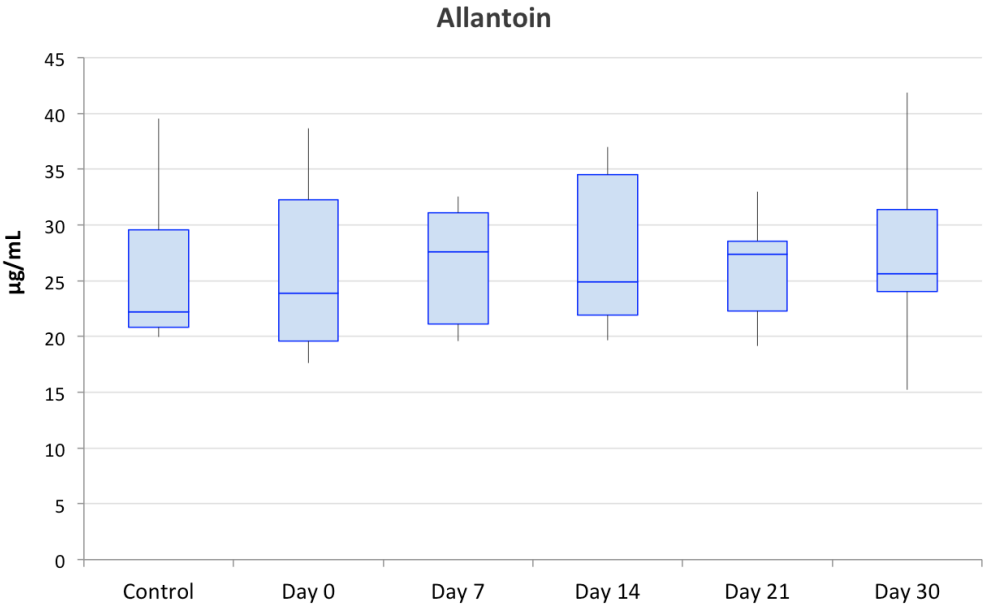

Figure 53. Allantoin concentration in control urine samples and during supplementation with GCBE. Day 0 corresponds to the first day of treatment, day 30 to the last.

The amounts of the two oxidative stress biomarkers were monitored in controls and in urine samples collected during supplementation with GCBE. Data are summarized in Figures 53 and 54. Amounts of both the markers were not affected by consumption of GCBE, in fact the concentrations monitored did not significantly

change along supplementation period, as well as if compared to controls. The average amount of allantoin in control samples was 25.82 ± 7.08 µg/mL, whereas the average concentration in urine collected during treatment was 26.70 ± 6.50 µg/mL. Similarly, the average concentration of 8-OHdG in controls was 1.37 ± 0.40 ng/mL, whereas in treated was 1.38 ± 0.70 µg/mL. Over all, the results show that a regular consumption of a 400 mg dose of GCBE for 30 days does not affect the oxidative status in humans, despite the high content in CGA (9% w/w).

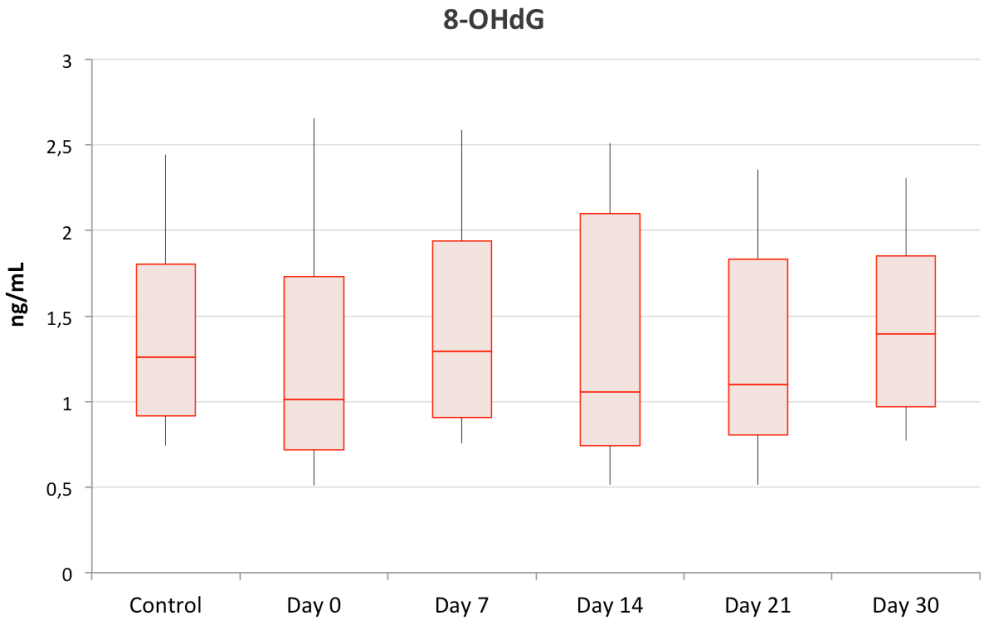

Figure 54. 8-OHdG concentration in control urine samples and during supplementation with GCBE. Day 0 corresponds to the first day of treatment, day 30 to the last.

3.5. Discussion

Products containing GCBE are frequently used to manage weight gain and to promote weight loss, due to the claimed activity of CGA on fatty acids and glucose metabolisms (Shimoda et al., 2006), and due to the content of caffeine, a well-known stimulant (Dulloo et al., 1989). On the other hand, although the efficacy of a treatment with isolated CGA on weight loss, induction of fatty acids and glucose metabolisms and lipid re-distribution were reported both in animals and humans (Dulloo et al., 1989), the efficacy of GCBE is still under debate. Furthermore, the mode of action of green coffee extract is not fully understood and the molecular targets that have been up to now discovered for CGA can be considered multiple. For example, CGA derivatives were

studied for their antioxidants and antibacterial activities and for their interaction with lipid and glucose metabolism (Arion et al., 1997, Brower, 1998, Cho et al., 2010, Sudeep et al., 2016, Huang et al., 2016, Huang et al., 2015, Li et al., 2009, Liang and Kitts, 2015, Liu et al., 2015, Meng et al., 2013). Metabolomics may offer the opportunity to study natural bioactive compounds, such as the green coffee extracts, with a new holistic approach aimed to assess the global metabolite composition of specific biofluids (Wolfender et al., 2013).

Hence, in this study we monitored the effects of a 30 days supplementation with an oral dose of 400 mg of dry GCBE (containing 9% w/w CGA and 0.5% w/w caffeine) in healthy non-obese volunteers, in order to mimic supplement consumption by healthy consumers. To perform the study, volunteers collected 24-h urine once a week during treatment, and these samples were finally analyzed using a metabolomics approach. Among variables significantly (p-value < 0.01) describing treatment with GCBE, none of them was identified as intact CGA; on the other hand, other variables, whose amounts were increased in urine during supplementation, were tentatively identified as benzoic acid, hippuric acid, 4-hydroxybenzoic acid, quinic acid, dihydrocaffeic acid sulfate, isoferulic acid, p-coumaric acid, 3(3-hydroxyphenyl)propanoic acid, 4-hydroxyphenylacetic acid and vanillic acid. Benzoic acid derivatives and hippuric acid are ascribable to intestinal and microbial degradation of CGAs and other polyphenols (Krupp et al., 2012, Olthof et al., 2003), and produced metabolites are mainly as 4-hydroxyphenylacetic acid (Gao et al., 2006). Also quinic acid, dihydrocaffeic acid sulfate, isoferulic acid, p-coumaric acid, 3(3-hydroxyphenyl)propanoic acid and vanillic acid can be considered as degradation products of CGA coming from catabolism by gut microbiota (Del Rio et al., 2010, Farah et al., 2008, Konishi and Kobayashi, 2004). Overall, the results of our study showed that CGA from dry GCBE were absorbed by intestine, but they were extensively subjected to microbial catabolism and subsequent phase II metabolism (as observed for dihydrocaffeic acid, that was detected as sulfate derivative), prior to be excreted with urine. This observation is in agreement with results previously published by other authors, whose reported that, after ingestion of coffee containing 3.395 μmol of caffeoylquinic acids (CQA), only CGA metabolites could be found in significant amounts in urine collected 0–24 h after coffee intake (Monteiro et al., 2007).

Other variables significantly describing treatment with GCBE were tentatively identified as endogen metabolites, namely medium-chain (C8-C10) acyl carnitines, two

dicarboxylic acids (3-hydroxysuberic acid and 3-hydroxyadipic acid) and acetone. Acyl carnitines are mainly involved in transportation of fatty acids inside the mitochondrion matrix (Sharma and Black, 2009), where they are further catabolized via β-oxidation to produce energy. On the other hand, 3-hydroxy dicarboxylic acids as 3-hydroxysuberic acid and 3-hydroxyadipic acid are derived from the ω-oxidation of 3-hydroxy fatty acids and the subsequent β-oxidation of longer chain 3-hydroxy dicarboxylic acids (Tserng, 1991), while acetone derives from degradation of ketone bodies, whose are produced mainly by 3-hydroxy-3-methylglutaryl-CoA synthase during ketogenesis. Overall, these markers belong to different pathways involved in lipid transportation and metabolism, whose are regulated by receptor PPAR-α, the major regulator of lipid metabolism in the liver (Gervois et al., 2000). Activation of this receptor promotes uptake, utilization, and catabolism of fatty acids by upregulation of genes involved in the transportation, binding and activation of fatty acids, and peroxisomal and mitochondrial fatty acid β-oxidation (Kersten et al., 1999). Purified CGA have been reported to act as agonists of PPAR-α (Meng et al., 2013), but few is known about the activity of the extract of GCBE. Li and coll. examined the effects of isolated CGA on lipid and glucose metabolism in hamsters under a high dietary fat burden, and they studied the role of PPAR-α in these effects (Li et al., 2009). After eight weeks of treatment they observed a reduction of the levels of fasting serum triglyceride, free fatty acid, total cholesterol LDL-Cholesterol, HDL-Cholesterol, fasting glucose and insulin. Furthermore, CGA significantly elevated the expression level of mRNA and protein expression in hepatic PPAR-α (Li et al., 2009). Our results showed that, after 30 days consumption of dry GCBE, the amounts of markers related to lipid metabolism in urine were increased, suggesting an induction of fat metabolism, although significant alterations of volunteers body weight were not observed (data not shown). Moreover, these markers were related to different pathways of fatty acids metabolism regulated by PPAR-α, so we postulate that the effects of GCBE could be related to the agonist activity exerted by CGA and CGA-derived metabolites on this receptor. This hypothesis is consistent with previously published data. In fact, 5-CQA was shown to up-regulate PPAR-*α* mRNA expression in the liver of rats in a dose-dependent manner (Huang et al., 2015).

Due to its chemical composition, green coffee is considered a rich natural source of antioxidants, with CGA being the most active compound (Babova et al., 2016).

Previous published studies assessed the antioxidant properties of CGA in animal models (Liang and Kitts, 2015) and of green coffee extracts in vitro (Babova et al., 2016, Liang and Kitts, 2015). In our study, we monitored the levels of two urinary markers of oxidative stress, namely allantoin and 8-OHdG. Allantoin is normally present in urine and is formed from uric acid through reactions with oxidative species, so its urinary amounts are increased with increasing oxidative stress (Tolun et al., 2010). On the other hand, 8-OHdG is one of the predominant forms of free radical-induced lesions of DNA. Because oxidative DNA lesion products are reasonably water soluble and excreted into the urine without being further metabolized, urinary 8-OHdG is considered a significant biomarker of oxidative stress (Cooke et al., 2002, Nakajima et al., 2012). Our results showed that the levels of both the markers were not affected by GCBE consumption and this finding suggest that in healthy subject the supplementation of green coffee is not changing levels of urinary markers of oxidative stress.

In conclusion, in this work, urine samples of human volunteers collected during 30 days of consumption of 400 mg of GCBE (containing 4.9% of 5-CQA, 0.5 % of caffeine and 0.3% trigonelline) were studied by metabolomics approach. Markers related to treatment were assigned to metabolites belonging to the pathways of fatty acid metabolism, showing an influence of green coffee extract on lipid metabolism. However, during the period of the experiment, the weight of volunteers did not change. Overall, these results could be considered, at least in part, as a further proof of the mode of action of GCBE, and they show that metabolomics-based studies offer new opportunities as new tools for the study of bioactive phytochemicals.

CONCLUSION

Nutraceuticals are non-medicinal products that, depending on their composition, are considered as food supplements or, in the case they contain natural products as pure or isolated compounds or as natural extracts, herbal products (non-registered medicinal herbal products). Nutraceuticals are commonly used to prevent diseases (as, for example, metabolic diseases associated to aging), or, more in general, to promote a healthy status. Generally, natural products used in the preparation of nutraceuticals are complex matrixes, whose quali-quantitative chemical composition is often not completely defined. In many cases, only scarce information regarding the bioactivity and safety of these products are reported in literature, as well as the mechanism(s) of action of their phytoconstituents and their pharmacokinetics. Furthermore, unlike in the case of single drugs, the components of complex natural extracts could interact among others, so possible synergic or antagonistic effects between them could be possible; for these reasons, the design and performance of bioactivity assays could be a challenge. However, for this purpose, urinary metabolomics could be a suitable tool. The analysis of the variation of urine composition following a supplementation with natural products can provide information on the effects of nutraceuticals on healthy subjects or animal models. Specimen collection is non-invasive, long-term experiments can be easily conducted and urinary biomarkers of oxidative stress can also be measured, offering the opportunity to evaluate the redox status of the considered organism. Compared to other biological fluids or matrices (plasma and feces for example), sample preparation is more straightforward in the case of urine because of lower sample complexity and lower protein/peptide content. Finally, urine samples the metabolic end-products from the organism destined for excretion, therefore, it is prone to high biological variation.

In this work, the application of urine metabolomics to bioactivity studies concerning herbal products was reported. Three natural extracts, namely *P. cuspidatum* (rich in resveratrol), cranberry (rich in type A procyanidins) and green coffee beans (rich in chlorogenic acids), were chosen on the basis of their importance and distribution on nutraceutical market and on the basis of the bioactivity studies already published in literature. For the study involving *P. cuspidatum*, a healthy animal model was used and metabolomics analyses were performed using an integrated approach

involving UPLC-MS and NMR. The results showed the complementarity of the two analytical platforms, yielding two different patterns of metabolites describing the changes ascribed to *P. cuspidatum* supplementation and to aging. UPLC-HRMS allowed to observe the decreasing of the levels of urinary oxidative stress markers following supplementation with *P. cuspidatum*, indicating an *in vivo* antioxidant effect exerted by the extract. Steroid derivatives were also identified as markers of treatment, among whom, more importantly, tetrahydrocortisol, suggesting a role for *P. cuspidatum* extract as stimulant of corticosurrenal hormones. Furthermore, an influence of the treatment on aging markers allowed to observe an effect of *P. cuspidatum* on aging processes, although the mechanisms of action involved are not yet clear. On the other hand, urinary changes observed with ^{1}H-NMR measurements were related to hippuric acid increase (indicating the microbial catabolism of polyphenols), and to some metabolites that suggest a relationship between *P. cuspidatum* treatment and energy metabolism.

Regarding the experiments involving cranberry, metabolomics was a valuable tool to explore its bioactivity both in healthy animal and human models. More importantly, similar results were obtained from the two independent experiments, showing a reproducibility of the effects related to treatment in rats and humans. An untargeted UPLC-MS approach showed the poor intestinal absorption of procyanidins from cranberry and their extensive degradation by gut microbiota, leading to the excretion of negligible amounts of intact PAC-A. Considering these results, the anti-adhesive effects of cranberry *in vivo* cannot be directly related PAC-A, or at least, they could be related to the interactions between its constituents and the degradation products formed by microbial catabolism. The study of the anti-adhesive activity of urine samples collected at different times after a single cranberry intake allowed to observe the highest activity after 6-8 hours. Untargeted analyses revealed the presence of polyphenol-derived microbial catabolites in the samples collected at these times. Furthermore, a targeted analysis on urine samples collected in the human trial showed a correlation between the excretion of valerolactone derivatives and anti-adhesive activity, being the peaks of excretion comprised between 6 and 8 hours after supplement consumption. Thus, these metabolites could play a crucial role against *E. coli* adhesion to epithelial cells and they can be, at least in part, responsible for cranberry activity.

Finally, LC-MS metabolomics analyses on 24-h urine samples collected during 30 days of supplementation with GCBE showed the absorption of CGA from green coffee

extract and their partial degradation by gut microbiota. The use of different combinations of stationary and mobile phases in the LC analyses allowed to detect different sets of metabolites related to treatment that were further identified as metabolites belonging to the pathways of fatty acid metabolism. Overall, the results showed an influence of supplementation on lipid metabolism, and they could be considered, at least in part, as a further proof of the mode of action of GCBE. Finally, despite the reported anti-oxidant effects of CGA *in vitro*, our results showed no significant activity in human volunteers, highlighting the differences between anti-oxidant activity data collected using the two experimental models.

In conclusion, metabolomics approaches could offer a unique opportunity to study the complex effects of natural product mixtures on healthy animal and human models. The use of integrated untargeted and targeted approaches, as well as LC-MS and NMR platforms, gives the opportunity to consider different sets of metabolites and to explore more exhaustively the effects of a nutritional intervention on the composition of urine in *in vivo* experiments.

REFERENCES

Anderssen, E., Dyrstad, K., Westad, F. and Martens, H. (2006). Reducing over-optimism in variable selection by cross-model validation. Chemometr Intelligent Lab Syst. 84, 69-74.

Andres-Lacueva, C., MacArulla, M.T., Rotches-Ribalta, M. et al. (2012). Distribution of resveratrol metabolites in liver, adipose tissue, and skeletal muscle in rats fed different doses of this polyphenol. J Agric Food Chem. 60, 4833-4840.

Arion, W.J., Canfield, W.K., Ramos, F.C. et al. (1997). Chlorogenic acid and hydroxynitrobenzaldehyde: New inhibitors of hepatic glucose 6-phosphatase. Arch Biochem Biophys. 339, 315-322.

Babova, O., Occhipinti, A. and Maffei, M.E. (2016). Chemical partitioning and antioxidant capacity of green coffee (Coffea arabica and Coffea canephora) of different geographical origin. Phytochemistry. 123, 33-39.

Bajko, E., Kalinowska, M., Borowski, P., Siergiejczyk, L. and Lewandowski, W. (2016). 5-O-Caffeoylquinic acid: A spectroscopic study and biological screening for antimicrobial activity. LWT - Food Science and Technology. 65, 471-479.

Bártíková, H., Boušová, I., Jedlicková, P., Lnenicková, K., Skálová, L. and Szotáková, B. (2014). Effect of standardized cranberry extract on the activity and expression of selected biotransformation enzymes in rat liver and intestine. Molecules. 19, 14948-14960.

Baur, J.A., Pearson, K.J., Price, N.L. et al. (2006). Resveratrol improves health and survival of mice on a high-calorie diet. Nature. 444, 337-342.

Beckman, K.B. and Ames, B.N. (1998). The free radical theory of aging matures. Physiol Rev. 78, 547-581.

Bell, J.D., Sadler, P.J., Morris, V.C. and Levander, O.A. (1991). Effect of aging and diet on proton NMR spectra of rat urine. Magn Reson Med. 17, 414-422.

Beneduci, A., Chidichimo, G., Dardo, G. and Pontoni, G. (2011). Highly routinely reproducible alignment of 1H NMR spectral peaks of metabolites in huge sets of urines. Anal Chim Acta. 685, 186-195.

Bernal, J., Mendiola, J.A., Ibáñez, E. and Cifuentes, A. (2011). Advanced analysis of nutraceuticals. J Pharm Biomed Anal. 55, 758-774.

Bhatt, J.K., Thomas, S. and Nanjan, M.J. (2012). Resveratrol supplementation improves glycemic control in type 2 diabetes mellitus. Nutr Res. 32, 537-541.

Blekherman, G., Laubenbacher, R., Cortes, D.F. et al. (2011). Bioinformatics tools for cancer metabolomics. Metabolomics. 7, 329-343.

Blumberg, J.B., Camesano, T.A., Cassidy, A. et al. (2013). Cranberries and their bioactive constituents in human health. Adv Nutr. 4, 618-632.

Boccard, J., Veuthey, J.-. and Rudaz, S. (2010). Knowledge discovery in metabolomics: An overview of MS data handling. J Sep Sci. 33, 290-304.

Brasnyó, P., Molnár, G.A., Mohás, M. et al. (2011). Resveratrol improves insulin sensitivity, reduces oxidative stress and activates the Akt pathway in type 2 diabetic patients. Br J Nutr. 106, 383-389.

Broadhurst, D.I. and Kell, D.B. (2006). Statistical strategies for avoiding false discoveries in metabolomics and related experiments. Metabolomics. 2, 171-196.

Brower, V. (1998). Nutraceuticals: Poised for a healthy slice of the healthcare market?. Nat Biotechnol. 16, 728-730.

Brown, A.O. and Mcneil, J.N. (2006). Fruit production in cranberry (Ericaceae: Vaccinium macrocarpon): A bet-hedging strategy to optimize reproductive effort. Am J Bot. 93, 910-916.

Buchanan, R. and Beckett, R.D. (2013). Green Coffee for Pharmacological Weight Loss. J Evid - Based Complement Alternat. 18, 309-313.

Butterweck, V. and Nahrstedt, A. (2012). What is the best strategy for preclinical testing of botanicals? A critical perspective. Planta Med. 78, 747-754.

Byrd, D.J., Kochen, W., Idzko, D. and Knorr, E. (1974). The analysis of indolic tryptophan metabolites in human urine. Thin-layer chromatography and situ quantitation. Journal of Chromatography A. 94, 85-106.

Caruso, F., Tanski, J., Villegas-Estrada, A. and Rossi, M. (2004). Structural basis for antioxidant activity of trans-resveratrol: Ab initio calculations and crystal and molecular structure. J Agric Food Chem. 52, 7279-7285.

Casteilla, L., Rigoulet, M. and Pénicaud, L. (2002). Mitochondrial ROS metabolism: Modulation by uncoupling proteins. IUBMB Life. 52, 181-188.

Chang, W.-., Choi, Y.H., Van Der Heijden, R. et al. (2011). Traditional processing strongly affects metabolite composition by hydrolysis in Rehmannia glutinosa roots. Chem Pharm Bull. 59, 546-552.

Chen, W., Rezaizadehnajafi, L. and Wink, M. (2013). Influence of resveratrol on oxidative stress resistance and life span in Caenorhabditis elegans. J Pharm Pharmacol. 65, 682-688.

Chen, Y., Tseng, S., Lai, H. and Chen, W. (2004). Resveratrol-induced cellular apoptosis and cell cycle arrest in neuroblastoma cells and antitumor effects on neuroblastoma in mice. Surgery. 136, 57-66.

Cho, A., Jeon, S., Kim, M. et al. (2010). Chlorogenic acid exhibits anti-obesity property and improves lipid metabolism in high-fat diet-induced-obese mice. Food Chem Toxicol. 48, 937-943.

Chong, I. and Jun, C. (2005). Performance of some variable selection methods when multicollinearity is present. Chemometr Intelligent Lab Syst. 78, 103-112.

Clarke, J.T.R. (2005). A Clinical Guide to Inherited Metabolic Diseases. Cambridge University Press.

Clifford, M.N., Johnston, K.L., Knight, S. and Kuhnert, N. (2003). Hierarchical scheme for LC-MSn identification of chlorogenic acids. J Agric Food Chem. 51, 2900-2911.

Clifford, M.N., Kirkpatrick, J., Kuhnert, N., Roozendaal, H. and Salgado, P.R. (2008). LC-MSn analysis of the cis isomers of chlorogenic acids. Food Chem. 106, 379-385.

Clifford, M.N., Knight, S. and Kuhnert, N. (2005). Discriminating between the six isomers of dicaffeoylquinic acid by LC-MSn. J Agric Food Chem. 53, 3821-3832.

Clifford, M.N., Marks, S., Knight, S. and Kuhnert, N. (2006). Characterization by LC-MS n of four new classes of p-coumaric acid-containing diacyl chlorogenic acids in green coffee beans. J Agric Food Chem. 54, 4095-4101.

Commisso, M., Strazzer, P., Toffali, K., Stocchero, M. and Guzzo, F. (2013). Untargeted metabolomics: An emerging approach to determine the composition of herbal products. Comput Struct Biotechnol J. 4.

Cooke, M.S., Lunec, J. and Evans, M.D. (2002). Progress in the analysis of urinary oxidative DNA damage. Free Radic Biol Med. 33, 1601-1614.

Craig, A., Cloarec, O., Holmes, E., Nicholson, J.K. and Lindon, J.C. (2006). Scaling and normalization effects in NMR spectroscopic metabonomic data sets. Anal Chem. 78, 2262-2267.

Davis, A.P., Govaerts, R., Bridson, D.M. and Stoffelen, P. (2006). An annotated taxonomic conspectus of the genus Coffea (Rubiaceae). Bot J Linn Soc. 152, 465-512.

Daykin, C.A., Van Duynhoven, J.P.M., Groenewegen, A., Dachtler, M., Van Amelsvoort, J.M.M. and Mulder, T.P.J. (2005). Nuclear magnetic resonance spectroscopic based studies of the metabolism of black tea polyphenols in humans. J Agric Food Chem. 53, 1428-1434.

De Llano, D.G., Esteban-Fernández, A., Sánchez-Patán, F., Martín-Álvarez, P.J., Moreno-Arribas, M.V. and Bartolomé, B. (2015). Anti-adhesive activity of cranberry phenolic compounds and their microbial-derived metabolites against uropathogenic escherichia coli in bladder epithelial cell cultures. Int J Mol Sci. 16, 12119-12130.

Del Rio, D., Rodriguez-Mateos, A., Spencer, J.P.E., Tognolini, M., Borges, G. and Crozier, A. (2013). Dietary (poly)phenolics in human health: Structures, bioavailability, and evidence of protective effects against chronic diseases. Antioxid Redox Signal. 18, 1818-1892.

Del Rio, D., Stalmach, A., Calani, L. and Crozier, A. (2010). Bioavailability of coffee chlorogenic acids and green tea flavan-3-ols. Nutr. 2, 820-833.

Dettmer, K., Aronov, P.A. and Hammock, B.D. (2007). Mass spectrometry-based metabolomics. Mass Spectrom Rev. 26, 51-78.

Dopazo, J. (2014). Genomics and transcriptomics in drug discovery. Drug Discov Today. 19, 126-132.

Dulloo, A.G., Geissler, C.A., Collins, A. and Miller, D.S. (1989). Normal caffeine consumption: Influence on thermogenesis and daily energy expenditure in lean and postobese human volunteers. Am J Clin Nutr. 49, 44-50.

Elliott, P.J., Walpole, S.M., Morelli, L. et al. (2009). Resveratrol/SRT501. Sirtuin SIRT1 activator treatment of type 2 diabetes. Drugs Future. 34, 291-295.

Eḿlia Juan, M., Pilar Vinardell, M. and Planas, J.M. (2002). The daily oral administration of high doses of trans-resveratrol to rats for 28 days is not harmful. J Nutr. 132, 257-260.

Espín, J.C., García-Conesa, M.T. and Tomás-Barberán, F.A. (2007). Nutraceuticals: Facts and fiction. Phytochemistry. 68, 2986-3008.

Fan, D., Zhou, X., Zhao, C., Chen, H., Zhao, Y. and Gong, X. (2011). Anti-inflammatory, antiviral and quantitative study of quercetin-3-O-β-D-glucuronide in Polygonum perfoliatum L. Fitoterapia. 82, 805-810.

Farah, A. and Donangelo, C.M. (2006). Phenolic compounds in coffee. Braz J Plant Physiol. 18, 23-36.

Farah, A., Monteiro, M., Donangelo, C.M. and Lafay, S. (2008). Chlorogenic acids from green coffee extract are highly bioavailable in humans. J Nutr. 138, 2309-2315.

Feliciano, R.P., Boeres, A., Massacessi, L. et al. (2016). Identification and quantification of novel cranberry-derived plasma and urinary (poly)phenols. Arch Biochem Biophys. 599, 31-41.

Fontana, L. and Klein, S. (2007). Aging, adiposity, and calorie restriction. J Am Med Assoc. 297, 986-994.

Foo, L.Y., Lu, Y., Howell, A.B. and Vorsa, N. (2000). The structure of cranberry proanthocyanidins which inhibit adherence of uropathogenic P-fimbriated Escherichia coli in vitro. Phytochemistry. 54, 173-181.

Gao, K., Xu, A., Krul, C. et al. (2006). Of the major phenolic acids formed during human microbial fermentation of tea, citrus, and soy flavonoid supplements, only 3,4-dihydroxyphenylacetic acid has antiproliferative activity. J Nutr. 136, 52-57.

Gerritsen, W.B., Aarts, L.P., Morshuis, W.J. and Haas, F.J. (1997). Indices of oxidative stress in urine of patients undergoing coronary artery bypass grafting. European Journal of Clinical Chemistry and Clinical Biochemistry. 35, 737-742.

Gertsch, J. (2011). Botanical drugs, synergy, and network pharmacology: Forth and back to intelligent mixtures. Planta Med. 77, 1086-1098.

Gervois, P., Torra, I.P., Fruchart, J. and Staels, B. (2000). Regulation of lipid and lipoprotein metabolism by PPAR activators. Clin Chem Lab Med. 38, 3-11.

Gomez-Sanchez, C.E., Clore, J.N., Estep, H.L. and Watlington, C.O. (1988). Effect of chronic adrenocorticotropin stimulation on the excretion of 18-hydroxycortisol and 18-oxocortisol. J Clin Endocrinol Metab. 67, 322-326.

Greenberg, J.A., Boozer, C.N. and Geliebter, A. (2006). Coffee, diabetes, and weight control. Am J Clin Nutr. 84, 682-693.

Gromski, P.S., Muhamadali, H., Ellis, D.I. et al. (2015). A tutorial review: Metabolomics and partial least squares-discriminant analysis - a marriage of convenience or a shotgun wedding. Anal Chim Acta. 879, 10-23.

Guarente, L., Baur, J.A. and Mai, A. (2012). Revelations into resveratrol's mechanism. Nat Med. 18, 500-501.

Guay, D.R.P. (2009). Cranberry and urinary tract infections. Drugs. 69, 775-807.

Gupta, A., Dwivedi, M., Mahdi, A.A., Gowda, G.A.N., Khetrapal, C.L. and Bhandari, M. (2012). Inhibition of adherence of multi-drug resistant E. coli by proanthocyanidin. Urol Res. 40, 143-150.

Gupta, K., Chou, M.Y., Howell, A., Wobbe, C., Grady, R. and Stapleton, A.E. (2007). Cranberry Products Inhibit Adherence of P-Fimbriated Escherichia Coli to Primary Cultured Bladder and Vaginal Epithelial Cells. J Urol. 177, 2357-2360.

Gupta, P., Song, B., Neto, C. and Camesano, T.A. (2016). Atomic force microscopy-guided fractionation reveals the influence of cranberry phytochemicals on adhesion of Escherichia coli. Food Funct. 7, 2655-2666.

Han, J., Danell, R.M., Patel, J.R. et al. (2008). Towards high-throughput metabolomics using ultrahigh-field Fourier transform ion cyclotron resonance mass spectrometry. Metabolomics. 4, 128-140.

Hausenblas, H.A., Schoulda, J.A. and Smoliga, J.M. (2015). Resveratrol treatment as an adjunct to pharmacological management in type 2 diabetes mellitus-systematic review and meta-analysis. Mol Nutr Food Res. 59, 147-159.

Herrero, M., Simõ, C., García-Cañas, V., Ibáñez, E. and Cifuentes, A. (2012). Foodomics: MS-based strategies in modern food science and nutrition. Mass Spectrom Rev. 31, 49-69.

Hisano, M., Bruschini, H., Nicodemo, A.C. and Srougi, M. (2012). Cranberries and lower urinary tract infection prevention. Clinics. 67, 661-667.

Howell, A.B., Reed, J.D., Krueger, C.G., Winterbottom, R., Cunningham, D.G. and Leahy, M. (2005). A-type cranberry proanthocyanidins and uropathogenic bacterial anti-adhesion activity. Phytochemistry. 66, 2281-2291.

Howell, A.B., Vorsa, N., Marderosian, A.D. and Foo, L.Y. (1998). Inhibition of the adherence of P-fimbriated Escherichia coli to uroepithelial-cell surfaces by proanthocyanidin extracts from cranberries. New Engl J Med. 339, 1085-1086.

Howitz, K.T., Bitterman, K.J., Cohen, H.Y. et al. (2003). Small molecule activators of sirtuins extend Saccharomyces cerevisiae lifespan. Nature. 425, 191-196.

Huang, C., Tung, Y., Huang, W., Chen, Y., Hsu, Y. and Hsu, M. (2016). Beneficial effects of cocoa, coffee, green tea, and garcinia complex supplement on diet induced obesity in rats. BMC Complement Altern Med. 16.

Huang, K., Liang, X., Zhong, Y., He, W. and Wang, Z. (2015). 5-Caffeoylquinic acid decreases diet-induced obesity in rats by modulating PPARa and LXRa transcription. J Sci Food Agric. 95, 1903-1910.

Inagami, K., Kaihara, M. and Price, J.M. (1965). The identification of 2,8-quinolinediol in the urine of rats fed a diet containing corn. J Biol Chem. 240, 3682-3684.

Jang, M., Cai, L., Udeani, G.O. et al. (1997). Cancer chemopreventive activity of resveratrol, a natural product derived from grapes. Science. 275, 218-220.

Jasinski, M., Jasinska, L. and Ogrodowczyk, M. (2013). Resveratrol in prostate diseases - A short review. Central European Journal of Urology. 66, 144-149.

Jepson, R.G., Williams, G. and Craig, J.C. (2012). Cranberries for preventing urinary tract infections. Cochrane Database Syst Rev. 10.

Johnson-White, B., Buquo, L., Zeinali, M. and Ligler, F.S. (2006). Prevention of nonspecific bacterial cell adhesion in immunoassays by use of cranberry juice. Anal Chem. 78, 853-857.

Juan, M.E., Alfaras, I. and Planas, J.M. (2010). Determination of dihydroresveratrol in rat plasma by HPLC. J Agric Food Chem. 58, 7472-7475.

Kaeberlein, M., McVey, M. and Guarente, L. (1999). The SIR2/3/4 complex and SIR2 alone promote longevity in Saccharomyces cerevisiae by two different mechanisms. Genes Dev. 13, 2570-2580.

Kalra, E.K. (2003). Nutraceutical - Definition and introduction. AAPS PharmSci. 5.

Kang, W., Hong, H.J., Guan, J. et al. (2012). Resveratrol improves insulin signaling in a tissue-specific manner under insulin-resistant conditions only: In vitro and in vivo experiments in rodents. Metab Clin Exp. 61, 424-433.

Kersten, S., Seydoux, J., Peters, J.M., Gonzalez, F.J., Desvergne, B. and Wahli, W. (1999). Peroxisome proliferator-activated receptor a mediates the adaptive response to fasting. J Clin Invest. 103, 1489-1498.

Kim, H.K., Choi, Y.H. and Verpoorte, R. (2011). NMR-based plant metabolomics: Where do we stand, where do we go?. Trends Biotechnol. 29, 267-275.

Kim, K.M., Henderson, G.N., Frye, R.F. et al. (2009). Simultaneous determination of uric acid metabolites allantoin, 6-aminouracil, and triuret in human urine using liquid chromatography-mass spectrometry. Journal of Chromatography B: Analytical Technologies in the Biomedical and Life Sciences. 877, 65-70.

Koehn, F.E. and Carter, G.T. (2005). The evolving role of natural products in drug discovery. Nat Rev Drug Discov. 4, 206-220.

Konishi, Y. and Kobayashi, S. (2004). Microbial metabolites of ingested caffeic acid are absorbed by the Monocarboxylic Acid Transporter (MCT) in intestinal Caco-2 cell monolayers. J Agric Food Chem. 52, 6418-6424.

Krastanov, A. (2010). Metabolomics - The state of art. Biotechnol Biotechnol Equip. 24, 1537-1543.

Krumsiek, J., Bartel, J. and Theis, F.J. (2016). Computational approaches for systems metabolomics. Curr Opin Biotechnol. 39, 198-206.

Krupp, D., Doberstein, N., Shi, L. and Remer, T. (2012). Hippuric acid in 24-hour urine collections is a potential biomarker for fruit and vegetable consumption in healthy children and adolescents. J Nutr. 142, 1314-1320.

Laparra, J.M. and Sanz, Y. (2010). Interactions of gut microbiota with functional food components and nutraceuticals. Pharmacol Res. 61, 219-225.

Lavrik, I.N. and Zhivotovsky, B. (2014). Systems biology: A way to make complex problems more understandable. Cell Death Dis. 5.

Lee, S.H., Park, S., Kim, H. and Jung, B.H. (2014). Metabolomic approaches to the normal aging process. Metabolomics. 10, 1268-1292.

Lees, H.J., Swann, J.R., Wilson, I.D., Nicholson, J.K. and Holmes, E. (2013). Hippurate: The natural history of a mammalian-microbial cometabolite. J Proteome Res. 12, 1527-1546.

Li, D., Dammer, E.B. and Sewer, M.B. (2012). Resveratrol stimulates cortisol biosynthesis by activating SIRT-dependent deacetylation of P450scc. Endocrinology. 153, 3258-3268.

Li, S., Chang, C., Ma, F. and Yu, C. (2009). Modulating effects of chlorogenic acid on lipids and glucose metabolism and expression of hepatic peroxisome proliferator-activated receptor-a in golden hamsters fed on high fat diet. Biomed Environ Sci. 22, 122-129.

Liang, N. and Kitts, D.D. (2015). Role of chlorogenic acids in controlling oxidative and inflammatory stress conditions. Nutrients. 8.

Liu, K., Zhou, R., Wang, B. and Mi, M. (2014). Effect of resveratrol on glucose control and insulin sensitivity: A meta-analysis of 11 randomized controlled trials. Am J Clin Nutr. 99, 1510-1519.

Liu, S., Peng, B., Zhong, Y., Liu, Y., Song, Z. and Wang, Z. (2015). Effect of 5-caffeoylquinic acid on the NF-κB signaling pathway, peroxisome proliferator-activated receptor gamma 2, and macrophage infiltration in high-fat diet-fed Sprague-Dawley rat adipose tissue. Food Funct. 6, 2779-2786.

Liu, Y., Gallardo-Moreno, A.M., Pinzon-Arango, P.A., Reynolds, Y., Rodriguez, G. and Camesano, T.A. (2008). Cranberry changes the physicochemical surface

properties of E. coli and adhesion with uroepithelial cells. Colloids Surf B Biointerfaces. 65, 35-42.

Liu, Y., Ma, W., Zhang, P., He, S. and Huang, D. (2015). Effect of resveratrol on blood pressure: A meta-analysis of randomized controlled trials. Clin Nutr. 34, 27-34.

Loke, W.M., Proudfoot, J.M., Stewart, S. et al. (2008). Metabolic transformation has a profound effect on anti-inflammatory activity of flavonoids such as quercetin: Lack of association between antioxidant and lipoxygenase inhibitory activity. Biochem Pharmacol. 75, 1045-1053.

Magyar, K., Halmosi, R., Palfi, A. et al. (2012). Cardioprotection by resveratrol: A human clinical trial in patients with stable coronary artery disease. Clin Hemorheol Microcirc. 50, 179-187.

McClements, D.J. (2015). Enhancing nutraceutical bioavailability through food matrix design. Curr Opin Food Sci. 4, 1-6.

McKay, D.L., Chen, C.O., Zampariello, C.A. and Blumberg, J.B. (2015). Flavonoids and phenolic acids from cranberry juice are bioavailable and bioactive in healthy older adults. Food Chem. 168, 233-240.

Mena, P., González de Llano, D., Brindani, N. et al. (2017). 5-(3′,4′-Dihydroxyphenyl)-γ-valerolactone and its sulphate conjugates, representative circulating metabolites of flavan-3-ols, exhibit anti-adhesive activity against uropathogenic Escherichia coli in bladder epithelial cells. J Funct Foods. 29, 275-280.

Meng, S., Cao, J., Feng, Q., Peng, J. and Hu, Y. (2013). Roles of chlorogenic acid on regulating glucose and lipids metabolism: A review. Evid -Based Complement Altern Med. 2013.

Miao, H., Chen, H., Zhang, X. et al. (2014). Urinary metabolomics on the biochemical profiles in diet-induced hyperlipidemia rat using ultraperformance liquid chromatography coupled with quadrupole time-of-flight SYNAPT high-definition mass spectrometry. Journal of Analytical Methods in Chemistry. 2014.

Militaru, C., Donoiu, I., Craciun, A., Scorei, I.D., Bulearca, A.M. and Scorei, R.I. (2013). Oral resveratrol and calcium fructoborate supplementation in subjects with stable angina pectoris: Effects on lipid profiles, inflammation markers, and quality of life. Nutrition. 29, 178-183.

Mishra, B.B. and Tiwari, V.K. (2011). Natural products: An evolving role in future drug discovery. Eur J Med Chem. 46, 4769-4807.

Monagas, M., Urpi-Sarda, M., Sánchez-Patán, F. et al. (2010). Insights into the metabolism and microbial biotransformation of dietary flavan-3-ols and the bioactivity of their metabolites. Food Funct. 1, 233-253.

Monteiro, M., Farah, A., Perrone, D., Trugo, L.C. and Donangelo, C. (2007). Chlorogenic acid compounds from coffee are differentially absorbed and metabolized in humans. J Nutr. 137, 2196-2201.

Movahed, A., Nabipour, I., Lieben Louis, X. et al. (2013). Antihyperglycemic effects of short term resveratrol supplementation in type 2 diabetic patients. Evid -Based Complement Altern Med. 2013.

Nakajima, H., Unoda, K., Ito, T., Kitaoka, H., Kimura, F. and Hanafusa, T. (2012). The relation of urinary 8-OHdG, a marker of oxidative stress to DNA, and clinical outcomes for ischemic stroke. Open Neurol J. 6, 51-57.

Neveu, V., Perez-Jiménez, J., Vos, F. et al. (2010). Phenol-Explorer: an online comprehensive database on polyphenol contents in foods. Database (Oxford). 2010.

Nguyen, D.V. and Rocke, D.M. (2002). Tumor classification by partial least squares using microarray gene expression data. Bioinformatics. 18, 39-50.

Ni, Y., Li, J. and Panagiotou, G. (2015). A molecular-level landscape of diet-gut microbiome interactions: Toward dietary interventions targeting bacterial genes. mBio. 6.

Nocerino, E., Amato, M. and Izzo, A.A. (2000). The aphrodisiac and adaptogenic properties of ginseng. Fitoterapia. 71, S1-S5.

Novelle, M.G., Wahl, D., Diéguez, C., Bernier, M. and De Cabo, R. (2015). Resveratrol supplementation: Where are we now and where should we go?. Ageing Res Rev. 21, 1-15.

Occhipinti, A., Germano, A. and Maffei, M.E. (2016). Prevention of urinary tract infection with Oximacro®, a cranberry extract with a high content of a-type proanthocyanidins: A pre-clinical double-blind controlled study. Urol J. 13, 2640-2649.

Olthof, M.R., Hollman, P.C.H., Buijsman, M.N.C.P., Van Amelsvoort, J.M.M. and Katan, M.B. (2003). Chlorogenic acid, quercetin-3-rutinoside and black tea phenols are extensively metabolized in humans. J Nutr. 133, 1806-1814.

Onakpoya, I., Terry, R. and Ernst, E. (2011). The use of green coffee extract as a weight loss supplement: A systematic review and meta-analysis of randomised clinical trials. Gastroenterol Res Pract.

Ozkan, E., Yaman, H., Cakir, E. et al. (2012). Plasma melatonin and urinary 6-hydroxymelatonin levels in patients with pulmonary tuberculosis. Inflammation. 35, 1429-1434.

Park, S., Ahmad, F., Philp, A. et al. (2012). Resveratrol ameliorates aging-related metabolic phenotypes by inhibiting cAMP phosphodiesterases. Cell. 148, 421-433.

Pavlovic, R., Cannizzo, F.T., Panseri, S. et al. (2013). Tetrahydro-metabolites of cortisol and cortisone in bovine urine evaluated by HPLC-ESI-mass spectrometry. J Steroid Biochem Mol Biol. 135, 30-35.

Pearson, K.J., Baur, J.A., Lewis, K.N. et al. (2008). Resveratrol Delays Age-Related Deterioration and Mimics Transcriptional Aspects of Dietary Restriction without Extending Life Span. Cell Metabolism. 8, 157-168.

Peron, G., Uddin, J., Stocchero, M., Mammi, S., Schievano, E. and Dall'Acqua, S. (2017). Studying the effects of natural extracts with metabolomics: A longitudinal study on the supplementation of healthy rats with Polygonum cuspidatum Sieb. et Zucc. J Pharm Biomed Anal. 140, 62-70.

Pferschy-Wenzig, E. and Bauer, R. (2015). The relevance of pharmacognosy in pharmacological research on herbal medicinal products. Epilepsy Behav. 52, 344-362.

Pham-Huy, L.A., He, H. and Pham-Huy, C. (2008). Free radicals, antioxidants in disease and health. Int J Biomed Sci. 4, 89-96.

Pimpão, R.C., Ventura, M.R., Ferreira, R.B., Williamson, G. and Santos, C.N. (2015). Phenolic sulfates as new and highly abundant metabolites in human plasma after ingestion of a mixed berry fruit purée. Br J Nutr. 113, 454-463.

Polewski, M.A., Krueger, C.G., Reed, J.D. and Leyer, G. (2016). Ability of cranberry proanthocyanidins in combination with a probiotic formulation to inhibit in vitro

invasion of gut epithelial cells by extra-intestinal pathogenic E. coli. J Funct Foods. 25, 123-134.

Possemiers, S., Bolca, S., Verstraete, W. and Heyerick, A. (2011). The intestinal microbiome: A separate organ inside the body with the metabolic potential to influence the bioactivity of botanicals. Fitoterapia. 82, 53-66.

Quick, M. and Kiefer, D. (2013). Weighing in: Green coffee bean extract - A potential safe and effective weight loss supplement?. Integr Med Alert. 16, 97-103.

Rajbhandari, R., Peng, N., Moore, R. et al. (2011). Determination of cranberry phenolic metabolites in rats by liquid chromatography-tandem mass spectrometry. J Agric Food Chem. 59, 6682-6688.

Reiter, R.J., Paredes, S.D., Korkmaz, A., Manchester, L.C. and Tan, D.X. (2008). Melatonin in relation to the "strong" and "weak" versions of the free radical theory of aging. Advances in medical sciences. 53, 119-129.

Ren, S., Hinzman, A.A., Kang, E.L., Szczesniak, R.D. and Lu, L.J. (2015). Computational and statistical analysis of metabolomics data. Metabolomics. 11, 1492-1513.

Revuelta-Iniesta, R. and Al-Dujaili, E.A.S. (2014). Consumption of Green Coffee Reduces Blood Pressure and Body Composition by Influencing 11 ß-HSD1 Enzyme Activity in Healthy Individuals: A Pilot Crossover Study Using Green and Black Coffee. BioMed Res Int. 2014.

Rietjens, I.M.C.M., Boersma, M.G., Haan, L.D. et al. (2002). The pro-oxidant chemistry of the natural antioxidants vitamin C, vitamin E, carotenoids and flavonoids. Environ Toxicol Pharmacol. 11, 321-333.

Rodríguez-Pérez, C., Quirantes-Piné, R., Uberos, J., Jiménez-Sánchez, C., Peña, A. and Segura-Carretero, A. (2016). Antibacterial activity of isolated phenolic compounds from cranberry (Vaccinium macrocarpon) against Escherichia coli. Food Funct. 7, 1564-1573.

Rogina, B. and Helfand, S.L. (2004). Sir2 mediates longevity in the fly through a pathway related to calorie restriction. Proc Natl Acad Sci U S A. 101, 15998-16003.

Sabbagh, G. and Berakdar, N. (2015). Docking studies of flavonoid compounds as inhibitors of β-ketoacyl acyl carrier protein synthase I (Kas I) of Escherichia coli. J Mol Graph Model. 61, 214-223.

Saiki, S., Sato, T., Kohzuki, M., Kamimoto, M. and Yosida, T. (2001). Changes in serum hypoxanthine levels by exercise in obese subjects. Metabolism: Clinical and Experimental. 50, 627-630.

Santana-Buzzy, N., Rojas-Herrera, R., Galaz-Ávalos, R.M. et al. (2007). Advances in coffee tissue culture and its practical applications. In Vitro Cell Dev Biol Plant. 43, 507-520.

Savorani, F., Rasmussen, M.A., Mikkelsen, M.S. and Engelsen, S.B. (2013). A primer to nutritional metabolomics by NMR spectroscopy and chemometrics. Food Res Int. 54, 1131-1145.

Schnackenberg, L.K., Sun, J., Espandiari, P., Holland, R.D., Hanig, J. and Beger, R.D. (2007). Metabonomics evaluations of age-related changes in the urinary compositions of male Sprague Dawley rats and effects of data normalization methods on statistical and quantitative analysis. BMC Bioinform. 8.

Seiger, L.A. (1996). Fallopia japonica. In Randall, J.M. and Marinelli, J. Invasive Plants: Weeds of the Global Garden. Brooklyn Botanic Garden Inc., New York. 77.

Sharma, S. and Black, S.M. (2009). Carnitine homeostasis, mitochondrial function and cardiovascular disease. Drug Discov Today Dis Mech. 6.

Shimoda, H., Seki, E. and Aitani, M. (2006). Inhibitory effect of green coffee bean extract on fat accumulation and body weight gain in mice. BMC Complement Altern Med. 6.

Singh, I., Gautam, L.K. and Kaur, I.R. (2016). Effect of oral cranberry extract (standardized proanthocyanidin-A) in patients with recurrent UTI by pathogenic E. coli: a randomized placebo-controlled clinical research study. Int Urol Nephrol. 48, 1379-1386.

Slominska, E.M., Rutkowski, P., Smolenski, R.T., Szutowicz, A., Rutkowski, B. and Swierczynski, J. (2004). The age-related increase in N-methyl-2-pyridone-5-carboxamide (NAD catabolite) in human plasma. Mol Cell Biochem. 267, 25-30.

Smolinska, A., Blanchet, L., Buydens, L.M.C. and Wijmenga, S.S. (2012). NMR and pattern recognition methods in metabolomics: From data acquisition to biomarker discovery: A review. Anal Chim Acta. 750, 82-97.

Stocchero, M. and Paris, D. (2016). Post-transformation of PLS2 (ptPLS2) by orthogonal matrix: A new approach for generating predictive and orthogonal latent variables. J Chemometr.

Sudeep, H.V., Venkatakrishna, K., Patel, D. and Shyamprasad, K. (2016). Biomechanism of chlorogenic acid complex mediated plasma free fatty acid metabolism in rat liver. BMC Complement Altern Med. 16.

Sut, S., Baldan, V., Faggian, M., Peron, G. and Dall'Acqua, S. (2016). Nutraceuticals, a New Challenge for Medicinal Chemistry. Curr Med Chem. 23, 1-26.

Szkudelska, K. and Szkudelski, T. (2010). Resveratrol, obesity and diabetes. Eur J Pharmacol. 635, 1-8.

Thom, E. (2007). The effect of chlorogenic acid enriched coffee on glucose absorption in healthy volunteers and its effect on body mass when used long-term in overweight and obese people. J Int Med Res. 35, 900-908.

Ting, Y., Jiang, Y., Ho, C. and Huang, Q. (2014). Common delivery systems for enhancing in vivo bioavailability and biological efficacy of nutraceuticals. J Funct Foods. 7, 112-128.

Tissenbaum, H.A. and Guarente, L. (2001). Increased dosage of a sir-2 gene extends lifespan in Caenorhabditis elegans. Nature. 410, 227-230.

Tiwari, V. and Chopra, K. (2011). Resveratrol prevents alcohol-induced cognitive deficits and brain damage by blocking inflammatory signaling and cell death cascade in neonatal rat brain. J Neurochem. 117, 678-690.

Tolun, A.A., Zhang, H., Il'yasova, D., Sztáray, J., Young, S.P. and Millington, D.S. (2010). Allantoin in human urine quantified by ultra-performance liquid chromatography-tandem mass spectrometry. Anal Biochem. 402, 191-193.

Tomé-Carneiro, J., Gonzálvez, M., Larrosa, M. et al. (2012). One-year consumption of a grape nutraceutical containing resveratrol improves the inflammatory and fibrinolytic status of patients in primary prevention of cardiovascular disease. Am J Cardiol. 110, 356-363.

Tomé-Carneiro, J., Larrosa, M., Yáñez-Gascón, M.J. et al. (2013). One-year supplementation with a grape extract containing resveratrol modulates inflammatory-related microRNAs and cytokines expression in peripheral blood mononuclear cells of type 2 diabetes and hypertensive patients with coronary artery disease. Pharmacol Res. 72, 69-82.

Trygg, J. and Wold, S. (2002). Orthogonal projections to latent structures (O-PLS). J Chemometr. 16, 119-128.

Tserng, K. (1991). Metabolic origin of urinary 3-hydroxy dicarboxylic acids. Biochemistry (NY). 30, 2508-2514.

Tsybin, Y.O., Fornelli, L., Kozhinov, A.N., Vorobyev, A. and Miladinovic, S.M. (2011). High-resolution and tandem mass spectrometry - the indispensable tools of the XXI century. Chimia. 65, 641-645.

Urbanczyk-Wochniak, E., Leudemann, A., Kopka, J. et al. (2003). Parallel analysis of transcript and metabolic profiles: A new approch in systems biology. EMBO Rep. 4, 989-993.

Van Breemen, R.B. (2015). Development of Safe and Effective Botanical Dietary Supplements. J Med Chem. 58, 8360-8372.

van den Berg, R.A., Hoefsloot, H.C.J., Westerhuis, J.A., Smilde, A.K. and van der Werf, M.J. (2006). Centering, scaling, and transformations: Improving the biological information content of metabolomics data. BMC Genomics. 7.

Van Der Hooft, J.J.J., De Vos, R.C.H., Mihaleva, V. et al. (2012). Structural elucidation and quantification of phenolic conjugates present in human urine after tea intake. Anal Chem. 84, 7263-7271.

Van Der Kooy, F., Maltese, F., Young, H.C., Hye, K.K. and Verpoorte, R. (2009). Quality control of herbal material and phytopharmaceuticals with MS and NMR based metabolic fingerprinting. Planta Med. 75, 763-775.

Van Dorsten, F.A., Daykin, C.A., Mulder, T.P.J. and Van Duynhoven, J.P.M. (2006). Metabonomics approach to determine metabolic differences between green tea and black tea consumption. J Agric Food Chem. 54, 6929-6938.

Verhaeghe, B.J., Van Bocxlaer, J.F. and De Leenheer, A.P. (1992). Gas chromatographic/mass spectrometric identification of 3-hydroxydicarboxylic acids in urine. Biol Mass Spectrom. 21, 27-32.

Verpoorte, R., Choi, Y.H. and Kim, H.K. (2007). NMR-based metabolomics at work in phytochemistry. Phytochem Rev. 6, 3-14.

Vettukattil, R. (2015). Preprocessing of raw metabonomic data. Methods Mol Biol. 1277, 123-136.

Vorkas, P.A., Isaac, G., Anwar, M.A. et al. (2015). Untargeted UPLC-MS profiling pipeline to expand tissue metabolome coverage: Application to cardiovascular disease. Anal Chem. 87, 4184-4193.

Wagner, H. and Ulrich-Merzenich, G. (2009). Synergy research: Approaching a new generation of phytopharmaceuticals. Phytomedicine. 16, 97-110.

Wahab, A., Gao, K., Jia, C. et al. (2017). Significance of resveratrol in clinical management of chronic diseases. Molecules. 22.

Wallace, T.C. and Giusti, M.M. (2010). Extraction and normal-phase HPLC-fluorescence-electrospray MS characterization and quantification of procyanidins in cranberry extracts. J Food Sci. 75, C690-C696.

Wang, D., Liu, W. and Chen, G. (2013). A simple method for the isolation and purification of resveratrol from Polygonum cuspidatum. Journal of Pharmaceutical Analysis. 3, 241-247.

Wang, J., Guleria, S., Koffas, M.A. and Yan, Y. (2016). Microbial production of value-added nutraceuticals. Curr Opin Biotechnol. 37, 97-104.

Wang, M., Lamers, R.A.N., Korthout, H.A.A.J. et al. (2005). Metabolomics in the context of systems biology: Bridging Traditional Chinese Medicine and molecular pharmacology. Phytother Res. 19, 173-182.

Watanabe, S., Tohma, Y., Chiba, H., Shimizu, Y., Saito, H. and Yanaihara, T. (1994). Biochemical significance of 19-hydroxytesterone in the process of aromatization in human corpus luteum. Endocr J. 41, 421-427.

Wehrens, R., Franceschi, P., Vrhovsek, U. and Mattivi, F. (2011). Stability-based biomarker selection. Anal Chim Acta. 705, 15-23.

Westerhuis, J.A., Hoefsloot, H.C.J., Smit, S. et al. (2008). Assessment of PLSDA cross validation. Metabolomics. 4, 81-89.

Wikoff, W.R., Anfora, A.T., Liu, J. et al. (2009). Metabolomics analysis reveals large effects of gut microflora on mammalian blood metabolites. Proc Natl Acad Sci U S A. 106, 3698-3703.

Wishart, D.S. (2008). Quantitative metabolomics using NMR. TrAC Trends in Analytical Chemistry. 27, 228-237.

Wojnicz, D., Sycz, Z., Walkowski, S. et al. (2012). Study on the influence of cranberry extract Zuravit S·O·S® on the properties of uropathogenic Escherichia coli strains, their ability to form biofilm and its antioxidant properties. Phytomedicine. 19, 506-514.

Wolfender, J.L., Marti, G., Thomas, A. and Bertrand, S. (2015). Current approaches and challenges for the metabolite profiling of complex natural extracts. J Chromatogr A. 1382, 136-164.

Wolfender, J.L., Rudaz, S., Choi, Y.H. and Kim, H.K. (2013). Plant metabolomics: From holistic data to relevant biomarkers. Curr Med Chem. 20, 1056-1090.

Worley, B., Powers, R. (2013). Multivariate Analysis in Metabolomics. Current Metabolomics. 1, 92-107.

Wu, B., Yan, S., Lin, Z. et al. (2008). Metabonomic study on ageing: NMR-based investigation into rat urinary metabolites and the effect of the total flavone of Epimedium. Mol Biosyst. 4, 855-861.

Yang, C., He, Z. and Yu, W. (2009). Comparison of public peak detection algorithms for MALDI mass spectrometry data analysis. BMC Bioinform. 10.

Yang, Y., Zhang, Z., Li, S., Ye, X., Li, X. and He, K. (2014). Synergy effects of herb extracts: Pharmacokinetics and pharmacodynamic basis. Fitoterapia. 92, 133-147.

Yuliana, N.D., Jahangir, M., Verpoorte, R. and Choi, Y.H. (2013). Metabolomics for the rapid dereplication of bioactive compounds from natural sources. Phytochem Rev. 12, 293-304.

Zhang, A., Sun, H., Wang, P., Han, Y. and Wang, X. (2012). Modern analytical techniques in metabolomics analysis. Analyst. 137, 293-300.

Zhang, L., Wang, Y., Li, D., Ho, C., Li, J. and Wan, X. (2016). The absorption, distribution, metabolism and excretion of procyanidins. Food Funct. 7, 1273-1281.

Zhang, S., Sun, X., Wang, W. and Cai, L. (2013). Determination of urinary 8-hydroxy-2'-deoxyguanosine by a combination of on-line molecularly imprinted monolithic solid phase microextraction with high performance liquid chromatography-ultraviolet detection. Journal of Separation Science. 36, 752-757.

Zhang, Y., Yan, S., Gao, X. et al. (2012). Analysis of urinary metabolic profile in aging rats undergoing caloric restriction. Aging Clin Exp Res. 24, 79-84.